MOLECULAR PHYSICS, 2001, VOL. 99, NO. 23, 1899–1940

INVITED PAPER

Density functional theory: coverage of dynamic and non-dynamic electron correlation effects

DIETER CREMER*

Department of Theoretical Chemistry, Göteborg University, Reutersgatan 2, S-41320 Göteborg, Sweden

(*Received 10 July 2001; accepted 10 July 2001*)

The electron correlation effects covered by density functional theory (DFT) can be assessed qualitatively by comparing DFT densities $\rho(\mathbf{r})$ with suitable reference densities obtained with wavefunction theory (WFT) methods that cover typical electron correlation effects. The analysis of difference densities $\rho(\mathrm{DFT})-\rho(\mathrm{WFT})$ reveals that LDA and GGA exchange (X) functionals mimic non-dynamic correlation effects in an unspecified way. It is shown that these long range correlation effects are caused by the self-interaction error (SIE) of standard X functionals. Self-interaction corrected (SIC) DFT exchange gives, similar to exact exchange, for the bonding region a delocalized exchange hole, and does not cover any correlation effects. Hence, the exchange SIE is responsible for the fact that DFT densities often resemble MP4 or MP2 densities. The correlation functional changes X-only DFT densities in a manner observed when higher order coupling effects between lower order N-electron correlation effects are included. Hybrid functionals lead to changes in the density similar to those caused by SIC-DFT, which simply reflects the fact that hybrid functionals have been developed to cover part of the SIE and its long range correlation effects in a balanced manner. In the case of spin-unrestricted DFT (UDFT), non-dynamic electron correlation effects enter the calculation both via the X functional and via the wavefunction, which may cause a double-counting of correlation effects. The use of UDFT in the form of permuted orbital and broken-symmetry DFT (PO-UDFT, BS-UDFT) can lead to reasonable descriptions of multireference systems provided certain conditions are fulfilled. More reliable, however, is a combination of DFT and WFT methods, which makes the routine description of multireference systems possible. The development of such methods implies a separation of dynamic and non-dynamic correlation effects. Strategies for accomplishing this goal are discussed in general and tested in practice for CAS (complete active space)-DFT.

1. Introduction

The primary goals of quantum chemical investigations are (a) the accurate prediction of molecular properties such as structure, stability, reactivity, etc. and (b) the rationalization and interpretation of (calculated or measured) molecular properties in terms of simple models and concepts [1–4]. These goals have been actively pursued ever since quantum chemical methods could be routinely applied with the help of powerful computers. Wavefunction theory (WFT) was for many decades the leading discipline in quantum chemistry. In particular, in the 1970s and 1980s research in quantum chemistry was driven by expectations that by a steady improvement of correlation corrected *ab initio* methods and the availability of faster supercomputers pending chemical problems could soon be solved just by calculation rather than experiment. By the end of the 1980s the most important methods for calculating atomic and molecular energies with high precision had been developed. However, it became clear that it would be impossible to attack basic problems in chemistry (such as complex reaction mechanisms in the polluted atmosphere, drug–receptor interactions in the human body or the folding of a protein) in the near future with the help of correlation-corrected WFT methods and next generation supercomputers. Clearly, it was necessary to sacrifice the precision of the available WFT methods to investigate pending chemical problems. However, quantum chemists did not want to revert back to semi-empirical methods, which had their peak time in the 1970s.

In this situation, in the late 1980s, density functional theory (DFT) [5–24] was introduced into the repertoire of standard quantum chemical methods available to the

* e-mail: cremer@theoc.gu.se

Molecular Physics ISSN 0026–8976 print/ISSN 1362–3028 online © 2001 Taylor & Francis Ltd
http://www.tandf.co.uk/journals
DOI: 10.1080/00268970110083564

widespread usership of quantum chemical methods and quantum chemical programs. This was triggered by important developments in DFT methodology, which facilitated the use of DFT in quantum chemistry. New density functionals leading to increased accuracy were introduced, the applicability of DFT was increased, and a better understanding of its advantages and disadvantages was gained. This work was connected with the names of Parr, Becke, Perdew, and many others. From a practical point of view even more important was the integration of DFT program codes into standard quantum chemical packages in a manner that allowed the reproducibility of DFT results: an aspect that had been questioned by many potential users of DFT in the decades before. Leading in this respect was the work by Pople and his group in the USA and, independently, the work by Handy and his coworkers in the UK. In this way, DFT became available in the 1990s as a routine method for a growing clientele of quantum chemical technology.

Actually, the roots of DFT reach as far back in history as those of WFT. DFT-based methods had their origin in the quantum mechanical work of the 1920s, in particular that of Thomas [25] and Fermi [26], who showed with the help of a functional derived for the homogeneous electron gas (HEG) that the kinetic energy of atoms or molecules can be calculated approximately by just utilizing the electron density rather than the molecular wavefunction. Following Thomas and Fermi, Dirac [27] demonstrated that the exchange energy of the electrons can be expressed as a functional of the density. Within the Thomas–Fermi–Dirac model the molecular energy can be determined because nucleus–electron attraction and the classical Coulomb repulsion of non-interacting electrons can be expressed anyway as functionals of the density.

In the early 1950s, Slater [28] pioneered the idea of blending WFT with DFT by replacing the Fock exchange term of HF theory by Dirac's exchange functional. A theoretical basis for DFT was laid by Hohenberg and Kohn in the mid-1960s [5]. Kohn and Sham [6] proved that Slater's *ad hoc* procedure can be justified theoretically. Provided that the correct functional of the electron density is known for the electron–electron interaction term (exchange and correlation where also a part of the kinetic energy is included that corrects the kinetic energy of non-interacting electrons for correlation effects), it is in principle possible to determine the Schrödinger energy of a molecule using self-consistent field (SCF) technology. This established Kohn–Sham (KS) DFT, by which it is possible to calculate the energy of atoms and molecules within an iterative SCF scheme [6].

Kohn's work plus that of Levy, Perdew, Parr, Becke, Pople, Handy, and others led to the DFT methods as they are available today. This feature article does not aim to summarize these developments in detail because they are discussed in literally dozens of monographs and review articles over recent years [7–24]. Instead, DFT is approached here from the basis of WFT, to assess its applicability to molecular problems requiring a detailed account of electron correlation. DFT is a correlation corrected method; however, it is by no means clear which electron correlation effects are covered by the various exchange–correlation (XC) functionals presently in use.

In this work, we shall summarize recent attempts to assess dynamic and non-dynamic correlation effects covered by KS-DFT when applying standard XC functionals [28–40]. For this purpose, electron density distributions and other molecular properties are analysed, where experience and knowledge of the coverage of electron correlation effects by correlation corrected *ab initio* methods [41–51] are used to specify correlation effects covered by DFT [52–59]. In particular, we shall focus on the following questions. (a) What does electron correlation actually mean at the DFT level? (b) What correlation effects are covered by the X, what by the C functional? (c) Are there considerable differences in the coverage of electron correlation effects when comparing different LDA, GGA or hybrid functionals? (d) What role does the self-interaction error play in connection with electron correlation? Do self-interaction corrected DFT methods provide a better account of correlation effects? (e) Does standard DFT include any non-dynamic correlation effects and, if so, in which way? (f) How can multireference systems be described by standard DFT methods? Does spin-unrestricted DFT cover any non-dynamic electron correlation effects? (g) What are the problems of combining WFT and DFT methods for the purpose of describing multireference systems in an accurate way?

Clearly, a more detailed knowledge about the correlation effects covered by DFT helps to predict the performance and reliability of DFT when applied to molecular systems. Therefore, answers to questions (a)–(g) will also lead to an assessment of the accuracy of standard DFT methods.

This feature article is organized in the following way. In § 2 and § 3, short overviews over commonly used XC functionals [28–40] and the correlation effects these functionals have to cover are given. Section 4 summarizes some of the advantages and disadvantages of DFT. In § 5, dynamic electron correlation effects described by exchange and correlation functional are discussed comparing electron difference densities obtained by WFT and DFT methods. In particular,

the role of hybrid functionals in connection with the self-interaction error will be considered. Section 6 is devoted to the question of whether nondynamic electron correlation errors can be introduced into DFT. In this connection, the usefulness of normal spin-unrestricted DFT (UDFT), permuted-orbital UDFT, and broken-symmetry UDFT for describing multireference systems is analysed. The explicit coverage of nondynamic correlation effects is possible by extending standard DFT, as is shown in § 7. Finally, conclusions and outlook are given in § 8.

2. Overview of commonly used exchange–correlation functionals

In the formulation of Levy [60], DFT is based on the functional

$$F[\rho] = \min_{\Psi\to\rho}\langle\Psi|\hat{T} + \hat{V}_{ee}|\Psi\rangle, \tag{1}$$

where the minimization is carried out over all properly antisymmetric trial wavefunctions Ψ that integrate to the density ρ. The ground-state energy for an external potential v is then found by a search over all ρ that integrate to the total number of electrons N as

$$E[v] = \min_{\rho\to N} F[\rho] + \int \mathrm{d}^3\mathbf{r}\,\rho(\mathbf{r})v(\mathbf{r}). \tag{2}$$

The form of the functional $F[\rho]$ is unknown. To transform equation (1) into a practical calculational scheme, one decomposes $F[\rho]$ into one term that covers the major part of the total energy and can be evaluated exactly and another term that represents the many-body problem of interacting electrons. Within KS-DFT [6] one partitions $F[\rho]$ into the KS energy $F_{KS}[\rho]$ and the exchange–correlation energy $E_{XC}[\rho]$:

$$F[\rho] = F_{KS}[\rho] + E_{XC}[\rho], \tag{3}$$

$$F_{KS}[\rho] = \min_{\Phi\to\rho}\langle\Phi|\hat{T}|\Phi\rangle + \tfrac{1}{2}\int d^3\mathbf{r}\int d^3\mathbf{r}'\,\frac{\rho(\mathbf{r})\rho(\mathbf{r}')}{|\mathbf{r}-\mathbf{r}'|}, \tag{4}$$

where the Φ are antisymmetric trial functions that can be built up from a set of orthonormal one-particle orbitals ψ_1, ψ_2, etc. The first term in equation (4) is related to the kinetic energy of the non-interacting electrons, while the second term is related to the Hartree repulsion energy E_J of non-interacting electrons. For standard KS-DFT, Φ is a single-determinant trial wavefunction. The exact XC functional should cover all non-dynamic and dynamic correlation contributions; however, the approximate XC functionals available today are considered to describe only dynamic correlation effects.

Three different generations of XC functionals [28–40] are used nowadays in standard DFT methods. Typical representatives of the first generation are the SVWN or the SVWN5 functional [28, 32], which were employed first within the local density approximation (LDA). They combine the Slater exchange functional [28] with the Vosko–Wilk–Nusair (VWN) correlation functional [32]. SVWN is based on the HEG, and covers local exchange and local correlation effects (tables 1 and 2). The correlation effects for the HEG were first determined by using the random phase approximation (RPA); later, a better description was achieved by a quantum Monte Carlo (QMC) treatment, which was then the basis of the VWN5 functional [32].

The second generation of density functionals is based on the 'generalized gradient approximation' (GGA). Typical members are the functionals BP86 [29, 33, 34], BPW91 [29, 30], and BLYP [29, 35]. All three use the Becke88 exchange functional [29] based on Slater exchange [28], and corrections involving the reduced gradient of the density, $\nabla\rho/\rho^{4/3}$, thus adding non-local exchange effects. P86 is Perdew's gradient-corrected correlation functional [33, 34], PW91 is the Perdew–Wang-1991 gradient-corrected correlation functional [30] and LYP is the correlation functional of Lee *et al.* [35], which is a modification of the Colle and Salvetti correlation energy formula [40].

Table 1. Overview over currently used exchange functionals.[a]

Acronym	Author	Year	Comment	Ref
S	Slater	1951	Local exchange from the HEG	[28]
B	Becke	1988	Local exchange as Slater Non-local correction term with one empirical parameter, which by construction (adjustment to exact HF exchange) corrects the asymptotical behaviour of $\varepsilon_X(\mathbf{r})$	[29]
PW91	Perdew, Wang	1991	Local exchange as Slater Non-local correction term based on the exchange hole in a weakly inhomogenous electron gas and some rigorous relations for $\varepsilon_X(\mathbf{r})$	[30]
mPW91	Barone	1998	Local exchange as Slater Non-local exchange based on PW91, readjusting some parameters to improve the performance in the low-density limit; adjustment is done with a fit to noble-gas dimers	[31]

[a] HEG, homogeneous electron gas; $\varepsilon_X(\mathbf{r})$, exchange energy per electron.

Table 2. Overview over correlation functionals in use today.[a]

Acronym	Author	Year	Comment	Ref
VWN	Vosko, Wilk, Nusair	1980	Local correlation: RPA for the HEG (i.e. just double excitations)	[32]
VWN5	Vosko, Wilk, Nusair	1980	Local correlation: QMC treatment of the HEG (i.e. all excitations)	[32]
PL	Perdew	1981	Local correlation: QMC for the HEG (i.e. all excitations)	[33]
P86	Perdew	1981, 1986	Local correlation: QMC for the HEG (i.e. all excitations) Non-local correlation: Coulomb hole for the weakly inhomogeneous electron gas	[33,34]
PW91	Perdew, Wang	1991	Local correlation: QMC for the HEG (i.e. all excitations) Non-local correlation: Coulomb hole for the weakly inhomogeneous electron gas	[30]
LYP	Lee, Yang, Parr	1988	Local and non-local correlation derived by a fit to the He density (i.e. no separation between local and non-local parts)	[35]

[a] HEG, homogeneous electron gas, RPA, random phase approximation; QMC, quantum Monte Carlo method.

Table 3. Overview over currently used hybrid functionals.

	Exchange					Correlation				
	HF	Local DFT		Non-local DFT		Local DFT		Non-local DFT		
Functional	%	%	Name	%	Name	%	Name	%	Name	Ref
B3P86	20	8	S	72	B	19	VWN	81	P86	[36]
P3PW91	20	8	S	72	B	19	PW91	81	PW91	[36]
B3LYP	20	8	S	72	B	19	VWN	81	(LYP-VWN)	[36]
B1LYP	25	0	S	75	B	0	LYP	100	LYP	[37,38]
mPW1PW91	25	0	S	75	mPW	0	PW91	100	PW91	[31]
BH&HP	50	50	S	0	—	0	LYP	100	LYP	[39]

The third generation of functionals is based on a mixing of HF and DFT exchange to obtain a more realistic account of the XC energy, as was first suggested by Becke [36, 39]. The hybrid functionals B3P86, B3PW91, and B3LYP all use the Becke exchange functional [29] in combination with one of the correlation functionals. Three parameters based on empirical calibration procedures determine a suitable admixture of HF, local and non-local exchange for the X functional and local and non-local correlation of the C functional. In table 3, the composition of these functionals is given explicitly.

The B1LYP functional uses just one parameter to define the composition of the X and C parts [37, 38]. This is also true for the one-parameter functional mPW1PW91 of Barone and Adamo [31], which is based on the modified Perdew–Wang exchange functional mPW91 [30] and the Perdew–Wang 91 correlation functional [30]. The one-parameter hybrid functionals were developed to extend the applicability of DFT [37].

When using the exchange and correlation functionals listed in tables 1, 2 and 3, or any other related functional, one has to remember that they were originally designed to describe all electron correlation effects in an electron system, but not to give an accurate account of exchange and correlation effects separately. Nevertheless, we will discuss correlation energies separately in the following to obtain a better understanding of electron correlation as it is covered by DFT. For this purpose, we shall review the different types of electron correlation effects that are described by WFT and DFT methods.

3. Electron correlation in WFT and DFT

The largest and most important part of electron correlation is the exchange correlation (*Fermi correlation*) of two electrons with identical spin. HF theory correctly accounts for exchange correlation via antisymmetry of the HF wavefunction, because antisymmetry implies that the amplitude of the wavefunction vanishes for the case when two electrons with the same spin are at the same position. The electron pair density of any antisymmetric wavefunction gives a zero probability of finding a second electron with the same spin at the position of the first electron. The result of Fermi correlation can be illustrated and investigated with the help of the Fermi hole, which was first discussed by Wigner and Seitz in 1934 [61], and later in 1951 examined by Slater

Table 4. Electron interaction energies of CO($^1\Sigma$) obtained with different functionals.[a]

Molecule	E_J	E_X	E_C	E_{XC}	E_{ee}
HF	76.247 63	−13.328 96	0	−13.328 96	62.918 67
S	75.898 98	−11.963 03	0	−11.963 03	63.935 95
B	76.235 97	−13.381 70	0	−13.381 70	62.854 27
PW91	76.205 17	−13.349 78	0	−13.349 78	62.855 39
mPW	76.222 22	−13.378 39	0	−13.378 39	62.843 83
SVWN	76.228 40	−12.001 91	−1.223 23	−13.225 13	63.003 27
SVWN5	76.197 87	−11.998 46	−0.948 38	−12.946 84	63.251 03
BPL	76.524 34	−13.417 99	−0.943 97	−14.361 96	62.162 38
BP86	76.374 44	−13.396 69	−0.495 25	−13.891 94	62.482 50
PW91PW91	76.395 75	−13.368 95	−0.485 25	−13.854 20	62.541 55
BPW91	76.424 50	−13.401 20	−0.485 72	−13.886 92	62.537 58
BLYP	76.387 49	−13.398 27	−0.485 32	−13.883 59	62.503 90
mPW91PW91	76.411 97	−13.397 73	−0.485 47	−13.883 20	62.528 77
B3LYP	76.391 77	−13.269 98	−0.625 66	−13.895 64	62.496 13
B3PW91	76.413 38	−13.272 14	−0.573 63	−13.845 77	62.567 61
B3P86	76.411 97	−13.273 09	−0.862 15	−14.135 24	62.276 73
MP2	76.247 63	−13.328 96	−0.426 79	−13.755 75	62.491 88
MP3	76.247 63	−13.328 96	−0.423 79	−13.752 75	62.494 88
MP4(SDQ)	76.247 63	−13.328 96	−0.432 91	−13.761 87	62.485 76
MP4(SDTQ)	76.247 63	−13.328 96	−0.454 61	−13.783 57	62.464 06
CCSD	76.247 63	−13.328 96	−0.430 28	−13.759 24	62.488 39
CCSD(T)	76.247 63	−13.328 96	−0.448 70	−13.777 66	62.469 97

[a] All energies are given in E_h. All calculations with the 6-311+G(3df) basis set [63] at the experimental geometry [64].

for the HEG [28]. Investigation of various atoms revealed that the Fermi hole for different atoms is remarkably unchanged, apart from a certain degree of contraction depending on the effective nuclear charge of the atom in question [62]. (As for the properties of the Fermi hole and its mathematical expression in terms of the pair density, see standard text books [7, 12, 24].)

The exchange–correlation energy as calculated with the HF method is given in table 4 for the CO molecule (all calculations [52] with the 6-311+G(3df) basis [63] at experimental geometry [64]). Comparison with the Coulomb correlation energy obtained for example at the CCSD(T) level of theory [65] suggests that Fermi correlation corresponds to more than 95% of the total correlation energy. Hence, the success of HF theory results from the simple fact that it covers correctly the larger part of the correlation energy, although in the common quantum chemical terminology HF is considered as an uncorrelated method because of its failure to cover Coulomb correlation. Nevertheless, it is didactically useful to speak of HF and all HF-based WFT approaches as exchange–correlated methods.

DFT includes exchange–correlation via the X functional; however, because of the approximate nature of the known X functionals (see tables 1 and 4), exchange is not covered exactly. Exchange functionals of the first generation, such as the S functional [28], underestimate exchange effects substantially (table 4), while Becke exchange [29] or the Perdew–Wang exchange [30] exaggerates slightly the magnitude of the exchange energy relative to the corresponding HF value. For the hybrid functionals, exchange effects are tuned down (table 4) by the admixture of both Slater and HF exchange, however *not to reproduce exact exchange energies but to provide a better total correlation energy*.

Fermi correlation applies only to electrons with the same spin whereas dynamic Coulomb electron correlation occurs for every pair of electrons. It is non-specific and in this sense a universal correlation effect, which always is present in many-electron systems ($N \geqslant 2$). Coulson and Neilson [66] described dynamic electron correlation with the help of the Coulomb hole: Around each electron, there is a region of space, in which another electron is less likely to be found relative to the HF description. However, the probability of finding another electron exactly at the position of the first electron is finite (provided the spins of the two electrons are different) rather than zero as found in the case of the Fermi hole. Coulson and Neilson [66] found that in the case of the He ground state the average radius of the Coulomb hole is about 0.56 Å and that 0.05 e is displaced by the Coulomb hole. The Coulomb correlation energy is about 42 mE_h for the electron pair of the He(^{1}S) atom, but it decreases to about 1 mE_h for

two electrons with the same spin, as in the He(^{3}S) state. Coulomb correlation enlarges somewhat the size of the Fermi hole, but both Fermi and Coulomb correlations are short range phenomena, as indicated by the dimensions of the corresponding correlation holes.

The absolute value of the correlation energy as obtained with the VWN [32] or PL functional [33] is more than twice the magnitude of the CCSD(T) correlation energy (table 4). The LYP [35] or PW91 functional [30] leads to correlation energies comparable in magnitude with those obtained with WFT methods. Hybrid functionals, on the other hand, yield correlation energies considerably more negative than those obtained at the CCSD(T) level of theory. This is justified in view of the differences in the definitions of the total correlation energy at the DFT and WFT levels of theory.

(1) While the exact HF exchange is calculated from the HF Slater determinant constructed from energy-optimized HF orbitals, the exact KS exchange energy is based on the Slater determinant formed from the KS orbitals. The KS orbitals are determined in such a way that they should reproduce the electron density of the real electron system, which means that they reflect the electron correlation effects of the molecule. In this sense, the KS exchange energy calculated with the help of the KS orbitals is influenced by the electron correlation in the system, even though it is calculated from the wavefunction of a non-interacting reference system. Accordingly, the DFT exchange energy cannot be equal to the HF exchange energy: orbitals calculated under the influence of electron correlation are more diffuse, so that the absolute value of the calculated exchange energy becomes smaller than the corresponding HF value even if the same functionals would be used.

(2) The correlation energy is defined as the difference between the exact energy of the interacting many-electron system and the energy of a suitable reference system, where both WFT and KS-DFT use the energy of a single-determinant wavefunction as reference. This reference function is optimized with respect to the total energy for HF, while in KS theory the reference function is optimized to provide the best density distribution $\rho(\mathbf{r})$. Consequently, the reference energy is more positive for KS than for HF, and thus the exact KS correlation energy becomes larger (by its absolute value) than the exact correlation energy in WFT. This is the reason why the DFT correlation energies listed in table 4 are all more negative than the WFT correlation energies.

(3) The DFT exchange–correlation energy covers also that part of the kinetic energy of the electrons that results from the correlated movement of the electrons. The DFT kinetic energy itself is just calculated for the non-interacting electrons. As correlation leads to an increase in the kinetic energy of the electrons of a molecule, the total correlation energy contains a kinetic energy correction due to electron correlation. (In the case of the HEG, the kinetic energy is increased.)

(4) Correlation and exchange functionals were developed in most cases to complement each other in the sense of determining the exact (best) electron density of a many-electron system rather than to lead to exact exchange or correlation energies. Other XC functionals were calibrated to provide accurate density-dependent molecular properties such as energy, geometry, etc., rather than to obtain exact X and C energies.

In view of considerations (1)–(4), a comparison of absolute WFT and DFT exchange and correlation energies is not meaningful. It is more useful to discuss trends in these energies in connection with calculated density distributions where, for the latter, WFT densities may be used as a suitable reference.

Standard KS-DFT is considered to cover just dynamic electron correlation, but not *non-dynamic* (*static*) Coulomb correlation. The latter is known to result from near-degeneracy effects, i.e. strong interactions of ground and excited states, which are close in energy. Hence, non-dynamic electron correlation is (contrary to dynamic correlation) system-specific. It leads to a substantial extension of the Coulomb correlation hole, indicating that non-dynamic correlation is a long range effect that clearly dominates the properties of the Coulomb hole. The straightforward procedure to cover non-dynamic electron correlation is to include all configuration state functions (CSFs) with similar energy into a self-consistent field calculation optimizing both the orbitals and the coefficients of the CSFs, as in the *full optimized reaction space* (FORS) method of Ruedenberg [67] of the equivalent (*complete active space*) CAS-SCF approach [68]. A basic problem of these approaches is that with the coverage of non-dynamic electron correlation an uncontrollable amount of dynamic electron correlation is introduced by the method. Hence, any improvement in standard KS-DFT to cover also non-dynamic electron correlation has to consider the basic features of the correlation hole resulting from system-specific, near-degeneracy correlation effects.

4. Advantages and disadvantages of DFT

The many-electron problem is simplified considerably when the variational principle is applied to the one-electron density distribution $\rho(\mathbf{r})$ rather than the many-electron wavefunction. Because of this simplification, advantages (A1–A6) result, which constitute the major reasons for the enormously increased use of DFT methods during the last decade [7–24].

(A1) In DFT the many-particle Hamiltonian is simplified in a way that its conceptual use becomes much easier. Energy parts that can be calculated exactly are written down explicitly, while all parts of the energy that are difficult to calculate are contracted in the XC functional.

(A2) Despite the fact that KS-DFT is based on a single-determinant description of the many-particle system, it will describe both single-reference and multi-reference systems correctly, provided the exact XC-functional is available.

(A3) The simplicity of DFT facilitates its extension when a more complete theory is needed (calculation of specific molecular properties, relativistic DFT, etc.).

(A4) For an adequate description of the XC functional it is sufficient to focus on the correct assessment of the exchange–correlation hole. The analysis of a simple many-particle system should provide a better understanding of the electron XC hole. Any improved insight into how to model the XC hole exactly leads to further developments in DFT and advances our knowledge of the electronic structure of molecules.

(A5) As long as the XC functional does not depend on the number N of electrons in a given electronic system, DFT is size-extensive [69, 70].

(A6) Within KS-DFT, basis functions are used to calculate KS orbitals. However, DFT as a theory based on the electron density is less sensitive to basis set truncation errors than WFT. VTZ+P and VQZ+P basis sets (in the language of Dunning: cc-pVTZ and cc-pVQZ basis sets [71]) are close to the basis set limit, which for correlation-corrected WFT methods is reached only at the cc-pV6Z basis set [72, 73]. A direct consequence of the decreased sensitivity of KS-DFT to basis set truncation errors is that basis set superposition errors play a much smaller role in DFT than in WFT.

The simplicity of DFT also implies disadvantages (D1–D10), which have hampered its acceptance by quantum chemists for a long time.

(D1) In contrast to WFT methods, DFT does not offer a systematic way of improving the Hamiltonian, and in particular the XC potential, so that a correct description of all many-electron interactions in a molecule cannot be achieved in a stepwise, well defined manner.

(D2) DFT is a correlation-corrected method; however, it is not clear which electron correlation effects are exactly covered by a given DFT method. This makes it difficult to predict the reliability of DFT results for a particular electronic system.

(D3) Because of the approximate nature of the density functionals in use nowadays, DFT is far from covering system-specific electron correlation effects as they occur in atoms and molecules with multi-reference character. The common understanding is that DFT covers just exchange and Coulomb correlation effects of the short range (dynamic) type.

(D4) As a consequence of D1, density functionals have been developed (e.g. the hybrid functionals) that are no longer based on first principles. Their composition was determined with the help of experimental data, thus converting DFT to a semiempirical method. Although clearly, LDA or GGA methods such as BLYP or PW91 are *ab initio* (non-empirical) methods [74], this is no longer true for hybrid functional methods.

(D5) In HF theory, the Coulomb interaction of an electron in a given orbital with itself is exactly cancelled out by an analogous interaction in the exchange term. Because of the approximate nature of the XC functional, DFT suffers from the self-interaction error (SIE) of the electrons (see, e.g. standard texts and reviews on DFT [7, 18, 20, 24, 32]). Methods to cure this error have been suggested [75–85], but turn out to complicate DFT in an undesirable way.

(D6) The conceptual understanding of WFT results is based strongly on the use of orbitals (HF orbitals, natural orbitals, etc. [86]). KS orbitals differ considerably from HF orbitals, although it has been argued that the former cover important properties of the latter [87–89]. Strictly speaking, one has to consider orbitals just as mathematical tools in a density theory, and therefore it has been pointed out [53, 54, 90] that KS orbitals, depending on the DFT method used, are physically not meaningful intermediates of the calculation, and that the conceptual understanding of DFT results has to start from the calculated density. Despite the progress in understanding the density distribution of a molecule (e.g. by virial partitioning as pioneered by Bader [91]), there are no simple density-based models and concepts that quickly help to understand the results of a DFT calculation.

Although it would be beyond the scope of this article to list all those cases in which KS-DFT reveals typical deficiencies because of the approximate nature of the density functionals in use, some characteristic failures of DFT should be mentioned.

(D7) A typical error of LDA descriptions is the exaggeration of bond strength [8–14]. This can be largely corrected for by using GGA and hybrid functionals, but nevertheless it can still represent a problem in bond forming/breaking processes.

(D8) It has been found that DFT underestimates in many cases the barrier of a chemical reaction, in particular low barriers of exothermic reactions [85, 92, 93]. Both D5 (SIE) and D7 (exaggeration of bond strength) can play a role in this connection. Connected with

deficiencies in describing transition states is often the appearance of spurious minima on a potential energy surface (PES) obtained by a DFT description [94].

(D9) Dispersion interactions in van der Waals complexes depend on fluctuations of the density in the tails of the monomers forming the complex, i.e. they depend strongly on a correct description of electron correlation in the van der Waals region. Most functionals in use are not able to describe these fluctuations correctly, which leads to the failure of KS-DFT in the case of van der Waals complexes held together predominantly by dispersion forces [95–99]. Better results are obtained for van der Waals complexes dominated by electrostatic forces (interactions between permanent or induced multipole moments).

(D10) Directly connected with D9 are failures of DFT in describing H bonding. While intermolecular H-bonds are described reasonably at the KS-DFT level with an appropriate basis set (mainly because H-bonding results from both covalent and electrostatic interactions) [100–102], intramolecular H-bonding often is not correctly covered by DFT [103].

In the following, we focus in particular on points D2 and D3 concerning the correlation effects covered by standard KS-DFT. A better understanding of these aspects is a prerequisite for increasing the predictability of DFT results (i.e. using DFT in a manner similar as WFT methods are used) and for obtaining a starting point for a more systematic improvement of DFT.

In WFT, a systematic improvement in the quantum chemical description of a many-particle system is accomplished by extending the single-particle, single-determinant description of HF stepwise. First, dynamic electron correlation effects are introduced, for which a well tested repertoire of WFT methods is available (for example, Møller–Plesset perturbation theory at *n*th order (MP*n*) [44, 104] or coupled cluster (CC) theory [2, 3, 105–108]). If needed, non-dynamic electron correlation can be added using multideterminant, multireference (MR) descriptions such as MR-CI [109] or MR-CC theory [110]. In WFT, there is the possibility of specifying those many-particle corrections introduced via the type of excitation (single (S), double (D), triple (T), quadruple (Q), etc.) covered by the method in question [44]. For example, MP2 is known to describe electron pair correlation in a somewhat exaggerated way, MP3 corrects pair correlation effects at MP2 by a coupling between D excitations, and MP4 introduces orbital relaxation effects (via the S excitations), three-electron correlation effects (via T excitations), and disconnected four-electron correlation effects via Q excitations. Higher order correlation effects as they are introduced at fifth-order (MP5) and sixth-order MP (MP6) theories are also described in the literature [45]. MP theory provides a platform for analysing electron correlation effects [46, 47] covered by more advanced methods, such as CCSD [111] or CCSD(T) [65]. For example, the former method contains all infinite order effects in the SD space, which means that for $2 \leqslant n \leqslant \infty$ all MP*n* energy terms built up by just S and D are automatically covered, as well as many (disconnected) higher order contributions [48]. Similarly, CCSD(T) covers (up to MP8) 77% of the terms of the SDT space of the more complete CCSDT method [49]. Hence, the systematic extension of MP and CC theories provides a firm basis for an understanding of the stepwise improvement of these methods.

5. Coverage of dynamic electron correlation by DFT

Despite the fact that generally the absolute value of the DFT correlation energy is larger than the corresponding values obtained by WFT methods, the changes in the density distribution caused by the correlation functional are not necessarily larger. The KS reference system has to reproduce the one-electron density distribution of the real system as much as possible, and therefore the influence of the DFT correlation functional on the density should be lower than that of electron correlation corrections introduced in WFT. Because of the simultaneous treatment of exchange and Coulomb correlation effects in the XC functional, the X functional can mimic electron correlation effects identified by WFT methods as Coulomb rather than exchange correlation effects. Accordingly, it is important to analyse the differences in the density distribution caused by HF and DFT exchange, and to see which correlation effects are already simulated by a particular choice of an X functional. Such an investigation was carried out by Cremer and coworkers [52], and in the following the major conclusions of this work are summarized.

Cremer and coworkers approached the problem of identifying correlation effects covered by the DFT XC functional by first establishing a list of reference densities covering well known correlation effects. A number of molecules with typical bonding situations between first row heavy atoms (H—H, $H_3C—CH_3$, $H_2C=CH_2$, HC≡CH, $H_2N—NH_2$, HN=NH, N≡N, O=O, HO—OH, F—F, $CH_3—OH$, $H_2C=O$, C≡O) was investigated for this purpose. Out of this group of test molecules we shall refer in particular to results obtained for carbon monoxide in its ground state, $CO(^1\Sigma^+)$ (basis: 6-311 + G(3df) [63]; experimental geometry [64]) because its calculated electron density distribution depends sensitively on the correlation effects covered by a given method [43, 112–114]. The exact electron density and other molecular properties of CO reflect a delicate balance between with-

drawal of σ-type electron density from the C to the O atom (due to the difference in electronegativities) and partial back-donation of π electron density from the O to the C atom, thus lending the molecule some triple-bond character. HF exaggerates the transfer of σ charge towards the O atom and underestimates π-back donation [52].

Electron pair correlation as introduced at the MP2 level of theory via the D excitations leads to an important redistribution of the electron density, which can be made visible when plotting the difference electron density distribution $\Delta\rho(\mathrm{MP2, HF}) = \rho(\mathrm{MP2}) - \rho(\mathrm{HF})$ (figure 1(*a*)) [41, 42]. (a) *Left–right correlation* causes a substantial charge transfer in the π space from the O to the C atom. (b) *Angular correlation* supports the first effect by shifting negative charge from the region of the σ bond close to the O to the π region at C. (c) *In–out correlation* shifts part of the charge in the outer valence region closer to the nucleus (inner valence region), in particular at O, while another part is moved into the van der Waals region, by which the σ electron lone pairs at C and O become more diffuse.

Although the pair correlation effects introduced at MP2 correct the density and other properties of the CO molecule in the right direction, their values are over-corrected because too much negative charge is transferred from the O to the C atom. MP3, in turn, corrects the exaggeration of pair correlation effects at the MP2 level by coupling pair correlation effects. The MP3 electron density changes partially back (π donation from C to O) to the HF density, i.e. again there is too little charge at the C atom (too much at the O atom). This is corrected a second time at the MP4 level, which introduces orbital relaxation effects, three-electron correlation, and pair–pair correlation effects. Again, there is a transfer of negative charge from the O to the C atom similar to as it occurs at the MP2 level; however, this time the accumulation of charge in the π space of C is not so strong. In total, the stepwise introduction of electron correlation effects at the MP*n* level leads to oscillations in the density distribution and other molecular properties of CO, where oscillations decay slowly with increasing order *n* of MP*n* theory.

The correlation effects covered at the CCSD level include infinite-order orbital relaxation and pair correlation effects, which means that both an exaggeration or underestimation of pair correlation effects is avoided. The difference density distributions $\Delta\rho(\mathrm{CCSD,MP}n) = \rho(\mathrm{CCSD}) - \rho(\mathrm{MP}n)$ shown in figure 1(*b*) ($n = 2$), (*c*) ($n = 3$) and (*d*) ($n = 4$: MP4(SDQ)) confirm this. The CCSD electron density distribution leads to lower π density at the C atom than that found at both the MP2 and the MP4(SDQ) levels of theory, but it leads to more π density at C than found at the MP3 level. The partial inclusion of three-electron correlation at either the MP4(SDTQ) or the CCSD(T) level of theory increases (decreases) the π density at the C (O) atom (figure 1(*e*)), where again this effect is exaggerated by the MP method. Figure 1(*f*) reveals that by including a large part of infinite-order three-electron correlation effects at the CCSD(T) level of theory (CCSD(T) covers more than 70% of the infinite-order effects in the T space, in particular DT and TT coupling effects, which help to avoid an exaggeration of three-electron correlation as it occurs at the MP4 level [48,49]), the exaggeration of the π density at the C atom caused by MP4 is reduced. CCSD(T) yields a reliable description of both electron density and the molecular properties of CO, and therefore, the CCSD(T) results represent an ideal reference for the analysis of the DFT results.

5.1. *What correlation effects are covered by DFT exchange functionals?*

In figure 2 the electron density distribution calculated with the commonly used BLYP functional [29, 35] is compared with the corresponding density obtained from HF, MP and CC calculations. The difference electron density distribution $\Delta\rho(\mathrm{BLYP,HF}) = \rho(\mathrm{BLYP}) - \rho(\mathrm{HF})$ (figure 2(*a*)) reveals changes in the charge distribution of CO that agree qualitatively with those obtained for $\Delta\rho(\mathrm{MP2,HF})$ (figure 1(*a*)), i.e. charge is transferred from the π space at O and the σ(CO) region to the π(C) space. Also negative charge is shifted from the σ lone pair regions either towards the nucleus or out into the van der Waals regions.

A direct comparison with $\rho(\mathbf{r})$ calculated with MP2, MP3, MP4, CCSD or CCSD(T) (figure 2(*b–f*)) confirms that the BLYP functional generates an electron density distribution similar to that of MP2, MP4 or CCSD(T), but different from that of HF, MP3 or CCSD. A detailed analysis reveals that the BLYP density is actually closer to the MP4 density than either the MP2 or CCSD(T) density distributions [52]. This observation is made also for other molecules, and suggests that the BLYP functional covers in addition to pair and pair–pair electron correlation effects also considerable three-electron correlation effects.

The difference electron density distribution $\Delta\rho(\mathrm{BLYP, MP4}) = \rho(\mathrm{BLYP}) - \rho(\mathrm{MP4})$ (figure 2(*d*)) indicates some typical deviations of the BLYP density from the MP4 density. (a) In the case of the BLYP density there is more negative charge in the van der Waals regions, a reminder of a well known deficiency of this functional, namely, to fail when describing van der Waals complexes stabilized just by dispersion forces [95–99]. The analysis of the BLYP density suggests that probably it is less due to a failure of covering dispersion

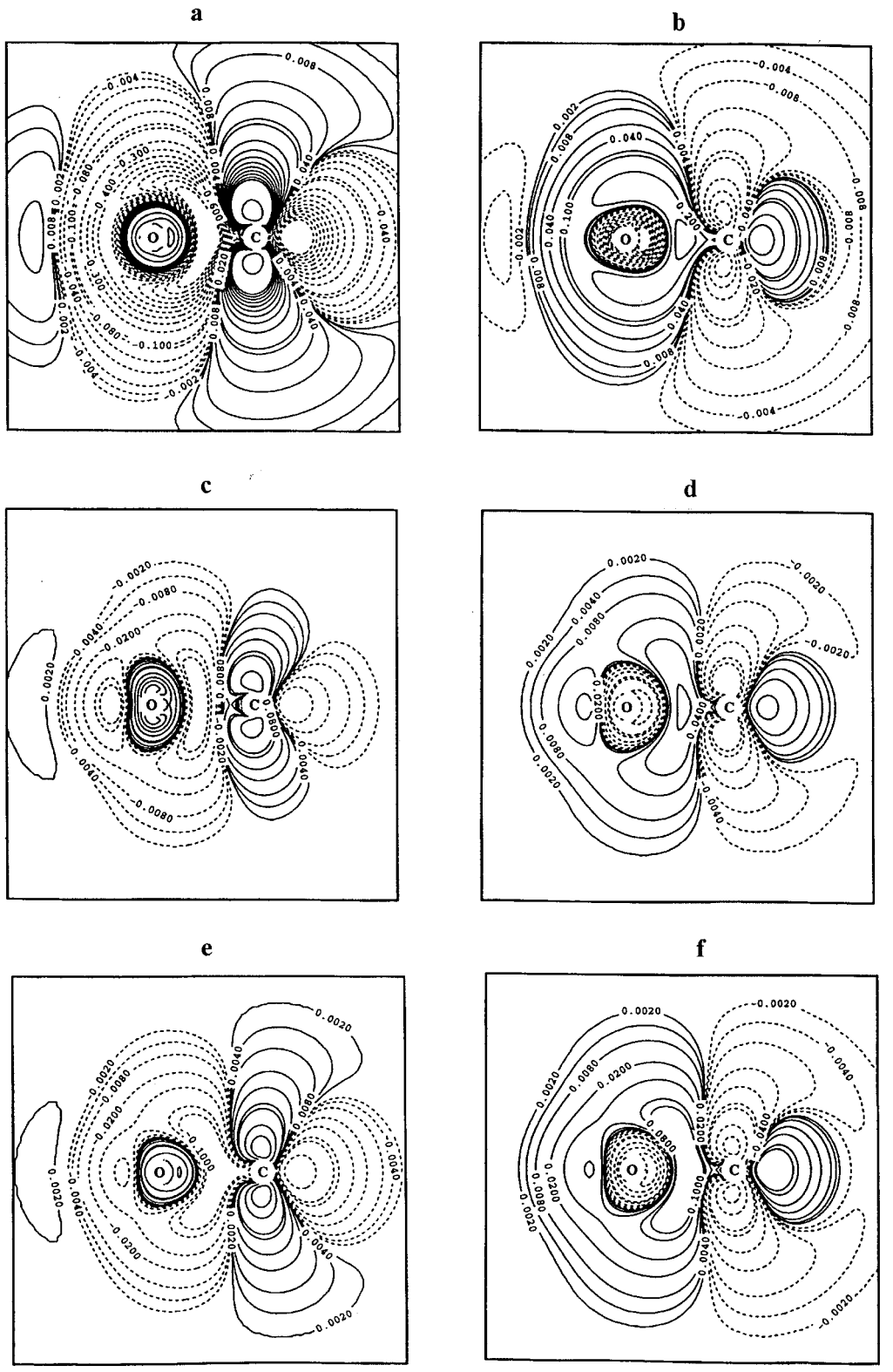

Figure 1. Contour line diagrams of the difference electron density distribution $\Delta\rho(\mathbf{r}) = \rho(\text{method I}) - \rho(\text{method II})$ of CO calculated with the 6-311+G(3df) basis at $r_e(CO) = 1.128$ Å. Solid (dashed) contour lines are in regions of positive (negative) difference densities. The positions of the C and the O nuclei are indicated. The contour line levels have to be multiplied by the scaling factor 0.01 and are given in $e\,a_0^{-3}$. (*a*) MP2-HF; (*b*) CCSD-MP2; (*c*) CCSD-MP3; (*d*) CCSD-MP4(SDQ); (*e*) CCSD(T)-CCSD; and (*f*) CCSD(T)-MP4.

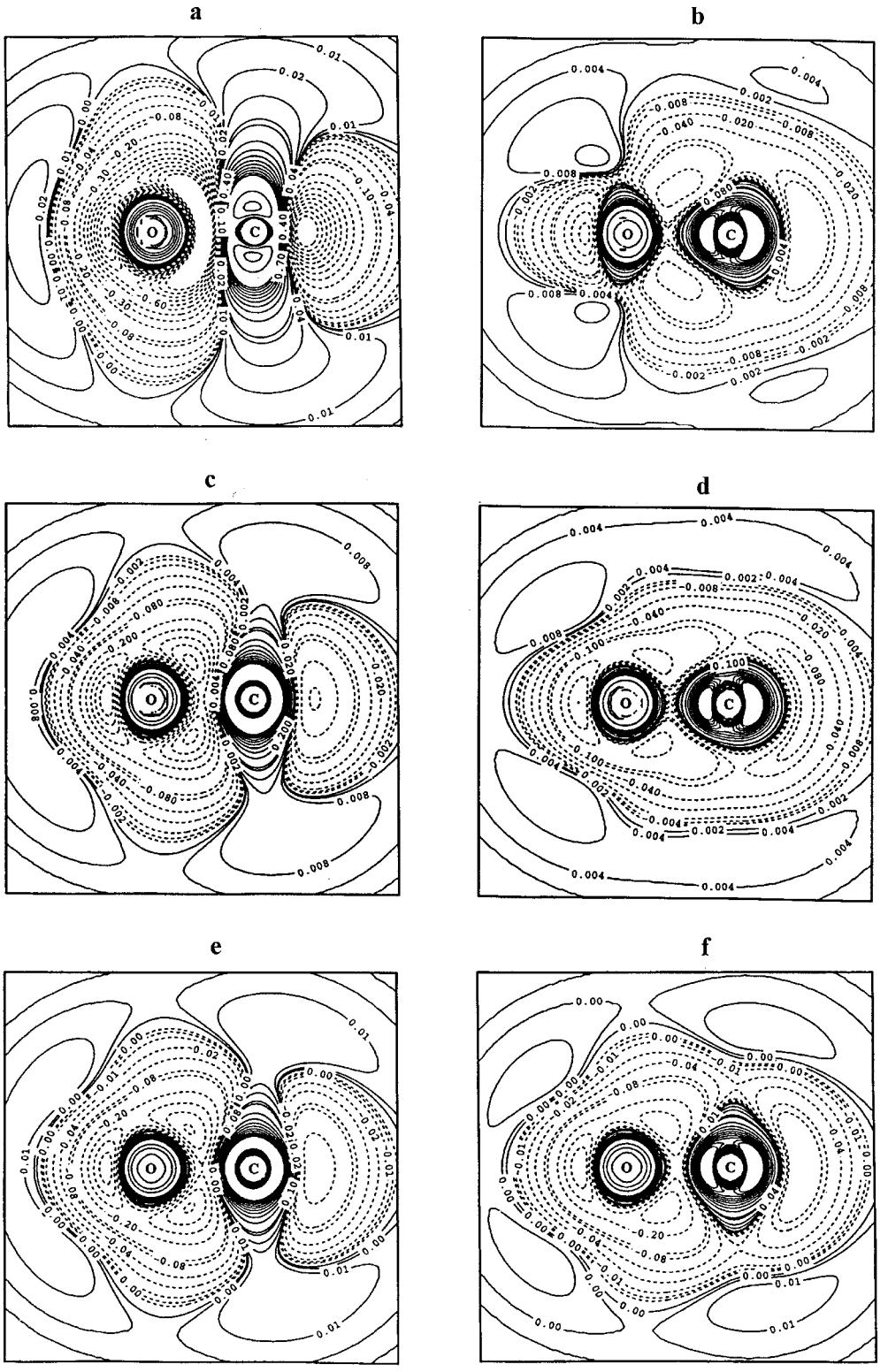

Figure 2. Contour line diagrams of the difference electron density distribution $\Delta\rho(\mathbf{r}) = \rho(\text{method I}) - \rho(\text{method II})$ of CO calculated with the 6-311+G(3df) basis at $r_e(\text{CO}) = 1.128$ Å. Solid (dashed) contour lines are in regions of positive (negative) difference densities. The positions of the C and the O nuclei are indicated. The contour line levels have to be multiplied by the scaling factor 0.01 and are given in $e\,a_0^{-3}$. (*a*) BLYP-HF; (*b*) BLYP-MP2; (*c*) BLYP-MP3; (*d*) BLYP-MP4; (*e*) BLYP-CCSD; and (*f*) BLYP-CCSD(T).

interactions correctly (pair and three-electron correlations are actually covered), and more due to an exaggeration of exchange repulsion caused by the relatively high electron density in the van der Waals regions. (b) The BLYP functional also concentrates more electron density to the inner shell and core region when compared with the MP4 density. The closer analysis carried out by Cremer and coworkers [52] revealed that the density distribution close to the nuclei is actually more complex in the BLYP representation than is obvious from the contour line diagrams of figure 2. There is a shell structure of the difference electron densities $\Delta\rho(\text{BLYP,WFT}) = \rho(\text{BLYP}) - \rho(\text{WFT})$ (figure 3) characterized by a strong increase in the BLYP density close to the nucleus surrounded by a shell of charge depletion and a second shell of (considerably less) density concentration in the inner valence region. This shell structure is an artefact of the B-exchange functional, as the profile plots of figure 3 show clearly.

There is a singularity in the Laplacian of the electron density caused by the cusp it possesses at the position of the nucleus. The singularity in the Laplacian of the density implies also a singularity in the exchange or correlation potential. The gradient corrections to the X functional increase the absolute value of the X energy and the corresponding contribution to the exchange potential is therefore attractive [115]. Consequently, the effective nuclear charge and the effective electronegativity of the atom in question are increased. The strongest influence of this extra potential is to be seen for the core orbitals, which are contracted compared with LDA, leading to an increase in charge density immediately at the nucleus and a decrease in the surrounding region. This generates a shell structure in the X-only density distribution (figure 3), the origin of which is mathematical rather than physical.

The shell structure of the B-only density observed in the nuclear region is an artefact typical of gradient corrected XC functionals. This has to be considered when calculating molecular properties such as nuclear magnetic shieldings [116] or NMR spin–spin coupling constants [117], which depend on a correct account of the electron density close to the nucleus.

Analysis of the BLYP density of CO and other molecules reveals that in general they resemble the corresponding MP4 densities, but does not indicate whether this is due to the exchange or the correlation functionals. Cremer and coworkers [52] answered this question by (a) comparing exchange-only densities directly with WFT densities and (b) investigating the changes caused by the correlation functionals separately. Four conclusions could be drawn from this investigation. (1)

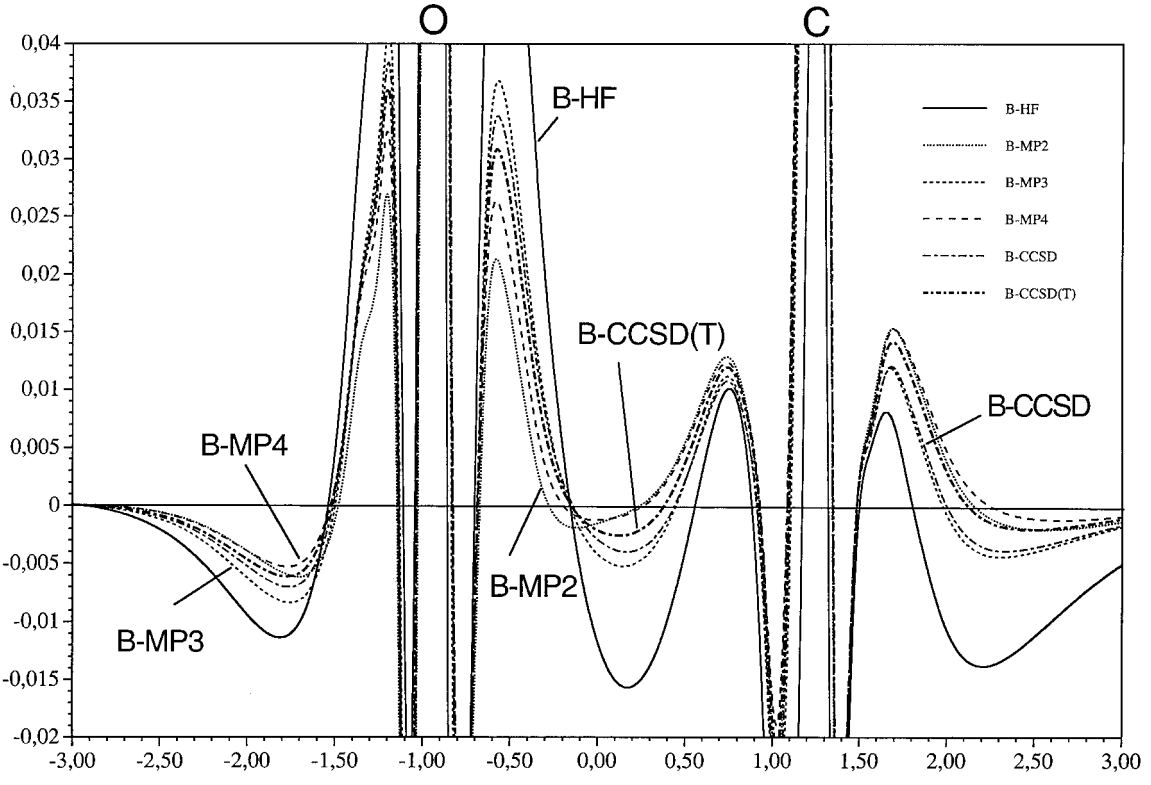

Figure 3. Profile diagrams of the difference electron density distribution $\Delta\rho(\mathbf{r}) = \rho(\text{B-only}) - \rho(\text{method II})$ (method II: HF, MP2, MP3, MP4, CCSD, CCSD(T)) of CO calculated with the 6-311+G(3df) basis at $r_e(\text{CO}) = 1.128$ Å and taken along the CO axis. The positions of the C and the O nuclei are indicated.

The XC density is dominated by the exchange part, to which the correlation part adds only minor corrections. (2) The replacement of HF exchange by DFT exchange leads to similar density changes as those observed when including dynamic electron correlation effects at the MP2, MP4 or CCSD(T) levels of theory (see figures 1 and 2). (3) GGA exchange functionals such as the B or PW91 functional lead to a density distribution that is close to MP4 density, i.e. they mimic already pair, pair–pair, and three-electron correlation effects. (4) LDA exchange functionals such as the S exchange functional [28] differ from this common behaviour only by the fact that they increase the density in the bond region, in the van der Waals region, and also in the inner valence regions of the atoms relative to that of a GGA functional. These observations are in line with the fact that LDA functionals significantly overestimate the bond density and the bond strength.

Although it is obvious that LDA and GGA X functionals simulate strong pair (and other low order diagonal N-electron) correlation effects, inspection of the difference density plots does not reveal whether these are of short range (dynamic) or long range (non-dynamic) nature. In the first case, negative charge is separated by a large number of short range electron–electron interactions, while in the latter case just a few strong long range interactions (mixing in of a few low lying CFSs into the wavefunction) lead to a similar density pattern. Before clarifying this point, we have to consider the influence of the correlation functional on the density generated by the exchange functional. The correlation functional should actually introduce the short range electron correlation effects, and therefore analysis of the density changes caused by the correlation functional can lead to a better understanding of the correlation effects simulated by the DFT exchange functional.

5.2. *What correlation effects are covered by DFT correlation functionals?*

The influence of the correlation functional on the DFT density was investigated by generating difference electron density distributions of the type $\Delta\rho(\text{C-only}) = \rho(XC) - \rho(\text{X-only})$. In this way, the density changes caused by the VWN, VWN5, PL, P86, PW91, and LYP correlation functionals were analysed [52]. Four of these functionals, namely VWN, VWN5, PL, and LYP, lead to similar changes in the electron density (figure 4(a, b)) while the changes caused by GGA functionals such as P86 or PW91 are different (figure 4(g, h)). The influence of the various correlation functionals on the density distribution can be summarized as follows.

(i) *In the case of the LDA correlation functionals, the electron density distribution is enhanced in the atom, bond, and (inner) non-bonding regions between the atoms; it is reduced in the van der Waals regions.* These changes are relatively small (compared with those caused by a replacement of the HF by the DFT exchange potential), but are typical and independent of the molecule investigated. In the case of the LDA functionals VWN, VWN5, and PL they can be explained in the following way. At the LDA level, electron correlation is described by an attractive local potential that becomes stronger the higher the density. Therefore the incorporation of an LDA correlation functional will transfer negative charge from regions with low electron density to regions with high electron density. This effect depends on the local density, and therefore is less specific than the charge transfer due to the explicit inclusion of electron correlation by a WFT correlation method. Also, it leads to an exaggeration of correlation effects.

(ii) *The differences between the various LDA correlation functionals are very small.* For example, the VWN5 correlation functional is based on the more complete QMC (all excitations) rather than RPA investigation (just D excitations) of the HEG (table 2), and therefore covers also the higher order correlation effects of the latter. VWN5 moves some minor amount of density from the bonding and valence regions of the atoms out into the van der Waals regions (figure 4(e)). Higher order correlation effects include more electrons in the correlated movements of an electron ensemble and, accordingly, lead to an expansion of the electron density. However, these changes are tiny die to the fact that the LDA functionals, although derived by different procedures, have a similar dependence on high densities.

(iii) *Although the density changes caused by the LYP functional are similar to those of the LDA functionals (figure 4(c, d)), LYP does not exaggerate bond and valence densities as much as LDA functionals do.* This becomes obvious when comparing the LYP and VWN5 density distributions (figure 4(f), $\rho(\text{LYP}) - \rho(\text{VWN5})$): LYP moves some of the density from the bond and valence regions back to the van der Waals regions. The LYP functional was derived to reproduce the true electron density of the He atom [35, 40], and therefore covers both local and non-local electron correlation effects, where the latter counterbalance partially the dependence of the local correlation effects on high densities.

(iv) *GGA correlation functionals (e.g. PW91; figure 4(g, h)) also shift density from the van der Waals region into the outer valence region and the non-bonding regions between the atoms. However, there are large depletion areas in the inner valence and the bond regions (between heavy atoms) not found for the LDA correlation densities.* Gradient corrected correlation functionals have a less

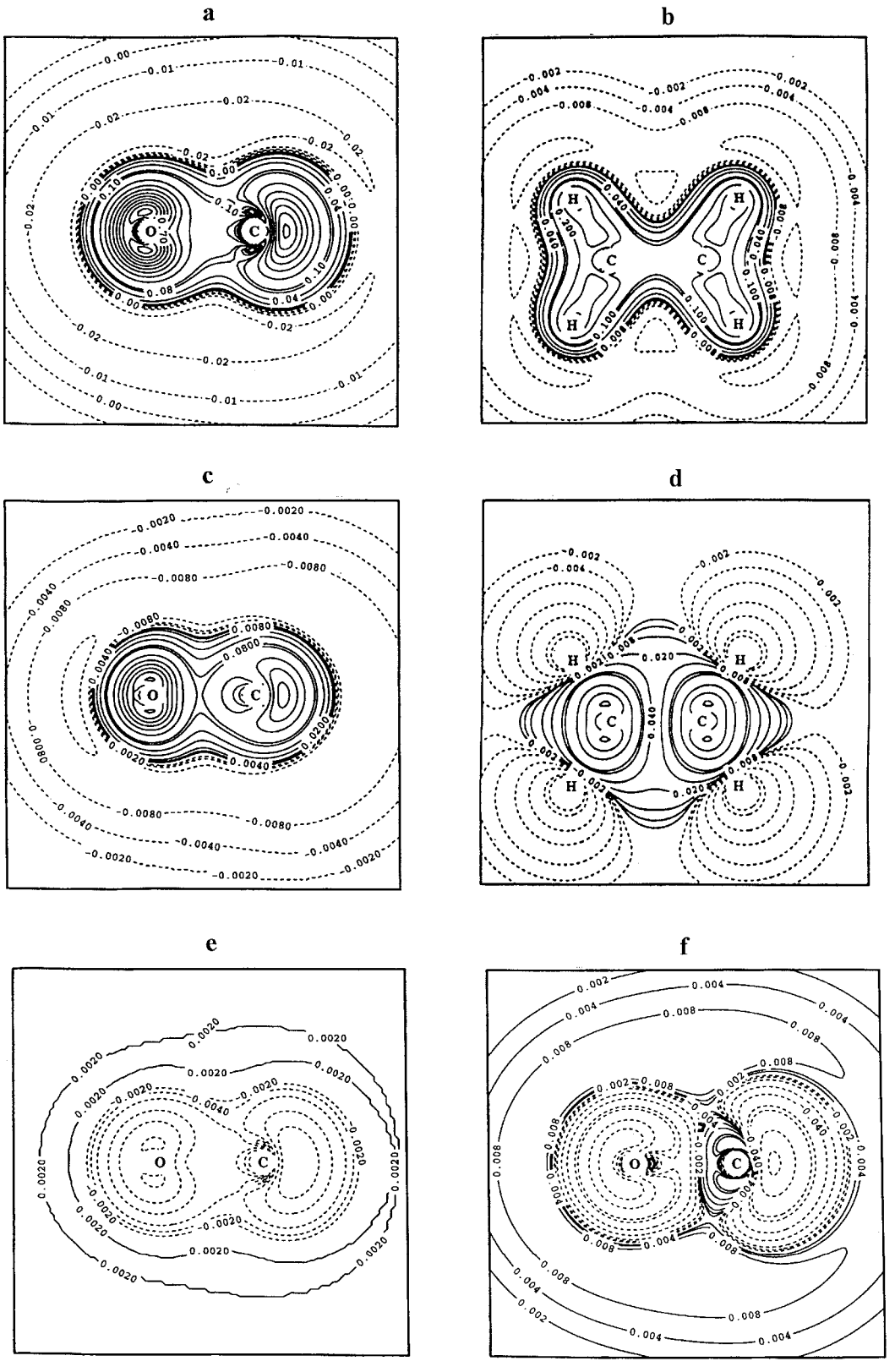
a
b
c
d
e
f

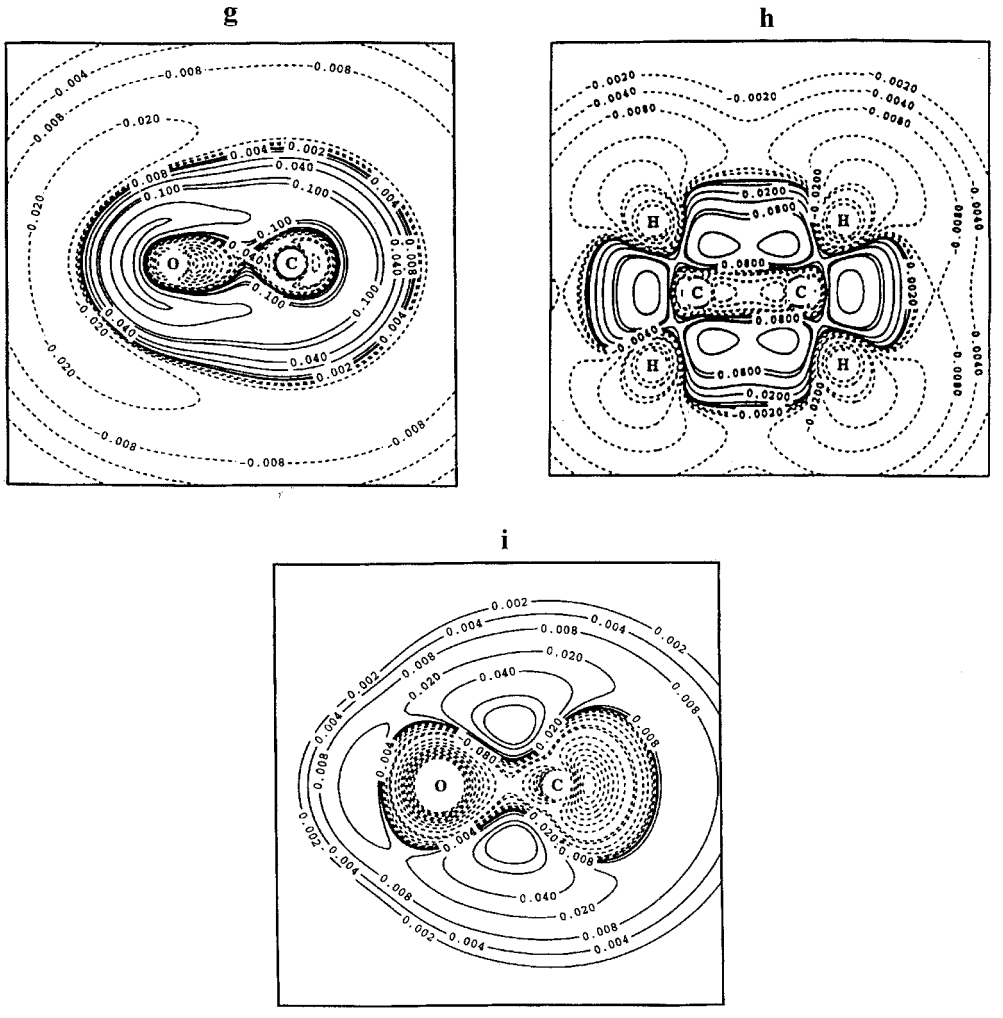

Figure 4. Contour line diagram of the electron density distribution $\rho(\mathbf{r})$ of CO and ethene calculated for various correlation functionals with the 6-311 + G(3df) (CO) and the cc-pVTZ basis (ethene). Solid (dashed) contour lines are in regions of positive (negative) difference densities. The positions of the nuclei are indicated. The contour line levels have to be multiplied by the scaling factor 0.01 and are given in $e\,a_0^{-3}$. (*a*) CO, VWN5 functional; (*b*) ethene, VWN5 functional; (*c*) CO, LYP functional; (*d*) ethene, LYP functional; (*e*) CO, VWN5-VWN; (*f*) CO, LYP-VWN5; (*g*) CO, PW91 functional; (*h*) ethene, PW91 functional; and (*i*) CO, P86-PL.

attractive correlation potential, in particular in regions where the reduced gradient of the density, $\nabla\rho/\rho^{4/3}$, is small, as for example in the bond regions between the heavy atoms ($\nabla\rho$ is small and ρ relatively large). However, in the non-bonding regions between the atoms (tail regions) the reduced gradient is relatively large ($\nabla\rho$ is large and ρ relatively small), thus leading to a larger correlation density than obtained from an LDA correlation functional (figure 4(*i*), which shows the difference density $\rho(\mathrm{P86}) - \rho(\mathrm{PL}) = \rho(\mathrm{GGA}) - \rho(\mathrm{LDA})$). At the nuclei, the GGA contribution to the correlation potential becomes singular for the same reasons as the GGA contribution to the exchange potential. The singularity for the correlation potential is repulsive and partly compensates for the attractive singularity of the exchange potential. The main impact of the gradient corrections to the correlation potential is thus that charge is transferred back from the core and bond regions into the outer valence regions of the molecule, which slightly reduces the effects of the LDA correla-tion potential, as is shown in figure 4(*f*) for PW91 functional.

Clearly, the DFT correlation functional corrects deficiencies in the exchange functionals where corrections are much smaller than the changes caused by the latter. This simply reflects the fact that DFT exchange correlation is much larger than DFT Coulomb correlation. The influence of the correlation potential on the density distribution resembles that of higher order

dynamic electron correlation effects observed for correlation-corrected WFT methods [44–47]. The addition of pair-, three-, and four-electron correlation effects at the MP*n* level of theory leads in general to an expansion of the orbitals and to a more diffuse charge distribution, which causes typical changes in calculated molecular properties, as for example a lengthening of the bond [44]. Higher order correlation effects are dominated by complicated coupling mechanisms between lower order correlation effects while diagonal *N*-electron correlation effects for $N > 4$ play a small role. Hence, the inclusion of higher order correlation effects always means a stronger emphasis of coupling effects that in general reduces trends caused by lower order correlation effects. The density becomes more contracted, bond lengths are reduced, but effective electronegativities, partial charges, and bond polarities are increased. This is the reason why (because of the presence of infinite order effects) perfectly *coupled* many-body methods such as CCSD or CCSDT lead to less extended orbitals and less diffuse charge distributions than MP*n* methods containing the same *N*-electron correlation effects (but not the complete set of possible coupling effects). *The DFT correlation functional seems to mimic these higher order correlation effects while the lower order correlation effects seem to be simulated by the DFT exchange functional.*

5.3. *The self-interaction error and electron correlation effects*

An electron interacts with other electrons in an atom or molecule via the Coulomb potential, but it does not interact with itself. This is clearly manifested in the many-particle Hamiltonian, in which the electron–electron interaction term excludes self-interaction. Consequently, WFT energies such as the HF energy do not include any self-interaction energies because the self-interaction part of the Coulomb energy exactly cancels out that of the exchange energy. Fermi and Amaldi [118], analysing the Thomas–Fermi density model, were the first to recognize that this is no longer true in the case of DFT. Their observation is valid for any modern form of DFT using approximate density functionals, as has been discussed widely [7, 18, 20, 24, 32]. Methods for curing this error have been suggested [75–85] but turn out to complicate DFT in an undesirable way.

If one considers the spin-density ρ_i^η of an electron with spin $\eta\,(\eta = \alpha, \beta)$ occupying the *i*th spin orbital, then the necessary requirement for a correct cancellation of self-interaction will be given by (see, e.g. [7])

$$E_J[\rho_i^\eta] + E_{XC}[\rho_i^\eta, 0] = 0 \tag{5}$$

or, explicitly,

$$E_J[\rho_i^\eta] + E_X[\rho_i^\eta, 0] = 0, \tag{6}$$

$$E_C[\rho_i^\eta, 0] = 0, \tag{7}$$

for a given value of spin η. E_J is the Coulomb repulsion energy of non-interacting electrons (table 4). Equation (6) is identical to the condition fulfilled by HF theory, while equation (7) simply states that Coulomb correlation has to vanish for one-electron systems. Conditions (6) and (7) are not fulfilled for most approximate DFT functionals, i.e. both exchange and correlation functionals may suffer from a self-interaction error (SIE), which is obtained by summing the terms on the left side of equation (5) over all occupied orbitals.

In this work, we use the self-interaction correction (SIC) suggested by Perdew and Zunger [75] to discuss the consequences of the SIE for the description of electron correlation effects by DFT. This SIC procedure can be carried out in a single-step SIC-DFT procedure [75, 76] to estimate the magnitude of corrections or within a self-consistent SIC-DFT (SCF-SIC-DFT) procedure [77–80, 119] to calculate molecular properties such as density distributions. The Perdew–Zunger method has the advantage of retaining the size-extensivity of DFT [69]. On the other hand, it leads to an orbital-dependent functional, and results are no longer invariant with regard to rotations among the occupied orbitals. Another problem inherent in the Perdew–Zunger approach is that the lowest SCF energy can be obtained only by minimizing the energy for localized orbitals [78]. Localization of the orbitals of a σ–π system leads, however, to bent bonds, so that SCF-SIC-DFT densities are no longer directly comparable with DFT or WFT densities. One can circumvent this problem by localizing σ and π orbitals separately and rotating the localized orbitals only within a given set. In this way, only a part of the SIE is recovered (about 80% for ethene [119]). However, a comparison of SCF-SIC-DFT and DFT densities becomes meaningful, in particular, when this is done in a qualitative rather than quantitative way. In any case, SIC-DFT and SCF-SIC-DFT lead to a considerable increase in computational cost, which hampers its application to larger molecules on a routine basis [119].

In table 5 some SIE energies obtained with the single-step SIC-DFT and the SCF-SIC-DFT procedures are listed for some commonly used functionals. LDA functionals lead to large, positive X-SIE and a considerably smaller, negative C-SIE (SIEs of those correlation functionals that do not fulfil equation (7)). GGA functionals such as BLYP or PW91PW91 reduce the SIE considerably, which in the exchange part can be either positive or negative (table 5) and which is always negative in the correlation part. By construction, the LYP correlation functional does not suffer from an SIE [35]. Since the X-SIE and C-SIE cancel each other partially for

Table 5. Self-interaction errors for various molecules calculated with various XC functionals.[a]

Molecule	XC functional	X-SIE	C-SIE	Total SIE	Δ (X-SIE)	Δ (C-SIE)	Δ (total SIE)	SCF-X-SIE	SCF-C-SIE	SCF total SIE
H_2	SVWN5	0.089 49	−0.045 29	0.044 20	0.002 73	−0.000 46	0.002 27	0.092 20	−0.045 75	0.046 45
	BLYP	0.000 23	0	0.000 23	0.002 88	0	0.002 88	0.003 11	0	0.003 11
	PW91PW91	0.007 21	−0.014 29	−0.007 07	0.002 88	−0.000 43	0.002 45	0.010 09	−0.014 72	−0.004 63
$H_2C{=}CH_2$	SVWN5	1.484 11	−0.445 16	1.038 95	0.033 95	−0.003 23	0.030 72	1.518 06	−0.448 39	1.069 67
	BLYP	−0.085 31	0	−0.085 31	0.038 29	0	0.038 29	−0.047 02	0	−0.047 02
	PW91PW91	0.095 07	−0.130 56	−0.035 49	0.031 04	−0.003 10	0.027 94	0.126 11	−0.133 66	−0.007 55
CO	SVWN5	1.589 91	−0.423 48	1.166 42	0.035 12	−0.002 66	0.034 47	1.625 03	−0.426 14	1.198 89
	BLYP	−0.210 65	0	−0.210 65	0.040 07	0	0.040 07	−0.170 58	0	−0.170 58
	PW91PW91	0.005 16	−0.109 43	−0.104 27	0.031 96	−0.002 26	0.029 70	0.037 12	−0.111 69	−0.074 57

[a] All energies are given in E_h. All calculations with the cc-pVTZ basis set [71] at experimental geometries. See [119]. X-SIE denotes the exchange self-interaction error, C-SIE the correction self-interaction error and total SIE the sum of C-SIE and X-SIE as calculated in a single-step SIC-DFT procedure. Δ (X-SIE), Δ (C-SIE), etc. give the change in the corresponding SIE energies during the SCF-SIC-DFT calculations, and SCF-X-SIE, SCF-C-SIE, etc. denote the final SIE energies obtained in the SCF-SIC-DFT algorithm. All occupied orbitals were localized in the SIC calculations.

GGA functionals, the BLYP functional, which does not benefit from this cancellation, leads to a larger total SIE than, e.g. the PW91PW91 functional (table 5). It is noteworthy that in the latter case the absolute magnitude of the C-SIE is actually larger than that of the X-SIE.

A single-step SIC-DFT procedure recovers a large part of the SIE, but the additional corrections gained in the SCF procedure are still substantial, in particular for the X functional (table 5). The general result of SIC-DFT relative to standard DFT is (a) a decrease in the exchange energy (increase in its absolute value) to fulfil equation (6) (for LDA and GGA functionals with the exception of BLYP) and (b) a reduction of correlation interactions (the correlation energy becomes more positive) to fulfil equation (7).

In figure 5 the difference density distribution $\Delta\rho(\text{SIC}) = \rho(\text{SIC-BLYP}) - \rho(\text{BLYP})$, which reflects the influence of the SIC on the electron density distribution, is shown for (*a*) ethene, (*c*) CO, and (*e*) N_2. The changes in the density distribution caused by SIC closely resemble the changes introduced by replacing the BLYP density by a B3LYP density (figure 5(*b*, *d*, *f*)) although changes are smaller in the latter cases. There is always a depletion of negative charge in the valence regions of the atoms and an increase in density in the (σ and π) bond regions and parts of the non-bonded regions. For CO, negative charge is transferred from the π space of the C atom into the bond region and the outer π space of the O atom. Both for CO and N_2 the electron density increases in the lone pair regions, but decreases in the van der Waals regions following the lone pair regions. Similar changes are found when comparing the corresponding difference densities of other SIC-XC/XC or hybrid-XC/XC functionals where greater changes occur when introducing SIC rather than a hybrid functional. In all cases, the changes observed suggest a significant reduction of left–right and other pair correlation effects. Both SIC-DFT and DFT with hybrid functionals seem to correct an exaggeration of correlation effects mimicked by the exchange functionals.

5.3.1. *SIE of exchange functionals*

The trends indicated by the difference density plots of figure 5 can be explained by analysing the impact of exchange, Coulomb self-interactions, and self-exchange on the electron density distribution of a molecule. Exchange will always be small in those regions where (a) there is only little density as in the van der Waals regions, (b) only one electron can be expected as in regions around the H atoms (particularly if bonded to a more electronegative atom), and (c) electron pairing as in the region of a single bond reduces the chance of finding a second electron of the same spin. In those regions where exchange is small Coulomb repulsion will be large, which leads to a reduction in the electron density.

Exchange is large in the valence region of the heavy atoms (C, N, O, etc.) and in the non-bonded regions between the atoms. For example, in the valence region of the C atom there can be up to 4 valence electrons of the same spin, thus leading to large exchange interactions between the electrons. In the non-bonded regions between the atoms there is no energy principle that requires $\alpha\beta$ spin coupling, but superposition of the density tails of the atoms makes it possible that electrons of the same spin are present in these regions. Relatively large exchange guarantees that Coulomb repulsion is low, and therefore the density increases in regions of large exchange (relative to a density that feels just the electrostatic Coulomb repulsion between the electrons). Hence, exchange interactions between the electrons lead to an increase in the electron density in the valence regions of the heavy atoms and in the non-bonded regions between the atoms, while there is a decrease of the density in the H atom, and the van der Waals regions (figure 6(*a*)).

The Coulomb SIE of the electrons removes density out of the space with large amplitudes of the orbitals ψ_i into the regions with small amplitudes of orbitals ψ_i, i.e. for molecules from the bond regions into the non-bonded and van der Waals regions. HF self-exchange has just the opposite effect, i.e. it transfers density from non-bonded and van der Waals regions into the bond regions (figure 6(*b*)). At the DFT level of theory, Coulomb self-interaction is larger than exchange self-interaction in the bond region if approximate functionals suffering from an SIE are used. Accordingly, density is removed artificially out of the bond region and transferred to the valence region, where exchange interactions are large, thus leading to lower Coulomb repulsion. This is the essence of the X-SIE, which simulates long range left–right correlation and other pair correlation effects. It is reasonable to say that the X-SIE mimics non-dynamic correlation effects, which in WFT are introduced by the mixing in of low lying, quasi-degenerate CSFs. Hence, the correlation effects simulated by a GGA functional such as B exchange are even stronger than the exaggerated pair correlation effects obtained at the MP2 level: the latter describe short range (dynamic) pair correlation effects while the former simulate long range (non-dynamic) correlation effects [99].

Since exact exchange does not cover any dynamic or non-dynamic correlation effects, it is necessary to clarify why DFT exchange introduces long range correlation effects. This can be done by comparing HF and DFT exchange holes. The HF exchange hole is localized for

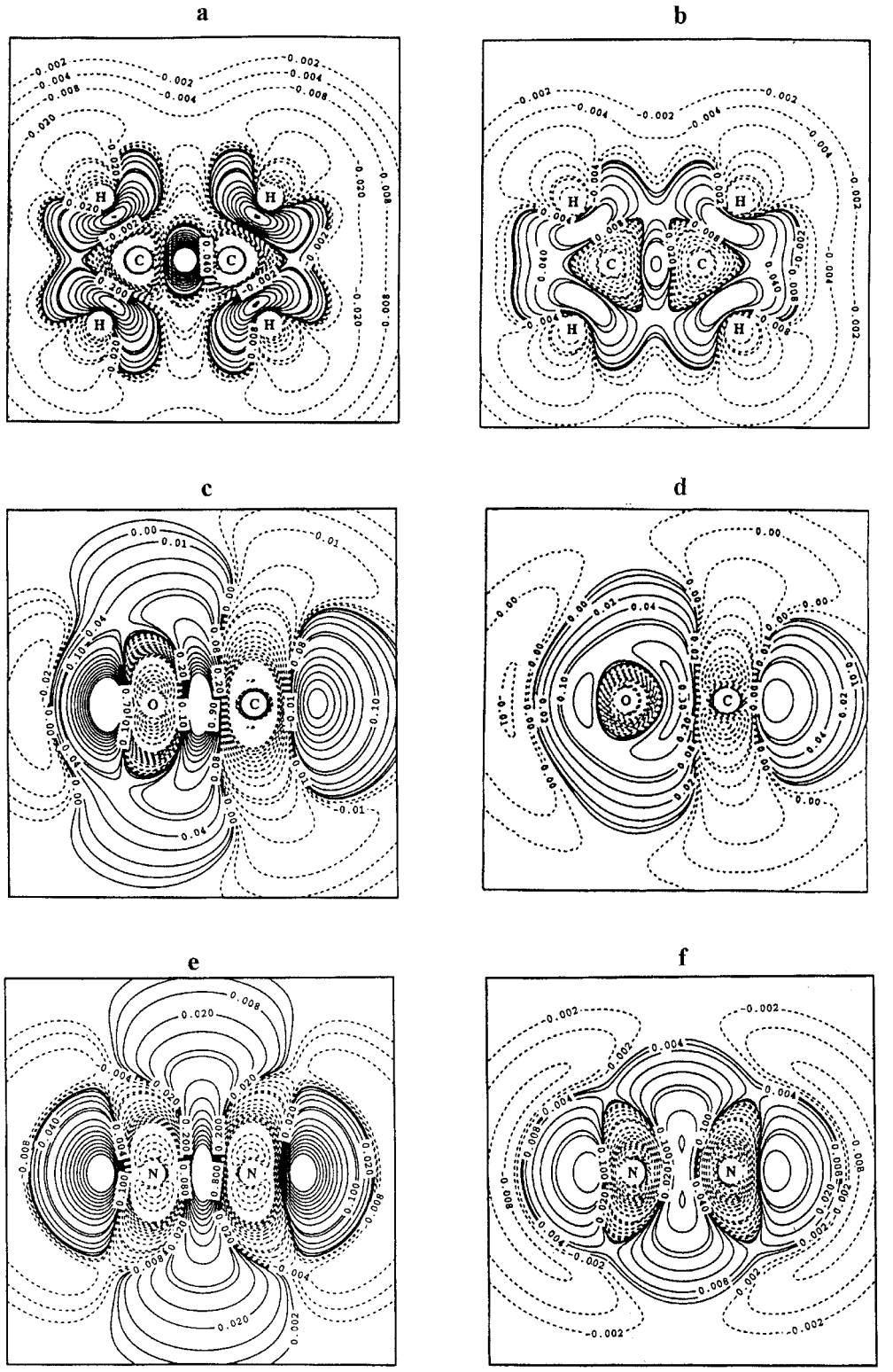

Figure 5. Contour line diagram of the electron density distribution $\Delta\rho(\mathbf{r}) = \rho(\text{method I}) - \rho(\text{method II})$ of ethene, N_2, and CO calculated with the cc-pVTZ basis (ethene, N_2) and the 6-311 + G(3df) basis (CO). Solid (dashed) contour lines are in regions of positive (negative) difference densities. The positions of the C and the O nuclei are indicated. The contour line levels have to be multiplied by the scaling factor 0.01 and are given in $e\,a_0^{-3}$. (*a*) Ethene, SIC-BLYP; (*b*) ethene, B3LYP-BLYP; (*c*) CO, SIC-BLYP-BLYP; (*d*) CO, B3LYP-BLYP; (*e*) N_2, SIC-BLYP-BLYP; and (*f*) N_2, B3LYP-BLYP.

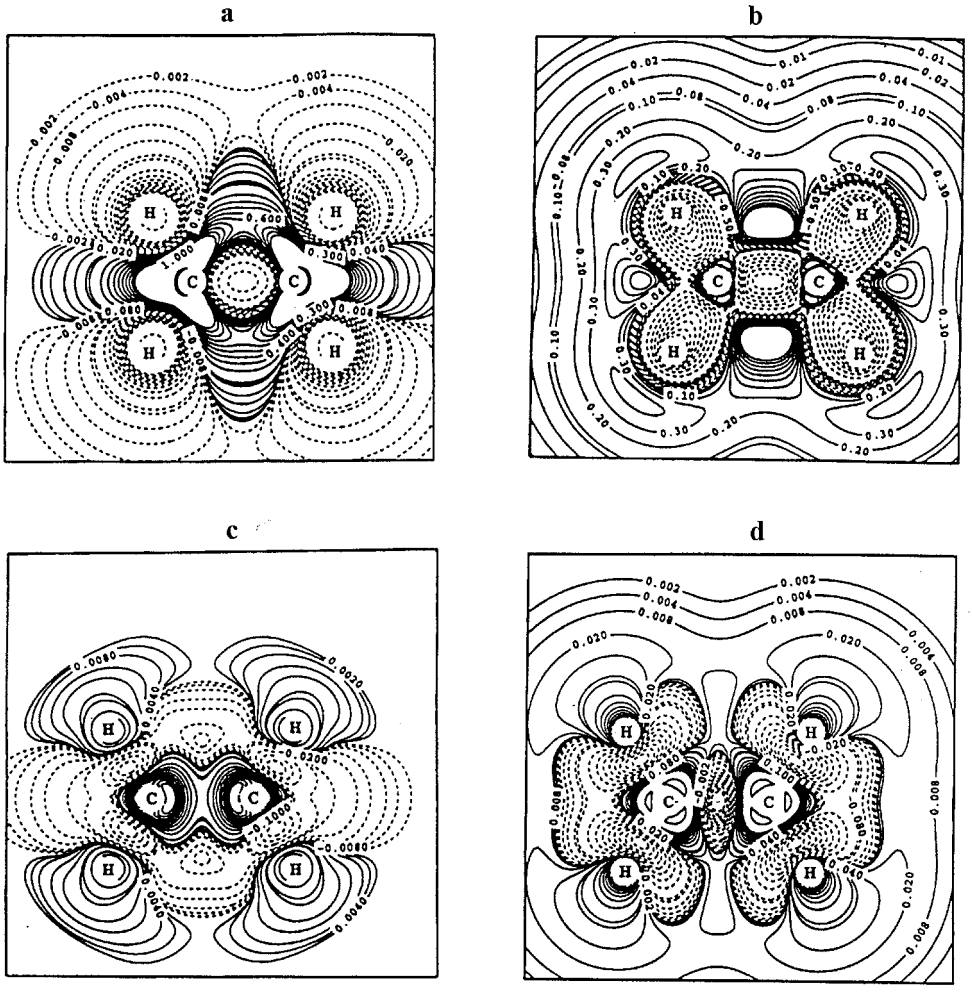

Figure 6. Contour line diagram of the electron density distribution $\Delta\rho(\mathbf{r}) = \rho(\text{method I}) - \rho(\text{method II})$ of ethene calculated with the cc-pVTZ basis at the experimental geometry. Solid (dashed) contour lines are in regions of positive (negative) difference densities. Reference plane is the plane containing the atoms. The positions of the atoms are indicated. The contour line levels have to be multiplied by the scaling factor 0.01 and are given in $e\,a_0^{-3}$. (*a*) HF exchange; (*b*) HF, Coulomb self-repulsion; (*c*) SIC-B-HF exchange; and (*d*) B-only-HF exchange.

an atom but tends to be delocalized for molecules, as was first pointed out by Slater [28, 120] and later emphasized in particular by Becke [121]. This can be demonstrated for the H_2 molecule, for which exchange is just the one-electron cancellation term for Coulomb self-interaction, and the exchange hole just the negative of the $1\sigma_g$ orbital density. Hence, the X hole is delocalized in H_2 over the whole bond region and independent of the position of the reference electron. The electron density related to the exchange hole is large close to the nuclei (deep X hole) and smaller in the bond region (flat X hole). If the reference electron moves out into the van der Waals region, the X hole will not follow, but will stay behind in regions of larger densities, which simply means that exchange interactions are small in the van der Waals region and, accordingly, the electron density is reduced due to a dominance of Coulomb interactions.

By construction the DFT X hole is localized and depends on the position of the reference electron. If the reference electron with spin η is close to the left nucleus, negative charge will be removed from this nucleus and piled up next to the right nucleus. This is typical of long range (non-dynamic) pair correlation effects not included into exact exchange. Since the properties of the DFT exchange hole are influenced by both the effects of normal exchange and self-exchange, the conclusion has to be drawn that the delocalized Fermi hole of correct exchange changes its nature under the impact of the SIE, which must be responsible for the long range left–right correlation effects. The SIE-part of the X hole must be strongly localized and by super-

position with a delocalized SIC-X hole must yield a localized X hole. This is in line with the density studies, and leads to the somewhat surprising conclusion that approximate DFT exchange, no matter whether presented by a LDA or a GGA functional, always covers non-dynamic (long range) pair correlation effects that actually exaggerate the separation of negative charge relative to WFT methods, which cover just dynamic correlation effects.

These consideration can be related to the difference densities shown in figure 6(*c*) (ρ(SIC-B) − ρ(HF exchange)) and (*d*) (ρ(B-only) − ρ(HF)). The SIC-B density is larger in the atomic regions. In the CC unit, the SIC-B density resembles that to be expected from a delocalized rather than localized exchange hole. There is high density at the positions of the C atoms (deep X hole) and lower density in the bond region (flat X hole). Hence, the peculiar density pattern resulting from the B-only calculation and reflected in the difference density of figure 6(*d*) clearly is a result of the X-SIE, which decreases the density in the CC bond region by long range left–right and in–out pair correlation effects.

5.3.2. *SIE of correlation functionals*

The SIE of the LDA correlation functional VWN5 has it strongest influence in the bond regions of a molecule (figure 7(*a*)) where it leads to a substantial increase in electron density. This can be explained by considering that the C functionals describe short range correlation, i.e. the localized Coulomb hole is surrounded at close range by a shell of somewhat increased density. This makes it possible that in the bond regions more density

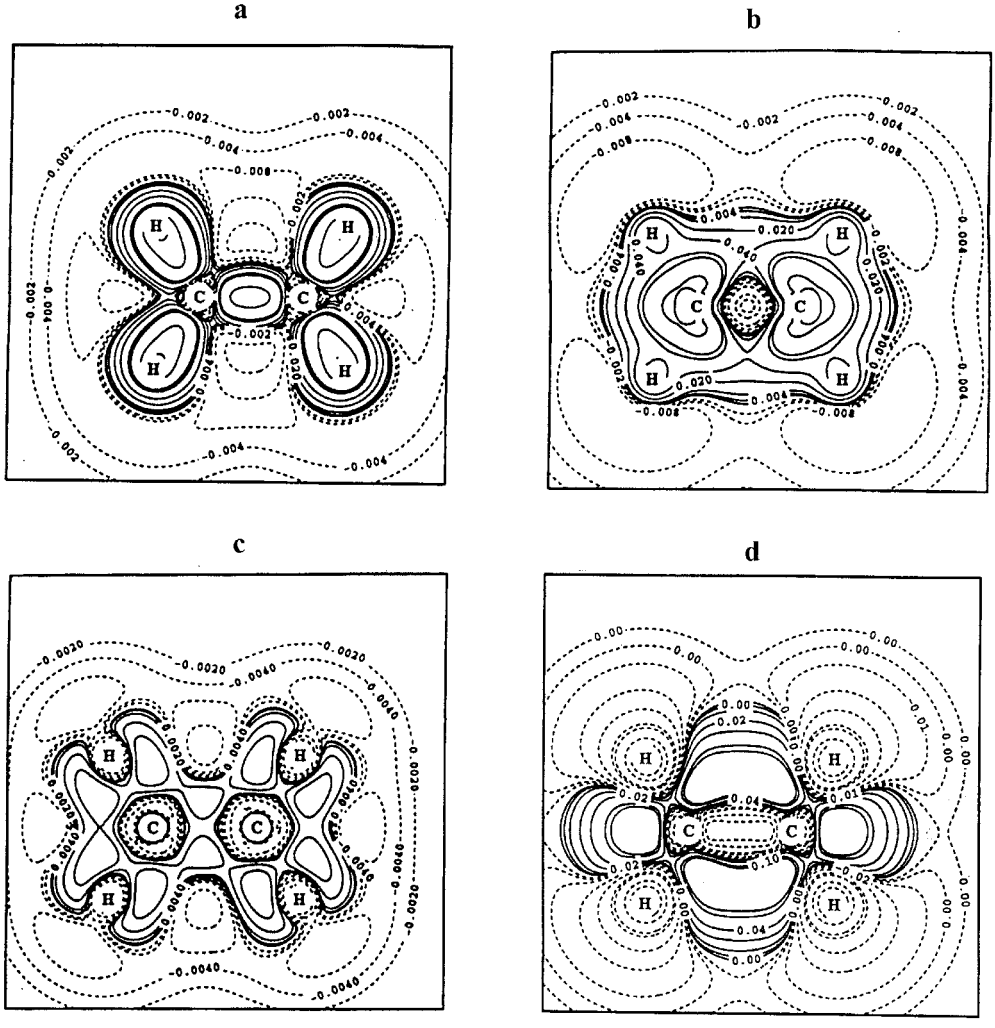

Figure 7. Contour line diagram of the electron density distribution of ethene calculated with the cc-pVTZ basis at the experimental geometry for various correlation functionals. Solid (dashed) contour lines are in regions of positive (negative) difference densities. Reference plane is the plane containing the atoms. The positions of the atoms are indicated. The contour line levels have to be multiplied by the scaling factor 0.01 and are given in $e\,a_0^{-3}$. (*a*) VWN5-SIE functional; (*b*) PW91-SIE functional; (*c*) SIC-VWN5 functional; and (*d*) SIC-PW91 functional.

is accumulated than allowed by the classical Coulomb repulsion interactions. LDA functionals such as VWN5 represent an attractive local potential that depends on the magnitude of the electron density. It is rather strong in the atomic, bond and (inner) non-bonded regions (superposition of atomic densities), but relatively weak in the van der Waals regions (compare figure 4(*a*)). The SIE depends on the same attractive potential and, accordingly, it is also large for large densities. In addition, it depends on the degree of electron localization in core, bond and lone pair orbitals so that, in contrast to the C functional, the SIE increases the density specifically around the centroids of the localized orbitals (figure 7(*a*)).

The C-SIE leads to a significant increase in bond density and compensates in this way somewhat for the effects of the X-SIE, which decreases the bond density. The correct SIC-VWN5 functional (figure 7(*b*)) decreases the density in the bond region between the heavy atoms and in the van der Waals regions, but increases it in the atomic and the non-bonded regions between the atoms. For GGA correlation functionals the corresponding changes are more complex, due to the influence of the reduced gradient. For example, for the PW91 C-functional the density of ethene is accumulated in the non-bonded regions but depleted in the CC bond region, at the H atoms, and in the van der Waals region (figure 4(*g*, *h*)). The density changes caused by the PW91-SIE partially enhance and partially oppose these effects (figure 7(*c*)), but changes are rather small (one third of the changes caused by VWN5-SIE), so that the overall pattern of the correlation density caused by SIC-PW91 is similar to that caused by PW91 (compare figures 4(*h*) and 7(*d*)).

Clearly, the SIE is dominated by the exchange part for commonly used functionals. The latter simulates correlation effects not covered by single determinant WFT methods, which can mean an advantage, for example if a stretched bond has to be described. However, in cases where a delocalized exchange hole plays an important role in the electronic structure of a molecule (1- and 3-electron bonds [84, 122–124], transition states involving an odd number of electrons [85, 93, 125], etc.), the SIE leads to nonsensical results, as has been documented in the literature. Then the SIC-DFT approach, although expensive, provides the only reasonable answer to the problem [126]. Also, from a general point of view, exclusion of the SIE, which actually leads to a more correct DFT, should lead to an improvement because for a description of the normal closed shell molecule there is no need to include long range correlation effects. We shall consider this point in more detail when discussing the changes in the density caused by hybrid functionals.

5.4. *Changes in electron correlation caused by hybrid functionals*

The similarity in the changes in molecular density obtained by SIC-DFT and hybrid functional calculations (figure 5) suggests that both correct (fully or partially) for the SIE. Hybrid functionals incorporate 20–25% exact exchange (table 3) and support, by this, a more delocalized X hole that compensates for some of the long range pair correlation effects invoked by the SIE-part of exchange [36, 121]. Of course, the LDA and GGA parts of the exchange covered by a hybrid functional (table 3) are not fully SIE-corrected so that the SIE of standard X functionals and the associated long range correlation effects are only partially reduced in an empirical way. This is reflected in the difference density distributions ρ(B3LYP) − ρ(SIC-BLYP) shown in figure 8(*a*, *b*): B3LYP densities still indicate a considerable amount of long range left–right and other pair correlation effects. The changes in density caused by the hybrid functional seem to be just a fraction of those caused by SIC-DFT, so that the pattern of density changes given by ρ(B3LYP) − ρ(BLYP) is just the mirror image of that found for the difference ρ(SIC-BLYP) − ρ(BLYP) (figure 5(*a*, *b*)).

When comparing B3LYP densities with WFT densities, similarities in the density distribution generated by a CCSD(T) calculation can be found (see, e.g. figures 5(*c*, *d*)). However, there are typical differences in the atomic, bond, and van der Waals regions where hybrid functionals predict a larger density irrespective of the WFT method used in the comparison. This reminds one of the typical changes found when comparing a SIC-B density with a HF exchange density (figure 6(*c*)). We may conclude that the SIE correction introduced into the hybrid functional by an admixture of exact exchange dominates the changes in the density in the atom and heavy atom bond regions where local and non-local correlation added by a mixing of LDA and GGA functionals (table 3) enhance these effects (compare with figure 4(*a–d*)).

We come to the (perhaps not unexpected) conclusion that commonly used XC functionals cover both non-dynamic (larger part) and dynamic (smaller part) correlation effects, but still fail to fully include important exchange delocalization effects. The hybrid functionals reduce the exaggeration of non-dynamic electron correlation by improving delocalization effects in the exchange. This can also be viewed as giving dynamic electron correlation a somewhat stronger impact relative to non-dynamic correlation. Since the hybrid functionals are fitted against experimental data, both the non-dynamic and dynamic electron correlation effects are covered in a more realistic and effective manner.

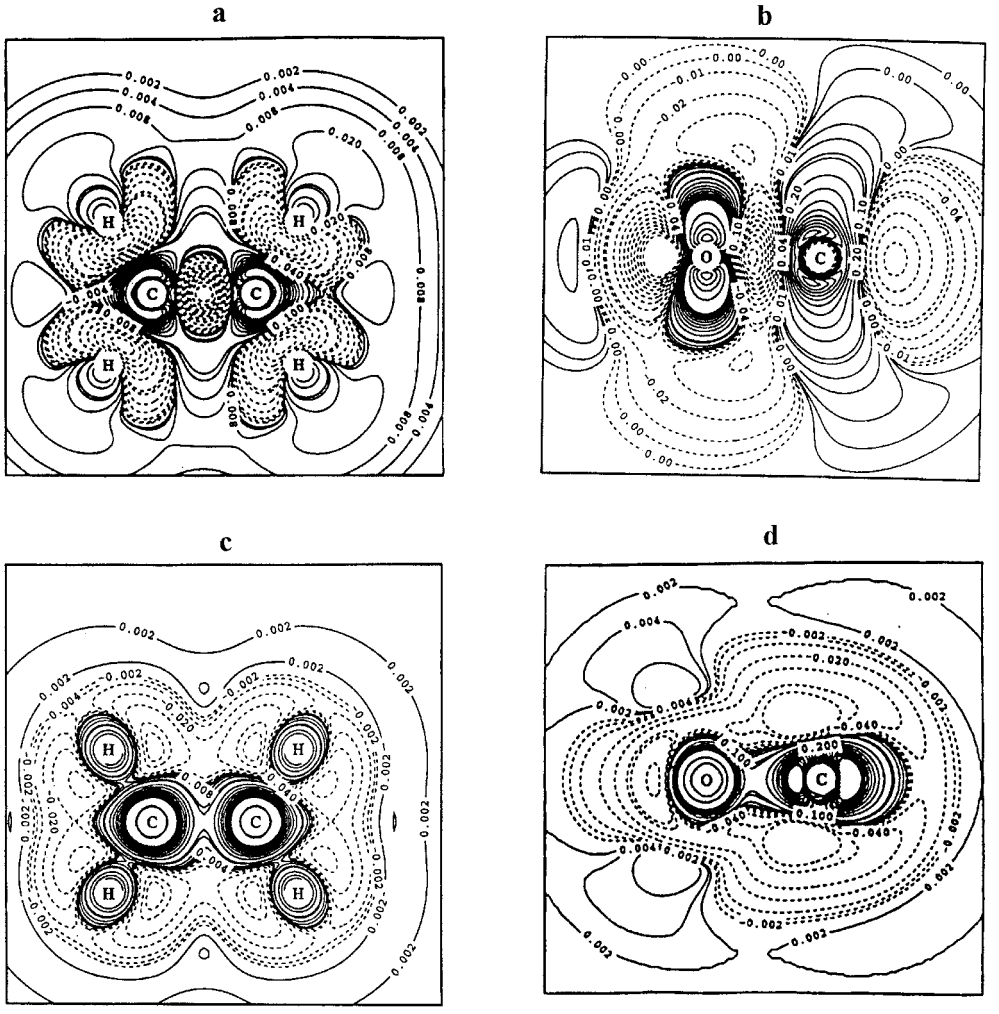

Figure 8. Contour line diagram of the difference electron density distribution $\Delta\rho(\mathbf{r}) = \rho(\text{method I}) - \rho(\text{method II})$ of ethene and CO calculated with the cc-pVTZ (ethene) and the 6-311+G(3df) basis at the experimental geometry. Solid (dashed) contour lines are in regions of positive (negative) difference densities. The positions of the nuclei are indicated. The contour line levels have to be multiplied by the scaling factor 0.01 and are given in $e\,a_0^{-3}$. (*a*) Ethene, B3LYP – SIC-BLYP; (*b*) CO, B3LYP – SIC-BLYP; (*c*) ethene, B3LYP-CCSD(T); and (*d*) CO, B3LYP-CCSD(T).

WFT methods that introduce higher order correlation effects (e.g. CCSD(T)) cover, in addition to dynamic, also a certain amount of non-dynamic electron correlation. In this way DFT with hybrid functionals simulates similar correlation effects to those of WFT methods. The changes in density due to the use of hybrid functionals also are reminiscent of the inclusion of higher order correlation effects that lead to coupling between *N*-electron (diagonal) correlation effects and contract the electron density towards the bond regions (figure 5(*b*, *d*)) [52]. The inclusion of more coupling effects (more ionic terms) by the hybrid functionals significantly improves calculated molecular properties, which often reach CCSD(T) quality.

Despite the fact that hybrid functionals suffer from a residual SIE, which, e.g. is reflected in the difference density plots of figure 8(*a*, *b*), their results are mostly better than those of SIC-DFT calculations. Correcting hybrid functionals for their residual SIE will not necessarily yield any improvement in molecular properties. Apart from special situations discussed above, SIC-DFT does not lead to any improvement in calculated molecular properties because the XC functionals used in such a calculation were optimized in the presence rather than the absence of the SIE. Several investigations show that SIC-DFT leads, e.g. to excessively short bond lengths and exaggerated stretching frequencies [80, 126]. However, orbital energies, excitation energies, and other properties can be considerably improved by SIC-DFT [77–79]. This indicates that, despite the empirical calibration of the hybrid functionals and the physically more correct SIC-DFT treatment of electron

interactions, there is room for further improvement of XC functionals. X Functionals based on delocalization indicators have been developed to replace hybrid functionals and to account for the SIE in a more basic way [37, 38, 127]. This will also lead to a more balanced coverage of correlation effects, in particular with regard to non-dynamic electron correlation.

6. Non-dynamic electron correlation effects and standard DFT

The KS formalism was derived originally without making any assumptions about the electronic character of the atoms and molecules to be described. If the correct XC functional were known, then simple closed shell systems, open shell systems, and even systems with distinct multireference character would be described correctly, because the XC functional would cover all dynamic and non-dynamic electron correlation effects. Problems results from the fact that the correct XC functional is not known, and therefore approximate XC functionals have to be used. The latter were developed to cover dynamic electron correlation effects using the HEG as an appropriate starting point. The discussion in the last section shows that approximate exchange functionals unintentionally mimic non-dynamic electron correlation although in an unspecified manner, which does not necessarily guarantee an improved description for a specific multireference system. Hence, single-determinant KS theory applied with the available functionals cannot be expected to perform satisfactorily when electronic systems with distinct non-dynamic electron correlation effects have to be calculated.

Nevertheless, KS theory is frequently applied for notorious multi-reference problems, mostly for the purpose of testing the limits of such an approach. A frequently posed question in current DFT research is how much multireference character can be adequately covered by single-determinant KS theory for a given functional and a given basis set. Answers to this question are often sought in a trial and error procedure using suitable reference values from experiment or WFT. However, this is a tedious approach, and therefore we shall consider here just some basic aspects of the problem. For this purpose, we distinguish between different types of multireference system and their description by KS DFT, following arguments first given by Gräfenstein and Cremer [58].

6.1. *Classification of electronic systems on the basis of standard DFT*

If one replaces the effective potential in the reference state characterized by non-interacting electrons adiabatically by the real electron–electron interaction with the help of the perturbation parameter λ, dynamic electron correlation will continuously increase from zero to its full magnitude, and a continuum of intermediate states will lead from the reference to the real state of the many-electron system in question (adiabatic connection scheme (ACS) [128, 129]). In WFT, the increase in dynamic electron correlation would be reflected by the fact that the weight of the (leading) ground state determinant Φ_0 decreases while those of the excited-state determinants Φ_1, Φ_2, etc., increase. In figure 9, this is schematically shown by giving the weight factor w of determinants Φ_i as a function of the ACS parameter λ. Also shown is the corresponding change in the KS energy E_{KS} and the exact energy E(exact), where it is assumed that the latter is always lower when expanding KS orbitals in an infinite basis set for a given value of λ. The difference between $E(\lambda = 0)$ and $E(\lambda = 1)$ is the dynamic correlation energy E_{C}. Figure 9(*a*) describes the situation for a typical closed shell system, the ground state wavefunction of which can be described by one CSF Ψ_0 (single-reference system), which is dominated by determinant Φ_0. Electronic systems of this type (*type 0 systems*) are described satisfactorily by standard DFT utilizing the available XC functionals, because the two basic requirements of KS-DFT are fulfilled [6, 7]. (1) The reference state is a single-determinant state. This assumption is essential for the calculation of E_{X}. In WFT, this corresponds to requiring that the ground state wavefunction is given by one CSF Ψ_0, which is well approximated by the Slater determinant Φ_0, i.e. the wavefunction reduces to a single-configurational, single-determinantal form. (2) The correlation hole in the real system is described reasonably well by the model correlation hole from the homogeneous or weakly inhomogeneous electron gas. This assumption is essential for the calculation of E_{C}. In WFT, this corresponds to requiring that for all $\lambda > 0$ the wavefunction is dominated by Φ_0, although excited determinants Φ_1, Φ_2, etc., describing dynamic electron correlation effects, appear in the wavefunction. Their weights w increase smoothly as λ increases, but their values remain small compared with the weight of Φ_0.

Type-I systems are also single-reference systems represented by one CSF, but this CSF must be constructed from two or more Slater determinants Φ_0, Φ_0', etc., which contribute with the same weight w each, but differ with regard to the spin orientation of the electrons in the open shell orbitals. The situation of a type-I system is indicated in figure 9(*b*) for a two-determinantal problem where the CSF Ψ_0 of the ground state is constructed from determinants Φ_0 and Φ_0' with weight factors $w = w'$. For increasing λ, dynamic electron correlation is covered in WFT by adding excited state determinants Φ_1, Φ_2, etc., thus reducing the weights of

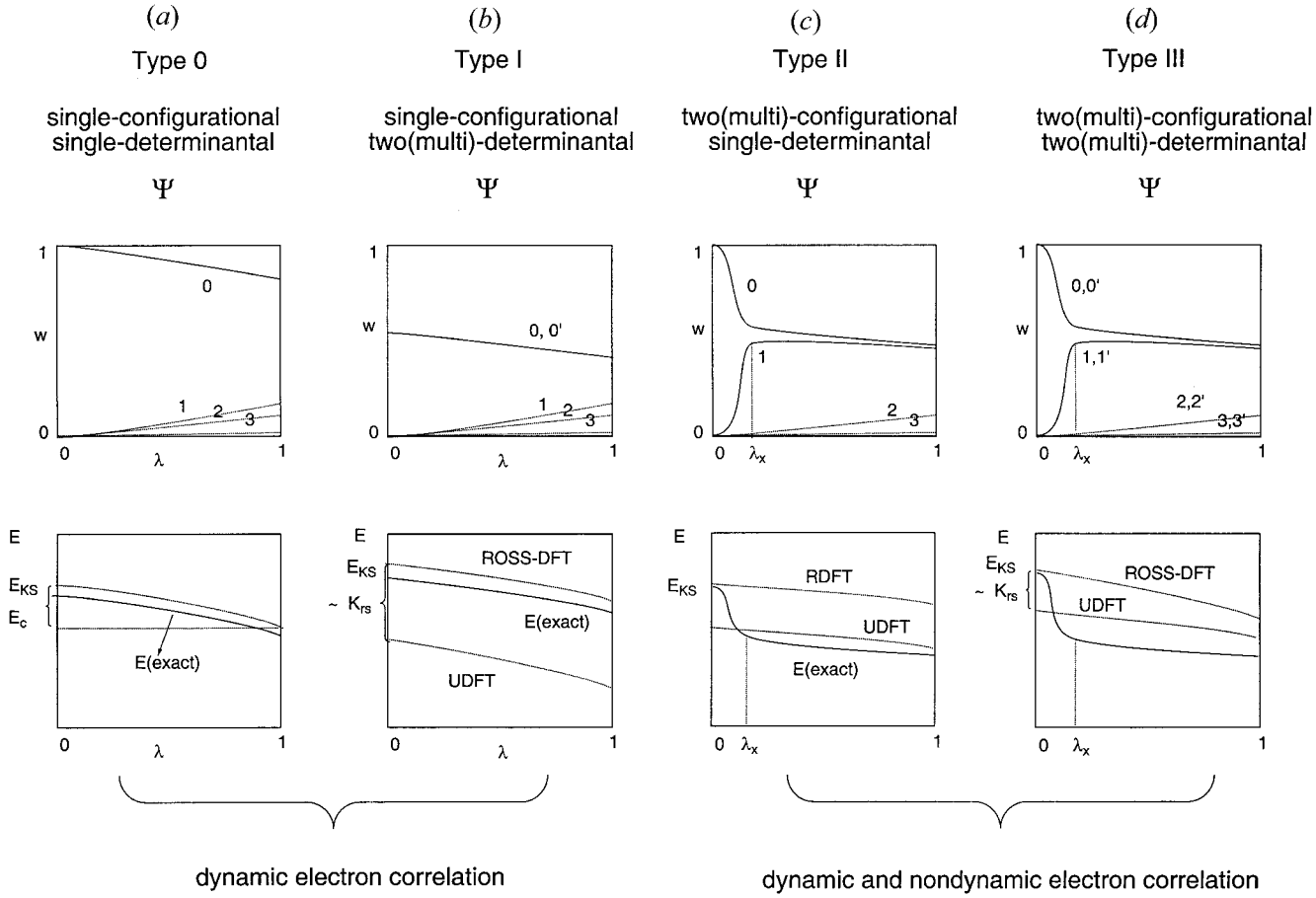

Figure 9. Schematic representation of wavefunction and energy of (*a*) type 0, (*b*) type I, (*c*) type II, and (*d*) type III electronic systems as described by RDFT or UDFT with approximate XC functionals or exact KS-DFT (thick lines). Numbers 0, 1, 2, etc., denote configuration state functions (CSFs) Ψ_0, Ψ_1, Ψ_2, etc. The weights w of the CSFs in the true wavefunction are schematically shown (first row of diagrams) in dependence of the parameter λ that continuously increases the electron correlation energy E_C from zero ($\lambda = 0$) to its true value ($\lambda = 1$). The corresponding changes in the Kohn–Sham energy K_{ES} and in the exact energy E(exact) are schematically given in the second row of diagrams.

Φ_0 and Φ_0' where the latter still dominate the ground state wavefunction Ψ.

Examples for type-I systems are σ–π or π–π open shell singlet (OSS) biradicals such as the $^1B_1$ state of methylene, the singlet state of 90°-rotated ethylene or that of the face-to-edge conformation of trimethylene (figure 10). For type-I systems, requirement (1) is not fulfilled, and therefore conventional KS-DFT is erroneous in principle, because the two-determinantal representation cannot be replaced by a single-determinant description [55, 56].

Type-II systems are multireference systems possessing a wavefunction that has to be constructed from two or more CSFs Ψ_0, Ψ_1, etc., each of which can be represented by a single determinant. Hence, the wave function can be expressed by a linear combination of determinants Φ_0 (reference), Φ_1, Φ_2, etc. (excited states). Considering a simple case (e.g. dissociation of H_2), the weight w_1 of Φ_1 increases dramatically with increasing λ at a point λ_x ($\lambda_x < 1$) so that the wavefunction is no longer dominated by Φ_0 (figure 9(*c*)). This indicates the importance of non-dynamic electron correlation effects, also reflected in the fact that, at λ_x, E(exact) drops substantially below the KS energy (figure 9(*c*)). Apart from the non-dynamic electron correlation effects, excited state determinants Φ_2, Φ_3, etc., contribute to the wavefunction with low but significant weight, thus covering dynamic electron correlation effects, as indicated by a smooth decrease in energy for $\lambda \to 1$.

Examples for type-II systems are (homolytically) dissociating molecules, the $^1A_1$ state of methylene, the ground states of ozone or of *p*-didehydrobenzene (*p*-benzyne, see figure 10), all of which are characterized by strong non-dynamic electron correlation effects.

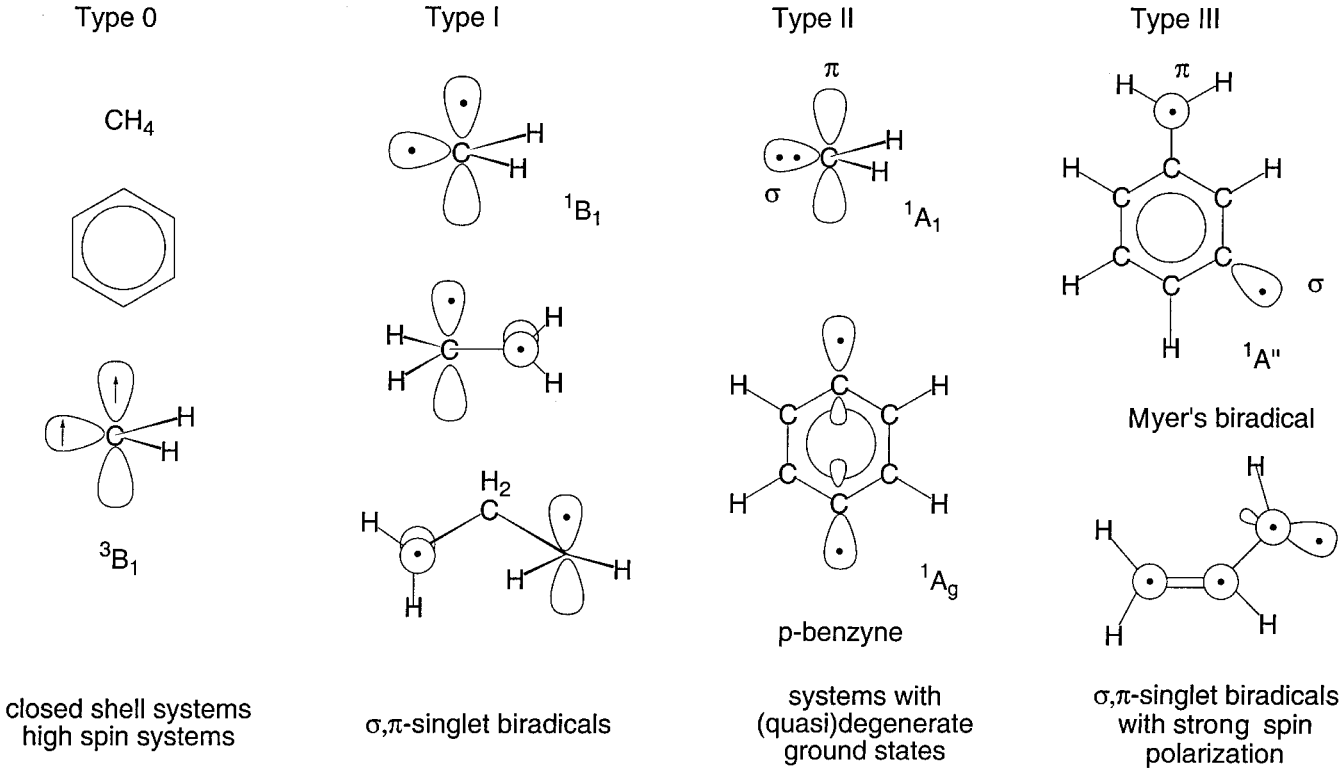

Figure 10. Some molecules with type-0, type-I, type-II, and type-III character. Electrons are denoted by dots or arrows (if spin has to be indicated).

For type-II systems, DFT is still valid in principle but will not work in practice, since the available approximations for the XC energy are based on condition (2).

In the case of a type-III system both conditions (1) and (2) are no longer valid because the wavefunction can be represented by only two or more CSFs Ψ_0, Ψ_1, etc., each of which must be spanned by two or more Slater determinants Φ_i, Φ_i', etc. Single-KS theory clearly fails in such a case because neither condition (1) nor condition (2) is fulfilled. An example of a type-III system is the Myers biradical (α,3-didehydrotoluene, figure 10), which possesses a singlet ground state because of spin polarization effects between the unpaired electrons. The latter can be correctly covered only by a multi-reference description.

The transition from type-0 to type-II system is continuous, so that for a given system with weak non-dynamic electron correlation effects it is difficult to predict whether KS theory fails or still provides reasonable results. One can actually use the accuracy of a DFT result to characterize a given electron system as representing a type-0 system (spin-restricted DFT (RDFT) provides a reasonable answer) or a type-II system (RDFT fails to provide useful results). Alternatively, one can use WFT to distinguish between a type-0 and a type-II system, gaining in this way an insight into which non-dynamic electron correlation effects are covered by standard DFT.

Type-0 and type-II are related by the fact that (a) their reference CSF can be approximated by Φ_0 and (b) it is difficult to define exactly a border between these systems. The same applies to type-I and type-III systems. However, there is a clear border between type-0 and type-I systems in so far as the form of the leading CSF is different, although both classes of systems are only characterized by dynamic electron correlation effects. In the following we shall discuss how the various DFT methods presently in use handle the four classes of electron systems.

A type-0 system that smoothly converts into a type-II system is given by a homolytically dissociating molecule A–A. The equilibrium geometry of the closed shell singlet system is described well by RDFT. However, with increasing bond length the closed shell singlet character of the electron system gradually changes into an open shell singlet system in which the electron pair responsible for bonding decouples while still keeping

the singlet configuration. The multireference character of the dissociating system increases and, by this, the spin-restricted DFT solution becomes qualitatively incorrect. Of course, it is not really possible to foresee the bond length at which the RDFT description is no longer reliable, and therefore an automated procedure determining the reliability of the RDFT solution is needed. This is achieved by testing the (internal and external) stability of the spin-restricted solution [130, 131] by procedures originally designed for HF theory [132] and later extended to DFT [133]. In case of an external instability of the spin-restricted DFT solution the constraint $\psi_\alpha = \psi_\beta$ must be lifted to obtain a stable spin-unrestricted DFT (UDFT) solution with lower energy. This leads to a breaking of the spin symmetry (and possible space symmetry). It also indicates that the RDFT solution no longer provides a reasonable description because a type-0 system is no longer given and one or both requirements (1) and (2) are not fulfilled. However, the question remains whether UDFT can represent a reasonable solution for type-II or even type-I (type-III) systems.

6.2. *Use of unrestricted DFT for multireference problems*

Spin-unrestricted DFT, like UHF, can be applied in different ways. For high spin open shell systems (type-0 systems such as doublet radicals, triplet biradicals, etc.) spin-unrestricted theory is used in the normal way and does not require any particular considerations. However, there are two other ways of using spin-unrestricted theory, namely permuted orbitals (PO)-UDFT and broken symmetry (BS)-UDFT [55]. The different applications of normal UDFT, PO-UDFT, and BS-UDFT can be demonstrated for the case of the three lowest states of methylene, $^3B_1$, $^1A_1$, and $^1B_1$, because they represent typical examples of a type-0, a type-II, and a type-I system (figure 10). (For carbenes such as vinyl carbene (figure 10) or allenyl carbene there are even OSS states with type-III character.) Normal UDFT is used for the $^3B_1$ state of methylene (type-0 character), PO-UDFT for the $^1B_1$ state (type-I character), and BS-UDFT for the $^1A_1$ state (type-II character).

The UDFT wavefunction (abbreviated to U because similar considerations are also valid for UHF theory [134]) is given by the following equation as a product of a (closed shell) core part Ψ_{core} and an open shell part Ψ_{open}:

$$\Psi^{\text{U}} = \mathcal{A}\{\Psi^{\text{U}}_{\text{core}}\Psi^{\text{U}}_{\text{open}}\} \tag{8}$$

($\mathcal{A}$ is the antisymmetrizer; note that $\Psi^{\text{U}}_{\text{core}}$ will no longer represent an exact closed shell function in the final unrestricted wavefunction due to the independent optimization of the α and β spin orbitals). In the case of methylene, $\Psi^{\text{U}}_{\text{open}}$ is constructed from the σ-type HOMO and the π-type LUMO of the RDFT description of the $^1A_1$ state (figure 10). This, however, is done for PO-DFT and BS-UDFT in different ways.

6.2.1. *Permuted orbitals (PO) UDFT*

In the $^1B_1$ OSS state of the methylene or similar type-I systems, the electron with α (β) spin can occupy either the σ (π) or the π (σ) orbital, and both possibilities have to be covered by the wavefunction, thus leading to a two-determinantal CSF. This does not imply any non-dynamic electron correlation; there is just dynamic electron correlation. The PO-UDFT wavefunction provides, under certain circumstances, a possibility of handling the multi-determinantal type-I problem at the single-determinant KS level. For the purpose of constructing the PO-UDFT wavefunction, the order of the orbitals is changed for one of the spin orientations. Typically, the HOMO and LUMO are exchanged for β spin orientation (figure 11).

$$\Psi^{\text{PO-U}}_{\text{open}} = |\psi_\sigma\overline{\psi_\pi}\rangle. \tag{9}$$

As shown in figure 11 for methylene, the resulting initial state is a mixture of a σπ singlet and a σπ triplet component with equal weights:

$$\Psi^{\text{PO-U}}_{\text{open}} = \frac{1}{\sqrt{2}}(|\psi_\sigma\overline{\psi_\pi}\rangle^{\text{T}} + |\psi_\sigma\overline{\psi_\pi}\rangle^{\text{S}}), \tag{10}$$

$$|\psi_\sigma\overline{\psi_\pi}\rangle^{\text{S}} = \frac{1}{\sqrt{2}}(|\psi_\sigma\overline{\psi_\pi}\rangle + |\psi_\pi\overline{\psi_\sigma}\rangle), \tag{11a}$$

$$|\psi_\sigma\overline{\psi_\pi}\rangle^{\text{T}} = \frac{1}{\sqrt{2}}(|\psi_\sigma\overline{\psi_\pi}\rangle - |\psi_\pi\overline{\psi_\sigma}\rangle). \tag{11b}$$

Hence, the correct two-determinantal CSF of the OSS state is contained in the PO-UDFT wavefunction so that the $^1B_1$ state of methylene should be described adequately. However, the price for recovering the singlet state within the single-determinantal PO-UDFT wavefunction is contamination by the two-determinantal triplet component with $M_S = 0$. Superposition of singlet and triplet components breaks the spin symmetry of the closed shell initial state. With regard to the spatial symmetry, the PO-UDFT reference state will belong to a 1-dimensional irreducible representation ($^{1,3}B_1$), which is antisymmetric with respect to the symmetry plane containing the molecule.

6.2.2. *Broken symmetry (BS) UDFT*

The $^1A_1$ closed shell state of methylene possesses some biradical and by this two-configurational character, where each CSF is represented by a single determinant (figure 11). Hence, a description of the $^1A_1$ state requires the inclusion of non-dynamic electron correlation effects

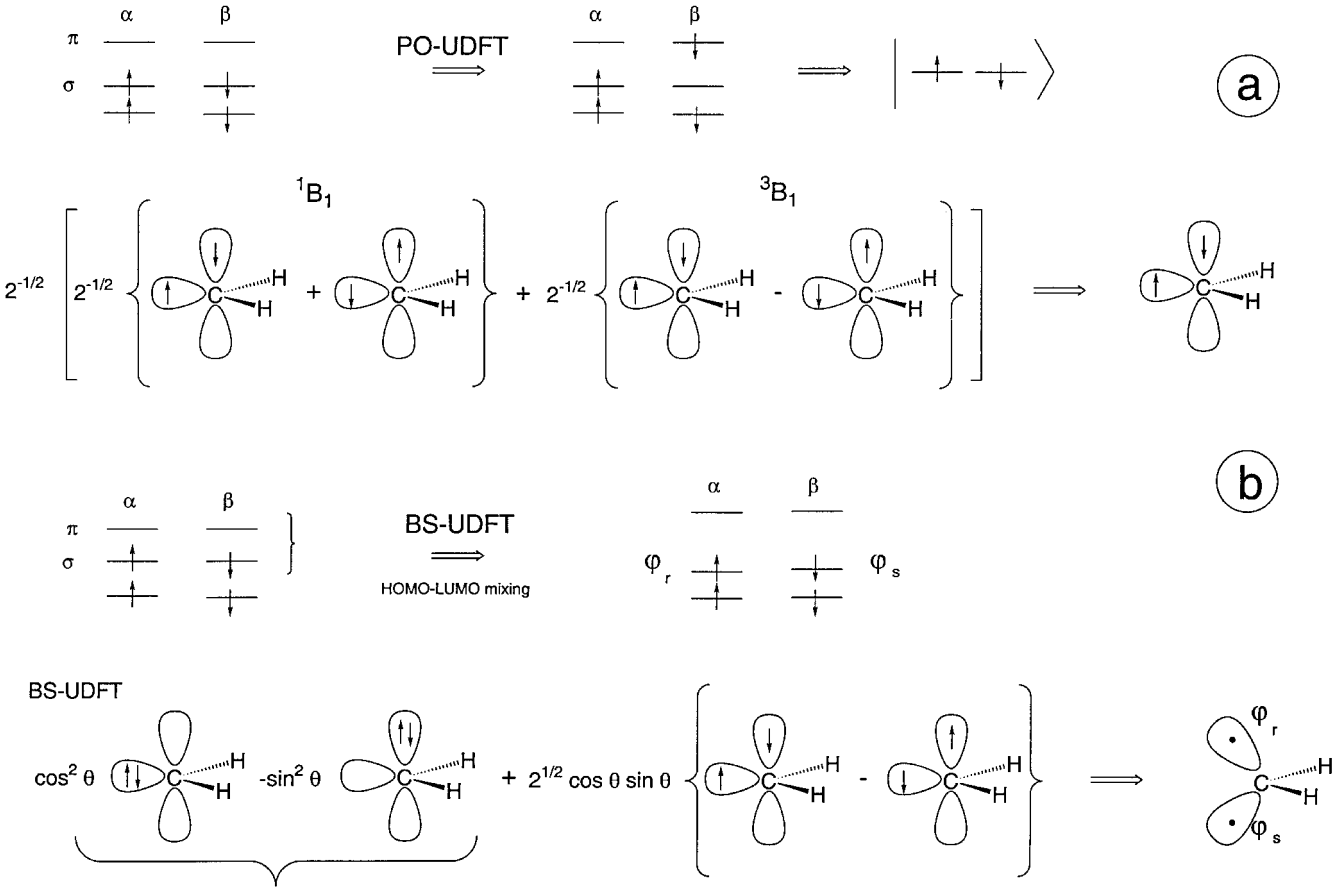

Figure 11. Schematic representation of the construction of the PO-UDFT and BS-UDFT wavefunctions in the case of (*a*) the $^1B_1$ state of methylene and (*b*) the $^1A_1$ state of methylene. The changes in the occupation (PO-UDFT) or the form (BS-UDFT: HOMO-LUMO mixing) of the frontier orbitals is given schematically (see text).

that are not necessarily covered by an RDFT description. The BS-UDFT wavefunction has two-configurational character, and therefore it may provide a reasonable description of the $^1A_1$ state. For the purpose of setting up the BS-UDFT wavefunction, an initial guess is constructed by mixing the σ-type HOMO and the π-type LUMO of the closed shell RDFT description of the $^1A_1$ state.

$$\Psi_{\text{open}}^{\text{BS-U}} = |\psi_{\text{r}}\overline{\psi_{\text{s}}}\rangle, \tag{12 a}$$

$$\psi_{\text{r}} = \cos\theta\psi_{\sigma} + \sin\theta\psi_{\pi} \tag{12 b}$$

$$\psi_{\text{s}} = \cos\theta\psi_{\sigma} - \sin\theta\psi_{\pi}, \tag{12 c}$$

where the orbital rotation angle θ is optimized during the SCF iterations. The resulting orbitals ψ_{r} and ψ_{s} are the localized counterparts of ψ_{σ} and ψ_{π}, respectively (figure 11). Using equation (12), the open shell part $\Psi_{\text{open}}^{\text{BS-U}}$ of the BS-UDFT wavefunction can be written as

$$\Psi_{\text{open}}^{\text{BS-U}} = \cos^2\theta|\psi_{\sigma}\overline{\psi_{\sigma}}\rangle - \sin^2\theta|\psi_{\pi}\overline{\psi_{\pi}}\rangle + \sqrt{2}\cos\theta\sin\theta|\psi_{\sigma}\overline{\psi_{\pi}}\rangle^{\text{T}}. \tag{13}$$

Hence, the BS-UDFT state is a mixture of the $|\sigma\overline{\sigma}\rangle$ and $|\pi\overline{\pi}\rangle$ singlet states and the $|\sigma\overline{\pi}\rangle$ ($M_{\text{S}} = 0$) triplet state. Again, the spin symmetry is broken as in the case of PO-UDFT. With respect to spatial symmetry, the BS-UDFT reference state does not belong to any irreducible representation but is part of a reducible representation that consists of a $^1A_1$ and a $^3B_1$ contribution for methylene. However, the BS-UDFT reference function is not completely asymmetric: it belongs to an irreducible representation of a mixed spin-space symmetry group where all reflections at the mirror plane are combined with a simultaneous flip of all spins in the system [55]. The PO-UDFT wavefunction is not symmetric with respect to this combined symmetry group.

The BS-UDFT wavefunction (13) has two-configurational character similar to that of the generalized valence

bond approach for one electron pair (GVB(1)) [135]. Hence, the BS-UDFT orbitals ψ_r and ψ_s resemble the corresponding GVB orbitals (figure 11).

6.3. *Non-dynamic electron correlation effects covered by UDFT*

The discussion of the various UDFT methods suggests that PO-UDFT may be appropriate to describe type-I systems (or even type-III systems) while BS-UDFT might be able to provide reasonable results for type-II systems. Both for type-II and type-III (but not for type-I) systems UDFT must cover non-dynamic correlation effects to lead to a useful description. The UDFT calculation of a high spin system explicitly includes dynamic correlation effects as the only type of electron correlation (where the unspecified amount of non-dynamic correlation effects included by the X functional is not considered here). The wavefunction contains small admixtures of higher CSFs, but these are too small to account for any significant amount of non-dynamic electron correlation. Also, there is no particular coverage of non-dynamic electron correlation effects by the PO-UDFT wavefunction for a type-I biradical, which of course are not needed in this case.

The form of the BS-UHF wavefunction (13) suggests that it includes similar non-dynamic electron correlation effects as GVB(1) or CASSCF(2,2). Important problems in chemistry such as the dissociation of a single bond are described reasonably by the latter. However, the BS-UDFT wavefunction never takes the explicit form of equation (13), which because of the triplet admixture collapses to a single-determinantal form. This means that the non-dynamic electron correlation effects covered by BS-UHF must be reflected by the form of the α and β spin orbitals calculated at the UDFT level of theory.

The UHF spin orbitals are known to be more localized than the RHF space orbitals, which becomes obvious when comparing the UHF and RHF orbitals of dissociating molecules such as H_2 and F_2. Localization of the orbitals leads to an increase in the Coulomb self-interactions of the electrons and, by this, also of the exchange interactions, which exactly annihilate the former by the self-exchange they contain. If one assumes that for the RHF and UHF description of the same electron system the Coulomb repulsion energy will be about the same, the subtraction of the exchange energy will give a smaller (more negative) electron interaction energy and total energy in the unrestricted case.

The same conclusion is reached when considering the impact exchange interactions have in general on the electron density (figure 6(*a*)). Since the chance of finding electrons with the same spin is greatest in the valence regions of the heavy atoms, exchange interactions in a molecule are strongest in these regions. A stronger localization of the orbitals (e.g. when ethene dissociates into two carbene molecules) implies a contraction of the valence regions and, accordingly, stronger exchange interactions, which in turn leads to a more negative energy relative to the corresponding RHF energy.

Alternatively, the decrease in the UHF energy can be considered to reflect the non-dynamic electron correlation effects resulting from the implicit two-configurational character of the BS-UHF wavefunction. Hence, breaking of the spin and space symmetry at the BS-UHF level is both an indication of and a compensation for the fact that the RHF description of a multireference electronic system lacks important non-dynamic electron correlation effects. These effects are covered by the exchange energy, and cause an increase in the magnitude of the latter.

The discussion in §5 clarified that DFT exchange covers non-dynamic electron correlation effects due to the local character of the exchange hole, where one has to recall that DFT exchange is not directly related to HF exchange because it is defined in a different way. Non-dynamic correlation effects covered by an LDA or GGA functional are unspecified and will not necessarily improve the description of a given multireference system. In addition to these effects, use of the UDFT rather than RDFT wavefunction introduces additional non-dynamic electron correlation effects of the type just described for the case of a UHF wavefunction (and indicated by the explicit form of the BS-UDFT wavefunction (13)). It cannot be excluded that (apart from problems such as spin contamination) *the UDFT description suffers from a double counting of non-dynamic correlation effects*. A simple corollary that may be drawn from this conclusion is that it is always better to carry out UDFT calculations with hybrid functionals, thus suppressing any double counting as much as possible (B3LYP is better than BLYP in the case of a UDFT description).

In view of these considerations, two important differences between BS-UHF and BS-UDFT must be stressed. (1) *The causes of symmetry breaking at the HF and DFT levels of theory are different*. In the former case, it is a failure of the method (which does not cover non-dynamic electron correlation needed for the description of a multireference system). In the latter case, however, the spin-restricted DFT description would be stable for the multireference system if the exact XC functional were available, i.e. a BS-UDFT description would not exist. Hence, the existence of a broken symmetry solution at the DFT level is not an indication of shortcomings of the method, but an indication of the shortcomings of the approximate functionals presently in use. Apart from this, an RDFT

description with an LDA or GGA functional will be always more stable than an RHF description because the former already contains non-dynamic correlation effects while the latter does not.

(2) *In contrast to HF, DFT can be improved by adjusting the XC functional.* This can be done in an empirical way, as in the case of the hybrid functionals [36], thus leading to semiempirical DFT [74]. The choice of reference compounds and of experimental reference data used in the empirical calibration decides on the dynamic and non-dynamic correlation effects covered by the hybrid functional. Alternatively, one can adjust the DFT exchange hole to the exact exchange hole using delocalization indicators and tuning down non-dynamic correlation effects in a molecule-specific way, which also leads to improved coverage of electron correlation [127].

It is of advantage to quantify the amount of non-dynamic electron correlation covered explicitly by a BS-UDFT description, for example, in the case of a dissociating molecule. The two-configurational character can be assessed directly from the rotational angle θ driving the mixing of HOMO and LUMO in the BS-UDFT description. Since for a given problem it may be difficult to determine the optimized θ and the exact form of equation (13), it is easier to calculate the natural orbitals of the BS-UDFT wavefunction. The fractional values of the natural orbital occupation numbers (NOONs) of the mixing orbitals then provide a simple measure of the amount of non-dynamic electron correlation covered by the BS-UHF wavefunction [55].

We conclude that BS-UDFT and in particular BS-UDFT with hybrid functionals should cover a considerable amount of non-dynamic electron correlation effects to lead to a reasonable description of many multireference systems. However, the price to be paid for this is spin contamination. From a practical point of view the question is whether spin contamination deteriorates results at the BS-UDFT level of theory in the same manner as it does at the UHF level. In UHF theory, the answer to this question is based on a quantitative assessment of spin contamination via the expectation value $\langle \hat{S}^2 \rangle$ [51, 136]. Therefore, we shall discuss the consequences of spin contamination in UDFT in the next section.

6.4. *Spin contamination in spin-unrestricted DFT*

There are three ways to investigate the consequences of spin contamination when using spin-unrestricted theory, which may also be applied at the UDFT level of theory.

(1) Comparison of calculated molecular properties such as the energy with the corresponding quantities calculated at the RODFT level of theory; alternatively, one can use for this purpose reliable WFT results or directly experimental values.

(2) Calculation of the expectation value $\langle \hat{S}^2 \rangle$. Its deviation from the ideal value $S(S+1)$ where S denotes the total spin of the electronic system should give the degree of spin contamination.

(3) Comparison of the UDFT spin density distribution with the correct spin density distribution taken from a reliable reference calculation.

In the literature, possibility 2 is mostly chosen, where the KS orbitals are used to calculate $\langle \hat{S}^2 \rangle$. There are, however, a number of arguments against the use of $\langle \hat{S}^2 \rangle$ as an indicator of spin contamination for the UDFT wavefunction [53, 54]. (a) The KS wavefunction corresponds to the situation of non-interacting electrons, and this differs considerably from the many-particle state represented by the KS density. Hence, one can not expect that $\langle \hat{S}^2 \rangle$ calculated from the KS Slater determinant has any physical significance. (b) The operator $\hat{S}^2$ is a two-electron operator, whereas the KS wavefunction should reproduce correctly only the expectation values of one-particle operators. There is no reason why the KS Slater determinant should yield the correct $\langle \hat{S}^2 \rangle$, and an expectation value for $\hat{S}^2$ that deviates from $S(S+1)$ does not necessarily indicate spin contamination. (c) At present, the correct calculation of $\langle \hat{S}^2 \rangle$ with the KS density is an unresolved problem.

Wang *et al.* [137] investigated a number of high spin states of atoms and small molecules (both doublet radicals and T biradicals) and compared the $\langle \hat{S}^2 \rangle$ values computed from the KS Slater determinant with values obtained by an approximate approach based on the correct Löwdin formula [138] for $\langle \hat{S}^2 \rangle$. They found that the values from the KS Slater determinant, though not exact, are at least reasonable for high spin radicals and biradicals. Gräfenstein and Cremer [54] used the spin (magnetization) density distribution $m_s(\mathbf{r}) = \rho_\alpha(\mathbf{r}) - \rho_\beta(\mathbf{r})$ to determine the value of $\langle \hat{S}^2 \rangle$ in the case of singlet biradicals where the UDFT description is highly contaminated (up to 50% and more triplet character). They found that spin contamination can be underestimated by more than 20% when using KS orbitals for the calculation of $\langle \hat{S}^2 \rangle$, where errors were largest for LDA functionals but smallest for hybrid functionals. These observations could be generalized in such a way that, for cases with equal mixing of singlet and triplet states in the BS-UDFT wavefunctions of singlet biradicals, $\langle \hat{S}^2 \rangle$ calculated from KS orbitals still possesses a useful diagnostic value, although this is no longer the case as soon as there is unequal mixing of these states [54].

Presently there is no reliable way to routinely calculate the correct magnitude of $\langle \hat{S}^2 \rangle$, and thus the diag-

nostic value of the latter as obtained with the help of KS orbitals has to be questioned in general. In this situation, arguments to disregard $\langle \hat{S}^2 \rangle$ and to consider the role of spin contamination in UDFT from a principle point of view are most welcome. For example, Pople *et al.* [139] argued that the spin-unrestricted KS formalism is the appropriate formulation of the KS approach for spin-resolved DFT, and that there is no motivation to avoid or remedy an incorrect value of $\langle \hat{S}^2 \rangle$ for the KS Slater determinant by a spin-restricted KS formalism. On the same basis, it is a contradiction in itself to use spin-projection methods developed within wavefunction theory in the case of UDFT [140].

6.5. *The usefulness of UDFT results*

BS-UDFT has been found to lead to surprisingly accurate descriptions in many cases where both the calculated value of $\langle \hat{S}^2 \rangle$ and the spin magnetization density indicate strong spin contamination. On this basis, the problem of spin contamination may be ignored altogether, as was suggested by Perdew *et al.* [90]. These authors developed an alternative interpretation of spin-unrestricted DFT that, while leaving the KS equations unchanged, avoids the symmetry-breaking problems of conventional UDFT. Their approach is based on the total and the on-top pair density distribution rather than spin densities ρ_α and ρ_β. The on-top pair density $P(\mathbf{r},\mathbf{r})$ gives the probability of finding two electrons at the same position $\mathbf{r}$ (one electron 'on top' of another), where $P(\mathbf{r})$ is approximated by using KS orbitals [141]:

$$P(\mathbf{r},\mathbf{r}) = \tfrac{1}{2}\rho^2(\mathbf{r})\{1-\zeta^2(\mathbf{r})\} = 2\rho_\alpha(\mathbf{r})\rho_\beta(\mathbf{r}), \qquad (14)$$

where $\zeta(\mathbf{r}) = [\rho_\alpha(\mathbf{r}) - \rho_\beta(\mathbf{r})]/\rho(\mathbf{r})$ is the relative spin polarization. By constrained minimization of the ground state energy with regard to total and on-top pair densities, Perdew *et al.* [90] determined the KS energy in a way that is more appropriate for approximate XC functionals than the conventional KS formalism. In standard DFT, the KS reference has to reproduce the correct total density $\rho(\mathbf{r})$ and the correct relative spin polarization ζ of the real state. Perdew *et al.* abandoned the latter requirement by the condition that the correct on-top pair density is reproduced.

There is a relationship between $\zeta(\mathbf{r})$, $P(\mathbf{r},\mathbf{r})$, and the amount of non-dynamic correlation effects covered by a UDFT calculation. A decrease in the on-top pair density can be caused in different ways. (a) Because of the Pauli principle, two electrons located at the same position must possess different spins. If spin polarization increases, i.e. one spin dominates the other, there will be a reduced probability of finding two electrons with opposite spin at a given position. Accordingly, the on-top density will decrease with increasing spin polarization for a given total density. (b) Non-dynamic electron correlation implies the long range separation of electrons, which also leads to a strong decrease in $P(\mathbf{r},\mathbf{r})$, even in those cases where there is no spin polarization. In view of (a) and (b), the on-top pair density contains information on both spin polarization and non-dynamic electron correlation effects. Hence, local spin polarization of the UDFT reference function may be related to either spin polarization or non-dynamic correlation effects in the real system where the former is reflected by differences between the KS spin orbitals and the latter by the exchange functional (see above).

As all the information needed is contained in the total and the on-top pair density of a UDFT calculation one can, as suggested by Perdew *et al.*, consider both KS orbitals and the KS spin density $m_s(\mathbf{r})$ as intermediate, physically not relevant quantities and analyse UDFT results exclusively on the basis of the calculated total and on-top densities [90]. This line of argument is supported by Gräfenstein *et al.* [53], who showed in the cases of singlet and triplet biradicals that the UDFT on-top pair densities give a reasonable account of electron correlation. (i) Contrary to the spin densities $m_s(\mathbf{r})$, $\rho_\alpha(\mathbf{r})$, and $\rho_\beta(\mathbf{r})$, the on-top pair densities comply with the symmetry of the molecule both in the singlet and the triplet state. (ii) For the singlet state, symmetry breaking at the UDFT level of theory leads to a twofold degenerate KS ground state, even though the real ground state is not degenerate. Within the alternative interpretation, these two ground states possess the same total and on-top pair densities, and therefore they are equivalent representations of the same KS ground state. (iii) The on-top pair densities for singlet and triplet state are very similar to each other in those cases where there is just a small energy difference between the two states. However, the spin densities $m_s(\mathbf{r})$ for the two states differ markedly from each other.

These considerations support the usefulness of UDFT calculations in cases where, because of non-dynamic electron correlation effects, RDFT fails. In line with this is the fact that UDFT, in contrast to RDFT, provides a reasonable description of bond dissociation [90]. However, there is no guarantee that UDFT will always provide a reasonable answer in such a situation, because clearly its success should depend on the amount of non-dynamic electron correlation that has to be covered for a given problem to get useful results. To make a better judgement about the performance of UDFT in cases with strong non-dynamic electron correlation, we turn first to those methods that explicitly incorporate non-dynamic electron correlation at the DFT level.

7. Extension of DFT: explicit coverage of non-dynamic electron correlation effects

An appropriate account of multi-determinantal (type-I systems) and/or multiconfigurational effects (type-II and type-III systems) within DFT seems to imply an extension of KS theory. It suggests itself that such an extension will be guided partially by the experience and knowledge obtained from WFT methods. Here, we shall discuss briefly two directions for developing multideterminantal/multiconfigurational DFT so that (a) type-I and (b) type-II (type-III) systems can be described reliably by DFT. Clearly, an extension of DFT can pursue different strategies and always has consequences with regard to the development of new density functionals and the incorporation of new calculational procedures, which cannot be discussed here in detail. Hence, we shall pick out only methods connected closely with the work of the present author [56–59].

7.1. *Restricted open shell theory for type-I systems*

The description of a type-I system such as the $^1B_1$ state of methylene requires a two-determinantal wavefunction, as discussed in § 6. This problem can be solved within single-determinant KS DFT by using techniques originally worked out for the application of restricted open shell HF (ROHF) theory in the case of low spin systems such as OSS biradicals [142], and latterly applied by Handy and coworkers at the MP2 level of theory with success to describe OSS states [143]. Gräfenstein *et al.* [56] used this technique to develop spin-restricted OSS DFT (ROSS-DFT). For this purpose, the authors constructed an appropriate XC functional, which accounts for the two-determinantal character of the OSS state and which is based on the two following considerations. (a) A (space and spin) symmetry-constrained energy minimization has to be applied in view of the fact that for the most interesting cases the OSS state possesses a symmetry differing from that of a lower singlet state. For example, in the case of methylene the lowest singlet state is the $^1A_1$ state, while OSS and the triplet state have B_1 symmetry. (b) A new density functional $F^{OSS}[\rho]$ for the OSS state is derived by using the fact that (i) the triplet state associated with the OSS state by spin-flip can be described well by DFT and that (ii) at the HF level the triplet state is exactly $2K_{rs}$ below the OSS state where $2K_{rs} = \langle\varphi_r\varphi_s|\varphi_s\varphi_r\rangle$ describes the exchange of the unpaired electrons in orbitals φ_r and φ_s.

The small Coulomb correlations between the unpaired electrons of the triplet state are covered in the way of weak equal-spin corrections. In the OSS case, the same interactions enter the energy expression as different-spin correlations, which can be handled by replacing the triplet correlation energy $E_C^{DFT}[\rho_c + \rho_r + \rho_s, \rho_c]$ by $E_C^{DFT}[\rho_c + \rho_r, \rho_c + \rho_s]$ where c denotes the core of doubly occupied orbitals. In this way, the ROSS-DFT energy functional for an OSS biradical is given by:

$$\begin{aligned} E = {} & 2\sum_i \langle\varphi_i|\hat{\boldsymbol{h}}|\varphi_i\rangle + \langle\varphi_r|\hat{\boldsymbol{h}}|\varphi_r\rangle + \langle\varphi_s|\hat{\boldsymbol{h}}|\varphi_s\rangle \\ & + \sum_i \langle\varphi_i|\hat{\boldsymbol{J}}|\varphi_i\rangle + \tfrac{1}{2}\langle\varphi_r|\hat{\boldsymbol{J}}|\varphi_r\rangle + \tfrac{1}{2}\langle\varphi_s|\hat{\boldsymbol{J}}|\varphi_s\rangle \\ & - a_{HF}\Bigg(\sum_i \langle\varphi_i|\hat{\boldsymbol{K}}_c + \tfrac{1}{2}(\hat{\boldsymbol{K}}_r + \hat{\boldsymbol{K}}_s)|\varphi_i\rangle \\ & + \tfrac{1}{2}\langle\varphi_r|\hat{\boldsymbol{K}}_c + \hat{\boldsymbol{K}}_r + \hat{\boldsymbol{K}}_s|\varphi_r\rangle + \tfrac{1}{2}\langle\varphi_s|\hat{\boldsymbol{K}}_c + \hat{\boldsymbol{K}}_r + \hat{\boldsymbol{K}}_s|\varphi_s\rangle\Bigg) \\ & + 2\langle\varphi_r\varphi_s|\varphi_s\varphi_r\rangle + E_X^{DFT}[\rho_c + \rho_r + \rho_s; \rho_c] \\ & + E_C^{DFT}[\rho_c + \rho_r; \rho_c + \rho_s]. \end{aligned} \tag{15}$$

In equation (15), a_{HF} is the weight factor for HF exchange in hybrid DFT schemes ($a_{HF} = 0$ for pure DFT). The functional $F^{OSS}[\rho]$ is readily obtained from expression (15) by omitting the external potential terms, i.e. replacing the core Hamiltonian $\hat{\boldsymbol{h}}$ by the kinetic energy operator $\hat{\boldsymbol{T}}$. For $a_{HF} = 1$ and $E_X^{DFT} = E_C^{DFT} = 0$, the energy expression for ROHF in the case of an OSS state is reproduced.

In an SCF procedure, the singly occupied orbitals φ_r and φ_s are rotated in such a way that the energy is minimized for otherwise fixed orbitals (such a rotation does not affect the total electronic structure in the high spin case but it does in the low spin case). For a molecule of high symmetry, φ_r and φ_s can represent different 1-dimensional irreducible representations (as, e.g. in the case of a σ and a π orbital) or span the basis for a 2-dimensional irreducible representation so that they are transformed into each other by some of the symmetry operations.

ROSS-DFT provides a reasonable description of OSS states of methylene and other type-I systems, as has been documented in the literature [56, 58]. However, ROSS-DFT does not include any non-dynamic correlation effects, and therefore its application to type-III systems is of little use. We note that other methods closely related to ROSS have been worked out as, e.g. the ROKS method (restricted open shell KS theory) of Filatov and Shaik [144]. Section 8 will discuss the performance of ROSS-DFT for some selected examples.

7.2. *Combination of multiconfigurational SCF and DFT*

Non-dynamic electron correlation effects are routinely covered by a multiconfigurational wavefunction with a moderate size active space. However, the available methods for a simultaneous inclusion of non-dynamic and dynamic correlation effects, such as CASSCF-PT2 [145], MR-CI [109] or MR-AQCC [110], are too costly to be applied on a routine basis.

If one could combine the advantages of a correct multiconfigurational description of non-dynamic electron correlation effects with those of a DFT coverage of dynamic correlation effects, one would have a method suitable for all problems that cannot be described correctly by conventional KS theory. By choosing FORS [67] or CASSCF [68] as a method for constructing the multiconfigurational wavefunction, CAS-DFT is obtained as a new, more generally applicable DFT method [57, 58]. CAS-DFT should be able to handle type-III systems and, by this, also all genuine type-I or type-II systems.

However, there is a basic problem accompanying all multiconfigurational descriptions that hinder a simple addition of CASSCF and KS-DFT. As mentioned in § 3, a multiconfigurational wavefunction will always contain, in addition to wanted non-dynamic correlation effects, dynamic electron correlation effects that will lead inevitably to a double-counting of dynamic electron correlation when combining CASSCF with DFT [57, 58]. Accordingly, any new development in the area of WFT-DFT methods has been automatically confronted with this problem, which also has been studied as part of the problem of fractionally occupied orbitals [146–148]. Closely related with this research are attempts at obtaining a better account of the interplay between dynamic and non-dynamic electron correlation effects for a multireference system (type-II and type-III systems) by improving virtual orbitals [149–155], by using a functional for non-dynamic correlation effects [156, 157], by partitioning the electron–electron interaction operator into a short range and a long range part [158, 159], or by partitioning the electron correlation energy [160–163]. An interesting attempt to identify dynamic and non-dynamic electron correlation effects was made at the MCSCF level by using properties of the calculated pair densities [163]. According to this approach, the electron–electron counterbalance density indicates the short or long range behaviour of electron correlation, defines their influence on the size of the Coulomb hole, and provides a basis for separating dynamic from non-dynamic electron correlation effects covered by a given multiconfigurational wavefunction. However, so far there is no obvious principle following from these investigations that helps in carrying out a self-consistent WFT-DFT calculation without any double-counting of dynamic correlation effects.

For the development of a generally applicable CAS-DFT method, one has to modify the KS approach (see equations (3) and (4)) in two ways: (a) the search over trial functions has to be done over all CAS wavefunctions for a given size of the active space, and (b) in equation (4), the Hartree energy E_J must be replaced by the full electron interaction energy of the CAS trial wavefunction. This implies that the exchange energy and the non-dynamic electron correlation energy are covered by a CAS-DFT analogue to $F_{KS}[\rho]$ in equation (3) and that $E_{XC}[\rho]$ is replaced by a term that covers the dynamic correlation energy only. Modifications (a) and (b) lead to the CAS-DFT scheme:

$$F[\rho] = F_{KS}^{\text{CAS-DFT}}[\rho] + E_C^{\text{CAS-DFT}}[\rho], \quad (16)$$

$$F_{KS}^{\text{CAS-DFT}}[\rho] = \min_{\Psi^{\text{CAS}} \to \rho} \langle \Psi^{\text{CAS}} | \hat{T} + \hat{V}_{ee} | \Psi^{\text{CAS}} \rangle. \quad (17)$$

One has to construct an approximation for $E_C^{\text{CAS-DFT}}[\rho]$ of the general form

$$E_C[\rho] = \int d^3r \, \varepsilon_C(\rho, \nabla\rho, \ldots)\Big|_{\mathbf{r}} \quad (18)$$

to apply CAS-DFT. However, in doing so a number of problems arise: (a) proper choice of input quantities (spin densities, total density, etc.); (b) avoidance of the double-counting of dynamic electron correlation effects; (c) the correct distinction between correlation effects involving core orbitals and those involving active space orbitals at the DFT level; (d) a balanced treatment of singly and doubly occupied CAS orbitals; and (e) appropriate choice of the DFT correlation functional for CAS-DFT calculations.

(a) *Choice of the input densities for the DFT correlation energy functional.* The use of spin densities ρ_α and ρ_β in CAS-DFT will lead to similar errors in the description of state multiplets as discussed in connection with ROSS-DFT. Therefore, it is of advantage to replace these densities, as in the case of UDFT, by the total density $\rho(\mathbf{r})$ and the on-top pair density $P(\mathbf{r},\mathbf{r})$ as input quantities for the correlation functional. Being a two-particle quantity, $P(\mathbf{r},\mathbf{r})$ can distinguish between states with different multiplicity and, in contrast to ρ_α, ρ_β, the on-top density is identical for the components of a state multiplet such as $T(M=-1)$, $T(M=0)$, and $T(M=1)$. Equation (19) can be used to convert existing correlation functionals so that they depend on total density $\rho(\mathbf{r})$ and on-top pair density $P(\mathbf{r},\mathbf{r})$ rather than spin densities $\rho_\alpha(\mathbf{r})$ and $\rho_\beta(\mathbf{r})$ [57]:

$$\varepsilon_C^{\text{on-top}}(\rho, P) = \varepsilon_C\left(\frac{\rho}{2} + \sqrt{\left(\frac{\rho}{2}\right)^2 - P}, \frac{\rho}{2} - \sqrt{\left(\frac{\rho}{2}\right)^2 - P}\right). \quad (19)$$

(b) *The double-counting of dynamic electron correlation effects.* As most of the expressions for the DFT correlation energy were derived using the HEG as starting basis, it is possible to use standard descriptions of the HEG to assess the amount of dynamic electron correlation effects [164, 165]. First, a reference density $\rho_{\text{ref}}(\mathbf{r})$ is determined by considering all core orbitals and active

space orbitals to be doubly occupied, so that the magnitude of $\rho_{\mathrm{ref}}(\mathbf{r})$ reflects the size of the active space. If compared with the true density of the system in question, $\rho(\mathbf{r})$, the ratio $\rho_{\mathrm{ref}}(\mathbf{r})/\rho(\mathbf{r}) \geqslant 1$ will increase with the size of the active space, as will the amount of dynamic electron correlation already covered by the CASSCF wavefunction. Hence, one has to scale the DFT correlation energy locally by a scaling factor f ($0 \leqslant f \leqslant 1$) to avoid this double counting. To determine f, one recalculates the correlation energy of the HEG with the density ρ in a way that is comparable with CASSCF, i.e. one allows excitations from the occupied orbitals only into virtual orbitals up to a certain energy limit, which is adjusted in the way that the active space has just the reference density ρ_{ref}. For the determination of the scaling factor f, the resulting correlation energy $\varepsilon_{\mathrm{C}}^{\mathrm{HEG}}(\rho, \rho_{\mathrm{ref}})$ is related to the value $\varepsilon_{\mathrm{C}}^{\mathrm{HEG}}(\rho, \infty)$ for all virtual orbitals being included.

$$f(\rho, \rho_{\mathrm{ref}}) = 1 - \frac{\varepsilon_{\mathrm{C}}^{\mathrm{HEG}}(\rho, \rho_{\mathrm{ref}})}{\varepsilon_{\mathrm{C}}^{\mathrm{HEG}}(\rho, \infty)}. \tag{20}$$

An analytical expression worked out for the scaling factor [165] facilitates the calculation of the correlation energy so that its scaled value can be determined readily:

$$E_{\mathrm{C}}^{\text{CAS-DFT}} = \int \mathrm{d}^3 r f(\rho, \rho_{\mathrm{ref}}) \varepsilon_{\mathrm{C}}^{\text{on-top}}(\rho, \nabla \ldots, P, \nabla P, \ldots)\Big|_{\mathbf{r}}. \tag{21}$$

(c) *Distinction between core and active space orbitals.* The original derivation of an analytical expression for the scaling factor f did not distinguish between core and active space orbitals, which is equivalent to assuming that the core part of a CASSCF description is always the same. However, it will change if different molecules are compared within a given reaction scheme. Gräfenstein and Cremer [58] suggested a procedure to compensate for this. However, a distinction between core and active space orbitals, which is possible via the electron density associated with them, has to be incorporated directly into the derivation of the expression of the scaling factor with the help of the HEG.

(d) *Treatment of singly and doubly occupied CAS orbitals.* Another shortcoming of the use of an analytical expression for the scaling factor is the fact that this expression does not distinguish between singly and doubly occupied orbitals. Because of this the scaling procedure assumes a larger Coulomb correlation energy for a triplet state (exchange–correlation between the single electrons keeps Coulomb correlation relatively small) than is actually covered by the CASSCF calculation. The CAS-DFT triplet energy is too high relative to that of the singlet state from which it is generated via a HOMO-LUMO excitation, thus yielding erroneous singlet–triplet splittings. Refined scaling procedures can compensate for this effect [166].

(e) *Choice of the DFT correlation functional for CAS-DFT.* It was shown that a gradient-corrected correlation functional is required because LDA functionals overestimate dynamic correlation effects. The LYP functional could be considered to represent an appropriate choice, in particular in view of its widespread successful use. Gräfenstein and Cremer [57], however, suggested reverting back to the Colle–Salvetti (CS) functional [12], from which the LYP functional was originally derived. The CS functional provides the advantage of using total density and pair density directly as input quantities, thus avoiding a conversion of the functional as just discussed under (a). However, other gradient-corrected correlation functionals should be equally suitable, where of course care has to be taken that they do not cover spurious non-dynamic correlation effects.

Once problems (a)–(e) are solved, a reasonable and computationally feasible account of both non-dynamic and dynamic electron correlation effects should be given at the CAS-DFT level of theory. The correct way to determine the CAS-DFT energy is to solve the CAS-DFT equations self-consistently. However, the orbitals do not depend strongly on the DFT correlation-energy contribution, as investigations with GVB-DFT [59] and first versions of CAS-DFT revealed [57, 58]. Hence, for energy calculations it is a reasonable approximation to insert Ψ^{CASSCF} into the CAS-DFT energy functional and to determine the CAS-DFT energy in a one-step procedure rather than obtaining $\Psi^{\text{CAS-DFT}}$ in an iterative procedure leading to self consistency. However, a generally applicable CAS-DFT method must be able to determine optimized geometries, frequencies, etc., which of course implies a self-consistent CAS-DFT wavefunction. First results obtained with CAS-DFT (discussed in the next section) clearly show its potential of (i) extending DFT methods to types-I, -II, and -III systems in a general way and (ii) offering a feasible alternative to the much more costly WFT methods such as CASPT2, MR-CI, or MR-CC.

7.3. *Performance of DFT methods covering non-dynamic electron correlation effects*

The performance of the various DFT methods that cover non-dynamic electron correlation effects was tested for a large number of electron systems with multi-reference character. Here, only a few typical examples are discussed, which illustrate the usefulness of DFT in these cases. In table 6, relative energies, geometries, and NOON values of the three lowest states of methylene [55–58, 167–171] are summarized. A number of conclusions can be drawn from these data.

Table 6. Energies, geometries, and NOON values for the three lowest states of methylene.[a]

Method	Functional	E or ΔE	r_{CH}	$\angle_{HCH}$	NOON(a_1)	NOON(b_1)
$^3B_1$ State						
RODFT	B3LYP	−39.166 68	1.077	133.9	1	1
UDFT	B3LYP	−39.168 74	1.077	135.0	1.000	1.000
ROHF-DFT[b]	LYP	−39.134 20	1.072	128.8	1	1
CAS(6,6)-DFT	CS	−39.120 67	1.102	131.0	1.000	1.000
Expt.[c]			1.070	134.0	1	1
$^1A_1$ State						
RDFT	B3LYP[d]	10.5 (11.8)	1.110	101.6	2	0
BS-UDFT	B3LYP	5.3	1.093	114.0	1.528	0.472
GVB-DFT	LYP	6.3	1.110	101.6	1.986	0.014
CAS(6,6)-DFT	CS	6.9	1.138	100.0	1.909	0.088
Expt.[c]		9.1	1.111	101.9	N/A	N/A
$^1B_1$ State						
ROSS-DFT	B3LYP	30.4	1.072	147.5	1	1
PO-UDFT	B3LYP	11.4	1.077	138.1	1.000	1.000
ROHF-DFT[b]	LYP	25.8	1.072	147.5	1	1
CAS(6,6)-DFT	CS	35.2	1.131	134.1	1.000	1.000
CI[e]		33.4	1.077	141.5	N/A	N/A

[a] Absolute energies E in E_h, relative energies ΔE in kcal mol^{-1}, bond lengths in Å, bond angles in deg. The natural orbital occupation numbers (NOON) are given for the two highest occupied MOs. Integer values denote NOON values fixed by the method used; floating point numbers are given when other than integer values are possible. All calculations used Dunning's cc-pVTZ basis set [71] unless otherwise noted. The CAS-DFT calculations were carried out with the Colle–Salvetti (CS) functional. Results from [55–58].

[b] Geometries taken from DFT.

[c] Experimental geometries from [168] ($^1A_1$) and [169] ($^1A_1$: 1.075 Å, 133.9°; and $^3B_1$). $E(^1A_1) - E(^3B_1)$ from [170], converted from T_0 to T_e according to [167].

[d] Energy difference in parentheses is given relative to the UDFT energy of the $^3B_1$ state.

[e] $E(^1B_1) - E(^3B_1)$ estimated by extrapolation to large basis sets [171a]; $E(^1A_1) - E(^3B_1)$ from SOCI + Q/ANO calculations [171b].

(1) RDFT provides a reasonable account of the $^1A_1$-$^3B_1$ splitting where the calculated value will be closer to the experimental value (9.1 kcal mol^{-1} [170]) if RODFT (10.5 kcal mol^{-1}, table 6) rather than UDFT (11.8 kcal mol^{-1}) is taken for the triplet state. The $^1A_1$ state has only little type-II character, as confirmed by the NOON values obtained by CAS-DFT; there is only little negative charge (0.014 e, table 6) in the b_1-symmetrical π MO of the singlet closed shell state.

(2) BS-UDFT exaggerates the type-II character of $^1A_1$ state as revealed by a population of 0.472 e of the b_1-symmetrical π MO. As a consequence, the singlet–triplet splitting is just 5.5 kcal mol^{-1}. Because of the low lying triplet state, the breaking of space and spin symmetry leads to unreasonable results. BS-UDFT is inappropriate for describing non-dynamic electron correlation effects in the singlet state. Those covered by the semiempirical B3LYP functional within spin-restricted theory are sufficient.

(3) The simple augmentation of a two-configurational approach such as GVB by the DFT correlation functional LYP leads to a reasonable account of the type-II character of the $^1A_1$ state but to a serious double counting of its dynamic electron correlation effects, thus exaggerating its stability.

(4) CAS-DFT largely avoids double-counting of dynamic electron correlation. However, in the version used the scaling back of dynamic correlation effects for the triplet is too strong, thus underestimating its stability. This emphasizes the necessity for differentiating between singlet and triplet states in the scaling procedure (see § 7.2).

(5) ROSS-DFT gives a reasonable account of OSS $^1B_1$ state and therefore will be the method of choice if the more costly CAS-DFT method cannot be used. We note that the latter predicts a more accurate value of $\Delta E(^1B_1 - ^3B_1)$ because of the similarity in the orbital occupation.

(6) Interesting is the dramatic failure of PO-UDFT, which predicts an energy difference (11.4 kcal mol^{-1}) between the $^1B_1$ state and the $^3B_1$ state, which is just one third of the best available WFT value

(33.4 kcal mol^{-1} [171], table 6). Although the orbital occupation of the $^1B_1$ state is correctly given by the PO-UDFT approach, the result is flawed by a large contribution from the $^3B_1$ state in the PO-UDFT wavefunction, thus artificially lowering the corresponding energy. The PO-UDFT energy of the $^1B_1$ state of methylene has to be too low by at least twice the magnitude of the exchange integral K_{rs}, which is $2 \times 7.8 = 15.6$ kcal mol^{-1} in the case of methylene. We conclude that even a qualitatively correct PO-UDFT description of the $^1B_1$ state is not possible.

One might conclude from this comparison that both BS-UDFT and PO-UDFT are methods one should not use for the description of type-I, type-II or type-III systems. However, the results listed in tables 7 and 8 reveal that such a conclusion would be precipitate.

In the case of α-3-didehydrotoluene (Myers biradical, figure 10) it is known that because of spin polarization between the unpaired electrons the singlet $^1A'$ state is the ground state [172]. The best estimates give a singlet–triplet splitting of about 2 kcal mol^{-1} [55, 58, 173]. For the Myers biradical, spin polarization is a long range effect, and therefore it corresponds to non-dynamic electron correlation, i.e. the Myers biradical is a typical example of type-III character, which in WFT implies a two(multi)-determinantal multiconfigurational description. On the basis of these considerations, the results listed in table 7 can be analysed [55, 58].

(7) Although the ROSS method (implicitly) provides a two-determinantal description, it must fail because it covers no extra non-dynamic correlation effects needed to account properly for spin polarization. Accordingly, ROSS predicts the $^1A'$ state to be above rather than below the $^3A''$ state (0.8 kcal mol^{-1}, table 7).

(8) PO-UDFT covers spin-polarization as a result of a separate optimization of α and β spin orbitals. As the two unpaired electrons are substantially separated, the magnitude of the exchange integral K_{rs} is very small, and therefore the basic failure of PO-UDFT (see conclusion 6 above) is disguised. In other words, the singlet–triplet splitting is rather small and any triplet contamination of the PO-UDFT wavefunction a negligible problem. The correct order of states and a reasonable value for the singlet–triplet splitting is obtained (−1.0 kcal mol^{-1}, table 7).

(9) BS-UDFT describes for the Myers biradical a type-II rather than a type-III state by mixing the $^1A'(\sigma^2)$ with the $^1A'(\pi^2)$ state. The calculated NOON values are 1.423 for the a′ symmetrical σ orbital and 0.577 for the a″ symmetrical π-orbital while the NOON values of the PO-UDFT description are both 1.000 as they should be. Hence, BS-UDFT describes an excited singlet state that is 22.5 kcal mol^{-1} higher in energy than the triplet state (table 7).

(10) As both the $^1A'$ and the $^3A''$ imply the same orbital occupation (apart from spin), the CAS-DFT calculation is not affected by a different scaling of dynamic electron correlation for the singlet and triplet states. It gives the singlet state 2.6 kcal mol^{-1} below the triplet state, in good accord with the best WFT results published so far (table 7). However, GVB-DFT is flawed by a double-counting of dynamic electron correlation, which plays a larger role in the singlet state, thus exaggerating its stability.

Table 7. Singlet–triplet splitting for α-3-didehydrotoluene (Myers biradical).[a]

Method	Functional	$E(^3A'')$	$\Delta E(^1A')$
ROSS	B3LYP	−270.319 71	0.8
PO-UDFT	B3LYP	−270.323 22	−1.0
BS-UDFT	B3LYP	−270.323 22	22.5
GVB-DFT[b]	LYP	−270.116 65	−7.4
CAS(8,8)-DFT[c]	CS	−270.039 09	−2.6
DDCI2[d]			−2.0

[a] Absolute energies E in E_h, relative energies ΔE in kcal mol^{-1}. All calculations were done with Dunning's cc-pVTZ basis set [71] unless otherwise noted. The method is given for the description of the OSS state while for the triplet state either RODFT or UDFT was used.
[b] Triplet calculated with ROHF-DFT. ROSS geometries used. See [59].
[c] Reference [58]. The Colle–Salvetti (CS) functional and the 6-31G(d,p) basis set were used.
[d] Reference [173].

Table 8. Singlet and triplet energies for 1,4-didehydrobenzene (*p*-benzyne).[a]

Method	Functional	$E(^3B_{1u})$	$\Delta E(^1A_g)$
RDFT	B3LYP	−230.952 54	13.1
BS-UDFT	B3LYP	−230.952 54	−2.6
PO-UDFT	B3LYP	−230.952 54	38.9
GVB-DFT	LYP	−230.777 58	−10.4
CAS(8,8)-DFT[b]	CS	−230.709 04	−2.5
Expt.[c]			−3.5 ± 0.5

[a] Absolute energies E in E_h, relative energies ΔE in kcal mol^{-1}. All calculations are based on Dunning's cc-pVTZ basis set [71] unless otherwise noted. The method is given for the description of the singlet state while for the triplet state either RODFT or UDFT was used. UDFT results are from [53].
[b] Reference [58]. The Colle–Salvetti (CS) functional and the 6-31G(d,p) basis set were used.
[c] Reference [174], converted to T_e according to [53].

The results for the Myers biradical show that PO-UDFT, despite its basic failure to describe the energy of type-I systems such as OSS states correctly, can be useful provided that the exchange interaction between the unpaired electrons in the triplet state associated with the OSS state is small. This situation occurs for singlet biradicals with the unpaired electrons located at different atoms. In such a case, the advantage of PO-UDFT to cover non-dynamic electron correlation effects dominates its disadvantages of being triplet contaminated, thus changing the energy by the term $2K_{rs}$. However, PO-UDFT is definitely not suitable for a type-II system as calculations for a third example, namely *p*-benzyne (table 8, figure 10), reveal. *p*-Benzyne possesses a singlet ground state, which has some biradical character because of mixing between the $^1A_g(HOMO^2)$ ground state with the $^1A_g(LUMO^2)$ singlet excited state [55]. The first excited triplet states, $^3B_{1u}(HOMO^1, LUMO^1)$, was measured to be 3.5 kcal mol^{-1} above the singlet ground state [53, 174].

(11) RDFT, which covers non-dynamic electron correlation effects only via the empirically calibrated B3LYP hybrid functional, underestimates the stability of the ^1A_g state and, accordingly, is not able to provide the correct state ordering (table 8).

(12) BS-UDFT, which covers non-dynamic electron correlation effects both via the approximate exchange functional used and the two-configurational character of the wavefunction, performs well in the case of *p*-benzyne and gives a splitting of 2.6 kcal mol^{-1}. The triplet contamination plays only a minor role.

(13) PO-UDFT is not able to describe the ^1A_g state, but describes an excited OSS state of *p*-benzyne which is 38.9 kcal mol^{-1} higher in energy.

(14) Because of a stronger double counting of non-dynamic correlation effects for the singlet state, GVB-DFT strongly exaggerates the stability of the ground state. CAS-DFT, however, provides a reliable account of the relative energies of the two states.

The three examples provide useful guidelines for the applicability of DFT methods in the case of multireference systems. UDFT methods are the 'poor-man's tools' for describing multireference effects, provided that appropriate care is taken and some knowledge of the electronic structure of the target system is available. Calculation of $\langle \hat{S}^2 \rangle$ with the help of KS orbitals provides little information on the accuracy of the UDFT description. A large $\langle \hat{S}^2 \rangle$ value does not necessarily imply a large error in the relative UDFT energies. A better way of assessing the accuracy of a given PO- or BS-UDFT description, e.g. of a singlet state with multireference character, is provided by an independent determination of the singlet–triplet splitting. If this is large and $E(S) < E(T)$, the stability of the target system and $\Delta E(T–S)$ will be underestimated because of the T contamination of the UDFT description. The stability of the target system, however, will be overestimated, and the magnitude of the singlet–triplet splitting again underestimated if $E(S) > E(T)$ and $\Delta E(S–T)$ is large. Reasonable results can be obtained only for relatively small singlet–triplet splittings. Hence, in all cases of large singlet-triplet splittings more advanced methods such as CAS-DFT rather than UDFT must be applied.

8. Conclusions and outlook

DFT defines and covers electron correlation effects in a way considerably different from WFT. Exchange correlation plays a strong role in DFT because it represents more than 95% of all electron correlation effects. Therefore, any investigation of electron correlation effects covered by DFT must especially consider the role of the exchange functional.

(1) Because of the local nature of the exchange hole of either LDA or GGA functionals, DFT exchange covers non-dynamic electron correlation effects in an unspecified way. This is reflected in the calculated difference densities, which suggest that Becke exchange leads to stronger left–right and in–out correlation effects than any of the MP or CC methods used in this work. Inspection of the difference densities does not clarify whether these pair correlation effects are of short or long range nature whereas the exaggeration of left–right correlation beyond that normally found for MP2 actually suggests that long range rather than short range effects are simulated by LDA or GGA exchange. For Slater exchange, pair correlation effects reflected by calculated difference densities are even stronger, indicating that the LDA functional covers even more non-dynamic correlation effects than the GGA exchange functionals.

(2) As the GGA exchange potentials possess a singularity at the nucleus, an artificial shell structure in the density surrounding the nucleus in the core and inner shell region is obtained, which should cause problems when calculating molecular properties strongly dependent on a correct description of the density distribution in this region.

(3) Correlation functionals such as LYP change the density distribution generally by contracting density from the van der Waals region to the bond region. GGA functionals differ in so far as they are also affected by a singularity at the nucleus that leads to a depletion of negative charge from the core region, thus balancing somewhat the opposite trends observed for the exchange functionals. The changes in density caused by the correlation functionals can be related to higher order correlation effects of WFT methods that have similar consequences with regard to the density distribution. This indicates that the correlation functionals contain

dynamic correlation effects not (or only partially) present in low order MP*n* methods.

(4) Despite the different nature of correlation effects covered, B-only DFT densities resemble MP2, MP4 or CCSD(T) density distributions, where the agreement with MP4 densities is often the best. The effects of the correlation functional do not change this agreement significantly. This explains why DFT results obtained with a GGA XC functional are often close to those obtained with either MP4, MP2 or CCSD(T).

(5) Investigation of SCF-SIC-DFT densities reveals that the long range (non-dynamic) correlation effects of commonly used exchange functionals are caused by the self-interaction error (SIE). Correct SIC-DFT exchange describes for the bond region of a molecule a delocalized exchange hole, which is not related to any dynamic or non-dynamic electron correlation effects. In this way it approaches but does not reach the delocalized hole of exact exchange.

(6) The SIE of correlation functionals leads to a stronger increase of the density in the bond regions of a molecule, thus slightly compensating for the dominating X-SIE. In the case of the BLYP functional this compensation is not given (LYP is by construction SIE-free) so that its total SIE is larger than in the case of the PW91PW91 functional, which has a rather small total SIE. The changes in the electron density caused by the PW91 correlation functional can be related to the influence of the reduced gradient. SIE corrected correlation functionals possess in general less density in the heavy atom bond regions and more in the non-bonded regions.

(7) Use of hybrid functionals invokes a similar pattern of changes in the molecular density as that caused by SIC-DFT, but changes are much smaller in the former case. The mixing-in of 20–25% HF exchange leads to a partial correction of the SIE and by this of the long range correlation effects without cancelling them completely. By construction, the hybrid functionals represent an economical way to correct partially for the SIE. However, this is done in a well balanced way using functionals that were calibrated including rather than excluding the SIE. In general, SIC-DFT will not pro-vide better results than DFT with hybrid functionals. However, there are molecular problems (odd-electron bonds and transition states) with distinctly delocalized exchange holes that require SIC-DFT to obtain a reasonable description.

(8) Hybrid functionals lead to electron densities that often agree well with CCSD(T) densities. This results from the fact that hybrid functionals suppress some of the long range correlation effects, which can be viewed as a coupling between diagonal *N*-electron correlation effects found at higher orders of MP or CC theory. Inclusion of the coupling effects is equivalent to adding ionic terms needed for a correct description of effective atomic numbers (effective electronegativities), bond polarities, etc.

(9) Spin restricted DFT covers both dynamic and non-dynamic correlation effects in an unspecified way, but this does not mean that electron systems with distinct multireference effects can always be described reasonably. Single-determinant RDFT fails on reasons of principle when describing type-I systems. For OSS states, this problem can be solved approximately by PO-UDFT, provided that the splitting between the singlet and the corresponding triplet state is relatively small (equivalent to a small magnitude of the term $2K_{rs}$ in the triplet state). Otherwise, ROSS-DFT or CAS-DFT must be applied.

(10) BS-UDFT covers non-dynamic electron correlation effects in two independent ways, namely in an unspecified way via the exchange functional and in a more specific way via the form of the UDFT wavefunction, which possesses two-configurational character. Hence, one cannot exclude that there will be a double counting of dynamic electron correlation effects if BS-UDFT is used. However, double counting can largely be suppressed if hybrid functionals are used.

(11) Because of the two-configurational character of BS-UDFT, the method is suitable for type-II systems. Nevertheless, it has to be used with care, always considering the influence of spin contamination on calculated energies, which is best monitored via the singlet–triplet splitting. We note in this connection that the expectation value $\langle \hat{S}^2 \rangle$ calculated using KS orbitals is less suitable as a diagnostic tool for the reliability of BS-UDFT. BS-UDFT is rather useful in cases or relatively small singlet–triplet splittings; for large singlet–triplet splittings, BS-UDFT becomes highly erroneous.

(12) BS-UDFT is not suitable for type-I and type-III systems. OSS states with type-III character can be described reasonably by PO-UDFT provided that the term $2K_{rs}$ and accordingly also the corresponding singlet–triplet splitting are small. Spin polarization is covered by an independent optimization of α and β spin orbitals.

(13) Any extensions of DFT methods to multireference problems with the help of WFT methodology will require the separation of dynamic and non-dynamic Coulomb correlation effects. Important steps in this direction have been made, but no rigorous principle to be used in setting up WFT-DFT methods is available yet.

(14) CAS-DFT is one of the WFT-DFT methods that because of its general applicability should have considerable potential when describing multireference systems. Early versions of the method are already available, but

the handling of the basic problem (scaling back of dynamic electron correlation effects) has to be improved to treat differently sized core and active spaces and different multiplicities of multireference systems appropriately.

This review can provide only a limited insight into the rapidly developing field of DFT methods that handle dynamic and non-dynamic correlation effects in an advanced manner. A central role in this connection is played by the SIE of standard DFT functionals, which was outlined and analysed here with the tools of density analysis and correlation corrected WFT methods. Since there are too many unsolved questions in connection with SIC-DFT (orbital dependence, invariance with regard to rotations between occupied orbitals, appropriate XC functionals to be used in connection with SIC-DFT, convergence problems, cost of SCF-SIC-DFT calculations, etc.), it makes little sense to invest in SIC-DFT methods intended for routine use in the future. However, SIC-DFT is useful in so far as it provides insight into some of the basic failures of standard DFT methods. This insight can trigger further developments of properly SIE-corrected XC functionals, which should replace the empirically calibrated hybrid functionals in the near future. As shown in this work, the balanced cancellation of the SIE is the key to new functionals that incorporate non-dynamic correlation effects in a more specific rather than unspecified manner. This goal is highly attractive, considering that within KS-DFT even a multireference system can be described by a single determinant approach, provided that an exact functional is used. Of course, the realization of this goal will involve many steps and cannot be achieved in a perfect way. Therefore, developments during the next few years will also focus on new WFT-DFT methods, which provide reasonable descriptions of multireference systems. The use of WFT-DFT methods will always imply increased computational cost, and therefore their application will be limited. In the long run, the goal must be to develop suitable multi-purpose XC functionals that preserve the simplicity of KS-DFT.

Fruitful discussions with Professor E. Kraka, Dr J. Gräfenstein, Victor Polo, and Dr M. Filatov are gratefully acknowledged. This work was supported by the Swedish Natural Science Research Council (NFR). Calculations were made on the supercomputers of the Nationellt Superdatorcentrum (NSC), Linköping, Sweden. D.C. thanks the NSC for a generous allotment of computer time.

References

[1] Curtis, L. A., Ragavachari, K., Trucks, G. W., and Pople, J. A., 1991, *J. chem. Phys.*, **94,** 7221; Curtis, L. A., Ragavachari, K., Redfern, P. C., Rassolov, V., and Pople, J. A., 1998 *J. chem. Phys.*, **109,** 7764.
[2] Schleyer, P. v. R., Allinger, N. L., Clark, T., Gasteiger, J., Kollman, P. A., Schaefer III, H. F., and Schreiner, P. R., 1998, *Encyclopedia of Computational Chemistry*, Vols 1–5 (Chichester: Wiley).
[3] Yarkony, R. D., 1995, *Advanced Series in Physical Chemistry*, Vol. 2., *Modern Electronic Structure Theory*, Part I and Part II (Singapore: World Scientific).
[4] Schaefer III, H. F., 1977, *Modern Theoretical Chemistry*, Vol. 3, *Methods of Electronic Structure Theory* (New York: Plenum Press).
[5] Hohenberg, P., and Kohn, W., 1994, *Phys. Rev.* B, **136,** 864.
[6] Kohn, W., and Sham, L., 1965, *Phys. Rev.* A, **140,** 1133.
[7] Parr, R. G., and Yang, W., 1989, *Density-Functional Theory of Atoms and Molecules* (Oxford University Press).
[8] Labanoswski, J. K., and Andzelm, J. W., 1990, *Density Functional Methods in Chemistry* (Heidelberg: Springer-Verlag).
[9] Trickery, S. B., 1990, *Density Functional Theory of Many-Fermion Systems* (San Diego: Academic Press).
[10] Dreizler, R. M., and Gross, E. K. U., 1990, *Density Functional Theory* (Berlin: Springer-Verlag) and references therein; Gross, E. K. U., and Dreizler, R. M., 1995, *Density Functional Theory* (New York: Plenum Press).
[11] Ellis, D. E., 1995, *Density Functional Theory of Molecules, Clusters and Solids* (Dordrecht: Kluwer).
[12] Chong, D. P., 1995, *Recent Advancees in Density Functional Methods*, Part II (Singapore: World Scientific).
[13] Seminario, J. M., and Politzer, P., 1996, *Modern Density Functional Theory—A Tool For Chemistry* (Amsterdam: Elsevier).
[14] Laird, B. B., Ross, R. B., and Ziegler, T., 1996, *Chemical Applications of Density Functional Theory* (Washington, DC: American Chemical Society).
[15] Nalewajski, R. F., 1996, *Density Functional Theory* I (Berlin: Springer-Verlag).
[16] Seminario, J. M., 1996, *Recent Developments and Applications of Modern Density Functional Theory* (Amsterdam: Elsevier).
[17] Joubert, D., 1997, *Density Functionals: Theory and Applications* (Heidelberg: Springer-Verlag).
[18] Springborg, M., 1997, *Density-Functional Methods in Chemistry and Material Science* (Chichester: Wiley).
[19] Dobson, J. F., Vignale, G., and Das, M. P., 1997, *Electronic Density Functional Theory, Recent Progress and New Directions* (New York: Plenum Press).
[20] Gill, P., 1998, *Encyclopedia of Computational Chemistry*, Vol. 1, edited by P. v. R Schleyer, N. L. Allinger, T. Clark, J. Gasteiger, P. A. Kollman, H. F. Schaefer III, and P. R. Schreiner (Chichester: Wiley), p. 678, and references therein.
[21] Chermette, H., 1998, *Coordination Chem. Rev.*, **178–180,** 699.
[22] Lowdin, P. O., 1999, *Density Functional Theory* (New York, Academic Press).
[23] March, N. H., 1992, *Electron Density Theory of Atoms and Molecules* (New York: Academic Press).
[24] Koch, W., and Holthausen, M. C., 2000, *A Chemist's Guide to Density Functional Theory* (New York: Wiley).
[25] Thomas, L. H., 1927, *Proc. Camb. Phil. Soc.*, **23,** 542.
[26] Fermi, E., 1927, *Rend. Accad. Lincei*, **6,** 602.

[27] Dirac, P. A. M., 1930, *Proc. Camb. Phil. Soc.*, **26,** 376.
[28] Slater, J., 1951, *Phys. Rev.*, **81,** 385.
[29] Becke, A. D., 1988, *Phys. Rev.* A, **38,** 3098.
[30] Perdew, J. P., 1991, *Electronic Structure of Solids '91* (Berlin: Akademie-Verlag), p. 11; Perdew, J. P., and Wang, Y., 1992, *Phys. Rev.* B, **45,** 13244.
[31] Adamo, C., and Barone, V., 1998, *J. chem. Phys.*, **108,** 664.
[32] Vosko, S. H., Wilk, L., and Nusair, M., 1980, *Can. J. Phys.*, **58,** 1200.
[33] Perdew, J. P., and Zunger, A., 1981, *Phys. Rev.* B, **23,** 5048.
[34] Perdew, J. P., 1986, *Phys. Rev.* B, **33,** 8822.
[35] Lee, C., Yang, W., and Parr, R. G., 1988, *Phys. Rev.* B, **37,** 785.
[36] Becke, A. D., 1993, *J. chem. Phys.*, **98,** 5648.
[37] Becke, A. D., 1996, *J. chem. Phys.*, **104,** 1040.
[38] Adamo, C., and Barone, V., 1997, *Chem. Phys. Lett.*, **272,** 242.
[39] Becke, A. D., 1993, *J. chem. Phys.*, **98,** 1372.
[40] Colle, R., and Salvetti, O., 1979, *Theoret. Chim. Acta*, **53,** 55; 1990, *J. chem. Phys.*, **93,** 534.
[41] Kraka, E., Gauss, J., and Cremer, D., 1991, *J. Molec. Struct. Theochem*, **234,** 95.
[42] Gauss, J., and Cremer, D., 1992, *Adv. Quantum Chem.*, **23,** 205.
[43] Kraka, E., 1985, Ph.D. thesis, Cologne.
[44] Cremer, D., 1998, *Encyclopedia of Computational Chemistry*, Vol. 3, edited by P. v. R. Schleyer, N. L. Allinger, T. Clark, J. Gasteiger, P. A. Kollman, H. F. Schaefer III, and P. R. Schreiner (Chichester: Wiley) p. 1706.
[45] Cremer, D, and He, Z., 1996, *J. phys. Chem.*, **100,** 6173; 1997, *J. Molec. Struct. Theochem*, **398–399,** 7; He, Z., and Cremer, D., 1996, *Intl J. Quantum Chem.*, **59,** 15, 31, 57, 71.
[46] He, Y., and Cremer, D., 2000, *Molec. Phys.*, **98,** 1415.
[47] He, Y., and Cremer, D., 2000, *Theoret. Chem. Accounts*, **105,** 110.
[48] He, Z., and Cremer, D., 1991, *Intl J. Quantum Chem. Symp.*, **25,** 43.
[49] He, Z., and Cremer, D., 1993, *Theoret. Chim. Acta*, **85**, 305.
[50] He, Y., He, Z., and Cremer, D., 2000, *Chem. Phys. Lett.*, **317,** 535.
[51] He, Y., and Cremer, D., 2000, *Chem. Phys. Lett.*, **324,** 389.
[52] He, Y., Gräfenstein, J., Kraka, E., and Cremer, D., 2000, *Molec. Phys.*, **98,** 1639.
[53] Gräfenstein, J., Hjerpe, A. M., Kraka, E., and Cremer, D., 2000, *J. phys. Chem.* A, **104,** 1748.
[54] Gräfenstein, J., and Cremer, D., 2001, *Molec. Phys.*, **99,** 981.
[55] Gräfenstein, J., Kraka, E., Filatov, M, and Cremer, D., 2001, *Int. J. Molec. Science*, in press.
[56] Gräfenstein, J., Cremer, D., and Kraka, E., 1998, *Chem. Phys. Lett.*, **288,** 593.
[57] Gräfenstein, J., and Cremer, D., 2000, *Chem. Phys. Lett.*, **316,** 569.
[58] Gräfenstein, J., and Cremer, D., 2000, *Phys. Chem. chem. Phys.*, **2,** 2091.
[59] Kraka, E., 1992, *Chem. Phys.*, **161,** 149; Kraka, E., Cremer, D., and Nordholm, S., 1991, *Molecules in Natural Science and Biomedicine*, edited by Z. Maksic and M. Eckert-Maksic (Chichester: Ellis Horwood) p. 351.
[60] Levy, M., 1979, *Proc. Natl Acad. Sci. USA*, **76,** 6062.
[61] Wigner, E. P., and Seitz, F., 1934, *Phys. Rev.*, **46,** 509.
[62] Boyd, R. J., and Coulson, C. A., 1974, *J. Phys.* B, **7,** 1805.
[63] Krishnan, R., Frisch, M., and Pople, J. A., 1980, *Chem. Phys.*, **72,** 4244.
[64] Huber, K. P., and Herzberg, G. H., 1979, *Molecular Spectra and Molecular Constants of Diatomic Molecules* (New York: Van Nostrand-Reinhold).
[65] Raghavachari, K, Trucks, G. W., Pople, J. A., and Head-Gordon, M., 1989, *Chem. Phys. Lett.*, **157,** 479.
[66] Coulson, C. A., and Neilson, A. H., 1961, *Proc. phys. Soc.*, **87,** 831.
[67] Ruedenberg, K., Cheung, L. M., and Elbert, S. T., 1997, *Intl J. Quantum Chem.*, **16,** 1069.
[68] Roos, B., 1980, *Intl J. Quantum Chem. Symp.*, **14,** 175; (b) 1987, *Ab Initio Methods in Quantum Chemistry*, Part II, edited by K. P. Lawley (Chichester: Wiley) p. 399.
[69] Perdew, J. P., 1990, *Adv. Quantum Chem.*, **21,** 113.
[70] Perez-Jimenez, A. J., Moscardo, F., Sancho-Garcia, J. C., Abia, L. P., San-Fabian, E., and Perez-Jorda, J. M., 2001, *J. chem. Phys.*, **114,** 2023.
[71] Dunning Jr, T. H., 1989, *J. chem. Phys.*, **90,** 1007.
[72] Wilson, A. K., van Mourik, T., and Dunning Jr, T. H., 1996, *J. Molec. Struct. Theochem*, **388,** 339; Woon, D. E., and Dunning Jr. T. H., 1993, *J. chem. Phys.*, **99,** 1914; Peterson, K. A., Kendall, R. A., and Dunning Jr., T. H., 1993, *J. chem. Phys.*, **99,** 1930, 9790.
[73] He, Y., and Cremer, D., 2000, *J. phys. Chem.* A, **104,** 7679; Kraka, E., He, Y., and Cremer, D., 2001, *J. phys. Chem.* A, **105,** 3269; Cremer, D., Kraka, E. and He, Y., 2001, *J. molec Struct.*, **567–568,** 275.
[74] However, it has to be pointed out that GGA functionals such as the Becke exchange functional are strictly seen also semiempirical because they were obtained by a fit procedure utilizing the HF exchange energies of the noble gas atoms [29].
[75] Perdew, J. P., and Zunger, A., 1981, *Phys. Rev.* B, **23,** 5048.
[76] Perdew, J. P., 1984, *Local Density Approximations in Quantum Chemistry and Solid State Physics*, edited by J. Avery and J. P. Dahl (New York: Plenum Press); Perdew, J. P., and Ernzerhof, M., 1998, *Electronic Density Functional Theory: Recent Progress and New Directions*, edited by J. F. Dobson, G. Vignale, and M. P. Das (New York: Plenum Press) p. 31.
[77] Harrison, J. G., Heaton, R. A., and Lin, C. C., 1983, *J. Phys.* B., **16,** 2079.
[78] Pederson, M. R., Heaton, R. A., and Lin, C. C., 1984, *J. chem. Phys.*, **80,** 1972; 1985, *J. chem. Phys.*, **82,** 2688.
[79] Svane, A., Temmerman, W. M., Szotek, Z., Laegsgaard, J., and Winter, H., 1999, *Intl J. Quantum Chem.*, **77,** 799.
[80] Goedecker, S., and Umrigar, C. J., 1977, *Phys. Rev.* A, **55,** 1765.
[81] Li, Y., and Krieger, J. B., 1990, *Phys. Rev.* A, **41,** 1701; Chen, J., Krieger, J. B., and Li, Y., 1996, *Phys. Rev.* A, **54,** 3939.
[82] Garza, J., Nichols, J. A., and Dixon, D. A., 2000 *J. chem. Phys.*, **112,** 7880; **113,** 6929; Garza, J., Vargas, R., Nichols, J. A., and Dixon, D. A., 2001, *J. chem. Phys.*, **114,** 639.

[83] Guo, Y., and Whitehead, M. A., 1991, *J. Comput. Chem.*, **12,** 803; Whitehead, M. A., and Suba, S., 1995, *Recent Advances in Density Functional Methods*, Part I, edited by D. P. Chong (Singapore: World Scientific) p. 53.

[84] Chermette, H., Ciofini, I., Mariotti, F., and Daul, C., 2001, *J. chem. Phys.*, **114,** 1447.

[85] Gill, P. M. W., Johnson, B. G., Gonzales, C. A., and Pople, J. A., 1994, *Chem. Phys. Lett.*, **221,** 100.

[86] Albright, T. A., Burdett, J. K., and Whangbo, M. H., 1984, *Orbital Interactions in Chemistry* (Chichester: Wiley).

[87] Kohn, W., Becke, A. D., and Parr, R. G., 1996, *J. phys. Chem.*, **100,** 12974.

[88] Baerends, E. J., and Gritsenko, O. V., 1997, *J. phys. Chem.* A, **101,** 5383.

[89] Stowasser, R., and Hoffmann, R., 1999, *J. Amer. chem. Soc.*, **121,** 3414.

[90] Perdew, J. P., Savin, A., and Burke, K., 1995, *Phys. Rev.* A, **51,** 4531.

[91] Bader, R. W. F., 1995, *Atoms in Molecules: A Quantum Theory* (Oxford: Clarendon Press).

[92] See, e.g. Baker, J., Muir, M., Andzelm, J., and Scheiner, A., 1996, *Chemical Applications of Density-Functional Theory*, edited B. B. Laird, R. B. Ross and T. Ziegler (Washington, DC: American Chemical Society) p. 343.

[93] Porezag, D., and Pederson, M. R., 1995, *J. chem. Phys.*, **102,** 9345.

[94] Wrobel, R., Sander, W., Kraka, E., and Cremer, D., 1999, *J. phys. Chem.* A, **103,** 3693.

[95] Kristyan, S., and Pulay, P., 1994, *Chem. Phys. Lett.*, **229,** 175.

[96] Perez-Jorda, J. M., and Becke, A. D., 1995, *Chem. Phys. Lett.*, **233,** 134.

[97] Hobza, P., Sponer, J., and Reschel, T., 1995, *J. comput. Chem.*, **16,** 1315.

[98] Ruiz, E., Salahub, D. R., and Vela, A., 1995, *J. Amer. chem. Soc.*, **117,** 1141.

[99] Wesolowski, T. A., Parisel, O., Ellinger, Y., and Weber, J., 1997, *J. phys. Chem.* A, **101,** 7818.

[100] Sosa, C. P., Carpenter, J. E., and Novoa, J. J., 1996, *Chemical Applications of Density-Functional Theory*, edited by B. B. Laird, R. B. Ross and T. Ziegler (Washington, DC: American Chemical Society) p. 131.

[101] Gonzales, L., Mo, O., and Yanez, M., 1996, *J. Comput. Chem.*, **18,** 1124; Gonzales, L., Mo, O., Yanez, M., and Elguerdo, J., 1996, *J. molec. Struct. Theochem*, **371,** 1; 1998, *J. chem. Phys.*, **109,** 139, 2685; Gonzales, L., Mo, O. and Yanez, M., 1999, *J. chem. Phys.*, **111,** 3855.

[102] For a recent review, see Koch, W., and Holthausen, M. C., 2000, *A Chemist's Guide to Density Functional Theory* (New York: Wiley) chap. 12.

[103] Christen, D., Coudert, L. H., Larsson, J. A., and Cremer, D., 2000, *J. Molec Spectrosc.*, **205,** 185.

[104] Møller, C, and Plesset, M. S., 1934, *Phys. Rev.*, **46,** 618.

[105] Gauss, J., 1998, *Encyclopedia of Computational Chemistry*, Vol. 1, edited by P. v. R. Schleyer, N. L. Allinger, T. Clark, J. Gasteiger, P. A. Kollman, H. F. Schaefer III, and P. R. Schreiner (Chichester: Wiley) p. 615.

[106] Crawford T. D., and Schaefer III, H. F., 2000, *Reviews in Computational Chemistry*, Vol. 14, edited by K. B. Lipkowitz and D. B. Boyd (Weinheim: VCH) p. 33.

[107] Bartlett, R. J., and Stanton, J. F., 1994, *Reviews in Computational Chemisry*, Vol. 5, edited by K. B. Lipkowitz and D. B. Boyd (Weinheim: Verlag Chemie) p. 65.

[108] Cremer, D., and He, Z., 1997, *Conceptual Perspectives in Quantum Chemistry*, Vol. III, edited by J.-L. Calais, and E. Kryachko (Dordrecht: Kluwer) p. 239.

[109] Werner, H.-J., 1987, *Ab Initio Methods in Quantum Chemistry*-II, edited K. P. Lawley (New York: Wiley) p. 1.

[110] Szalay, P. G., 1997, *Modern Ideas in Coupled-Cluster Methods*, edited by R. J. Bartlett (Singapore: World Scientific) p. 81; Szalay, P. G., and Bartlett, R. J., 1993, *Chem. Phys. Lett.*, **214,** 481.

[111] Purvis III, G. D., and Barlett, R. J., 1982, *J. chem. Phys.*, **76,** 1910.

[112] Siu, A. K., and Davidson, E. F., 1970, *Intl J. Quantum Chem.*, **4,** 233; Green, S., 1971, *Chem. Phys.*, **54,** 827; Billingsley, F. P., Krauss, I. I., and Krauss, M., 1974, *J. chem. Phys.*, **60,** 4130; Kirby-Docken, K., and Liu, B., 1977, *J. chem. Phys.*, **66,** 4309; Jasien, P. G., and Dykstra, C. E., 1985, *Intl J. Quantum Chem.*, **28,** 411; Jaquet, R., Kutzelnigg, W., and Staemmler, V., 1980, *Theoret. Chim. Acta*, **54,** 205.

[113] Krishnan, R., and Pople, J. A., 1981, *Intl J. Quantum Chem.*, **20,** 1067; Sadlej, A. J., 1978, *Theoret. Chim. Acta*, **47,** 205.

[114] Scuseria, G. E., and Schaefer III, H. F., 1988, *Chem. Phys. Lett.*, **148,** 205; Watts, J., Trucks, G. W., and Bartlett, R. J., 1989, *Chem. Phys. Lett.*, **157,** 359.

[115] See, e.g., Perdew, J. P., Burke, K., and Ernzerhof, M., 1996, *Phys. Rev. Lett.*, **77,** 3865; 1997, *Phys. Rev. Lett.*, **78,** 1396 (E).

[116] Olsson, L., and Cremer, D., 1996, *J. chem. Phys.*, **105,** 8995.

[117] Sychrovsky, V., Gräfenstein, J., and Cremer, D., 2000, *J. chem. Phys.*, **113,** 3530.

[118] Fermi, E., and Amaldi, E., 1934, *Accad. Ital. Rome*, **6,** 117.

[119] Polo, V., Kraka, E., and Cremer, D., 2001, *Molec. Phys.*, in press.

[120] Slater, J. C., 1974, *The Self-Consitent Field for Molecules and Solids* (New York: McGraw-Hill).

[121] Becke, A. D., 1995, *Modern Electronic Structure Theory*, Part II, edited by D. R. Yarkony (Singapore: World Scientific) p. 1022; Schipper, P. R. T., Gritsenko, O. V., and Baerends, E. J., 1999, *J. chem. Phys.*, **111,** 4056.

[122] Bally, T., and Sastry, G. N., 1997, *J. phys. Chem.* A, **101,** 7923.

[123] Sodupe, M., Bertran, J., Rodriguez-Santiago, L., and Baerends, E. J., 1999, *J. phys. Chem.* A, **103,** 166.

[124] Zhang, Y., and Yang, W., 1998, *J. chem. Phys.*, **109,** 2604; see also [26].

[125] Gritsenko, O. V., Ensing, B., Schipper, P. R. T., and Baerends, E. J., 2000, *J. phys. Chem.* A, **104,** 8558.

[126] Polo, V., Kraka, E., and Cremer, D., unpublished.

[127] See, e.g., Becke, A., 2000, *J. chem. Phys.*, **112,** 4020 and references therein.

[128] Langreth, D. C., and Perdew, J. P., 1975, *Solid State Commun.*, **17,** 1425; Gunnarsson, O., and Lundqvist, B. I., 1976, *Phys. Rev.* B, **13,** 4274.
[129] Harris, J., 1984, *Phys. Rev.* A, **29,** 1648.
[130] Paldus, J., and Cizek, J., 1967, *J. chem. Phys.*, **47,** 3976; 1970, *J. chem. Phys.*, **52,** 2919; 1971, *J. chem. Phys.*, **54,** 2293; Paldus, J., and Veillard, A., 1978, *Molec. Phys.*, **35,** 445.
[131] Davidson, E. R., and Borden, W. T., 1983, *J. phys. Chem.*, **87,** 4783; Hrovat, D. A., Du, P., and Borden, W. T., 1986, *Chem. Phys. Lett.*, **123,** 337.
[132] Seeger, R., and Pople, J. A., 1977, *J. chem. Phys.*, **66,** 3045.
[133] Bauernschmitt, R., and Ahlrichs, R., 1996, *J. chem. Phys.*, **104,** 9047.
[134] Fukutome, H., 1981, *Intl J. Quantum Chem.*, **20,** 955.
[135] Bobrowicz, F. W., and Goddard III, W. A., 1977, *Methods of Electronic Structure Theory, Modern Theoretical Chemistry*, Vol. 3, edited by H. F. Schaefer III (New York: Plenum Press) p. 79.
[136] Amos, T., and Hall, G. G., 1961, *Proc. R. Soc. Lond.* A, **263,** 483; Chen, W., and Schlegel, H. B., 1994, *J. chem. Phys.*, **101,** 5957; Schlegel, H. B., 1988, *J. phys. Chem.*, **92,** 3075; 1986, *J. chem. Phys.*, **84,** 4530; Purvis, G. D., Sekino, H., and Bartlett, R. J., 1988, *Collect. Czech. chem. Commun.*, **53,** 2203; Rittby, M., and Bartlett, R. J., 1988, *J. phys. Chem.*, **92,** 3033; Andrews, J. S., Jauatilaka, D., Bone, R. G., Handy, N. C., and Amos, R. D., 1991, *Chem. Phys. Lett.*, **183,** 423.
[137] Wang, J., Becke, A. D., and Smith, V., 1995, *J. chem. Phys.*, **102,** 3477.
[138] Löwdin, P. O., 1995, *Phys. Rev.*, **97,** 1474.
[139] Pople, J., Gill, P. M. W., and Handy, N. C., 1995, *Intl J. Quantum Chem.*, **56,** 303.
[140] Wittbrodt, J. M., and Schlegel, H. B., 1996, *J. chem. Phys.*, **105,** 6574.
[141] Burke, K., Perdew, J. P., and Ernzerhof, M., 1998, *J. chem. Phys.*, **109,** 3760. Perdew, J. P., Ernzerhof, M., Burke, K., and Savin, A., 1997, *Intl J. Quantum Chem.*, **61,** 197.
[142] Davidson, E. R., 1973, *Chem. Phys. Lett.*, **21,** 565.
[143] Andrews, J. S., Murray, C. W., and Handy, N. C., 1993, *Chem. Phys. Lett.*, **201,** 458.
[144] Filatov, M., and Shaik, S., 1998, *Chem. Phys. Lett.*, **288,** 689; Filatov, M. and Shaik, S., 1999, *J. chem. Phys.*, **110,** 116.
[145] Andersson, K., and Roos, B. O., 1995, *Modern Electron Structure Theory*, edited by R. Yarkony (Singapore: World Scientific) p. 55.
[146] Slater, J., Mann, J. B., Wilson, T. M., and Wood, J. H., 1969, *Phys. Rev.*, **184,** 672.
[147] Dunlap, B. I., 1987, *Adv. chem. Phys.*, **69,** 287.
[148] Goddard, J. D., and Orlova, G., 1999, *J. chem. Phys.*, **111,** 7705.
[149] Wang, S. G., and Schwarz W. H. E., 1996, *J. chem. Phys.*, **105,** 464.
[150] Borowski, P., Jordan, K. D., Nichols, J., and Nachtigall, P., 1998, *Theoret. Chem. Accounts*, **99**, 135.
[151] Filatov, M., and Shaik, S., 1999, *Chem. Phys. Lett.*, **304,** 429.
[152] Sherill, C. D., Lee, M. S., and Head-Gordon, M., 1999, *Chem. Phys. Lett.*, **302,** 425.
[153] Gutle, C., Savin, A., Krieger, J. B., and Chen, J. O., 1999, *Intl J. Quantum Chem.*, **75,** 885.
[154] Grimme, S., and Waletzke, M., 1999, *J. chem. Phys.*, **111,** 5645.
[155] Lee, M. S., and Head-Gordon, M., 2000, *Intl J. Quantum Chem.*, **76,** 169.
[156] Choi, C. H., Kertesz, M., and Karpfen, A., 1997, *J. chem. Phys.*, **107,** 6712.
[157] Gritsenko, O. V., Schipper, P. R. T., and Baerends, E. J., 1997, *J. chem. Phys.*, **107,** 5007; Schipper, P. R. T., Gritsenko, O. V., and Baerends, E. J., 1999, *J. chem. Phys.*, **111,** 4056.
[158] Savin, A., and Flad, H.-J., 1995, *Intl J. Quantum Chem.*, **56,** 327; Savin, A., 1996, *Recent Advances in Density Functional Methods*, edited by D. P. Chong (Singapore: World Scientific) p. 129; *Recent Developments and Applications of Modern Density Functional Theory*, edited by J. Seminario (Amsterdam: Elsevier) p. 327. Leininger, T., Stoll, H., Werner, H.-J., and Savin, A., 1997, *Chem. Phys. Lett.*, **275,** 151.
[159] Rassolov, V. A., 1999, *J. chem. Phys.*, **110,** 3672.
[160] Cioslowski, J., 1991, *Phys. Rev.* A, **43,** 1223.
[161] Mok, D. K., Neumann, R., and Handy, N., 1996, *J. phys. Chem.*, **100,** 6225.
[162] Valderrama, E., Ludena, E. V., and Hinze, J., 1997, *J. chem. Phys.*, **106,** 9227.
[163] Valderrama, E., Mercero, J. M., and Ugalde, J. M., 2001, *J. Phys.* B, **34,** 275.
[164] Savin, A., 1998, *Intl J. Quantum Chem. Symp.*, **22**, 59.
[165] Miehlich, B., Stoll, H., and Savin, A., 1997, *Molec. Phys.*, **91,** 527.
[166] Gräfenstein, J., unpublished.
[167] Bettinger, H. F., Schleyer, P. v. R., Schreiner, P. R., and Schaefer III, H. F., 1998, *The Encyclopedia of Computational Chemistry*, edited by P. v. R. Schleyer, N. Allinger, T. Clark, J. Gasteiger, P. A. Kollman, H. F. Schaefer III, and P. R. Schreiner (Chichester: Wiley) p. 183.
[168] Petek, H., Nesbitt, D. J., Darwin, D. C., Ogilby, P. R., Moore, C. B., and Ramsay, D. A., 1989, *J. chem. Phys.*, **96,** 6566.
[169] Jensen, P., and Bunker, P. R., 1988, *J. chem. Phys.*, **89,** 1327.
[170] McKellar, A. R. W., Bunker, P. R., Sears, T. J., Evenson K. M., Saykally, R. J., and Langhoff, S. R., 1983, *J. chem. Phys.*, **79,** 5251.
[171] (a) Bauschlicher, C. W., 1980, *Chem. Phys. Lett.*, **74,** 273; (b) Bauschlicher, C. W., and Langhoff, S. R., 1987, *J. chem. Phys.*, **87,** 387.
[172] Wenthold, P. G., Wierschke, S. G., Nash, J. J., and Squires, R. R., 1993, *J. Amer. chem Soc.*, **115,** 12611; Logan, C. F., Ma, J. C., and Chen, P., 1994, *J. Amer. chem Soc.*, **116,** 2137.
[173] Cabrero, J., Ben-Amor, N., and Caballol, R., 1999, *J. phys. Chem.* A, **103,** 6220.
[174] Wenthold, P. G., Squires, R. R., and Lineberger, W. C., 1998, *J. Amer. chem Soc.*, **120,** 5279.
[175] Crawford, D., Kraka, E., Stanton, J., and Cremer, D., 2001, *J. chem. Phys.*, **114,** 10638.